Unusual Signs in Quantum Field Theory

Thesis by

Dónal O'Connell

In Partial Fulfillment of the Requirements

for the Degree of

Doctor of Philosophy

California Institute of Technology

Pasadena, California

2007

(Defended May 16, 2007)

To Dísa

The Collar

I Struck the board, and cry'd, No more.
I will abroad.
What? shall I ever sigh and pine?
My lines and life are free; free as the rode,
Loose as the winde, as large as store.
Shall I be still in suit?
Have I no harvest but a thorn
To let me bloud, and not restore
What I have lost with cordiall fruit?
Sure there was wine
Before my sighs did drie it: there was corn
Before my tears did drown it.
Is the yeare onely lost to me?
Have I no bayes to crown it?
No flowers, no garlands gay? all blasted?
All wasted?
Not so, my heart: but there is fruit,
And thou hast hands.
Recover all thy sigh-blown age
On double pleasures: leave thy cold dispute
Of what is fit, and not. Forsake thy cage,
Thy rope of sands,
Which pettie thoughts have made, and made to thee
Good cable, to enforce and draw,
And be thy law,
While thou didst wink and wouldst not see.
Away; take heed:
I will abroad.
Call in thy deaths head there: tie up thy fears.
He that forbears
To suit and serve his need,
Deserves his load.
But as I rav'd and grew more fierce and wilde
At every word,
Me thoughts I heard one calling, *Childe*:
And I reply'd, *My Lord*.

George Herbert

Acknowledgements

I thank my advisor, Mark Wise, for teaching me quantum field theory, for his frequent amusing jokes, and especially for saving projects which seemed to be doomed. I thank him for showing me what it really means to do physics, for sharing his ideas with me and for patiently answering my many questions. I also thank Mark for educating my taste in Chateauneuf du Pape.

I thank Martin Savage for teaching me that nuclei are every bit as interesting as the high energy frontier. Martin taught me a useful skill—that is, how to complete papers, and I think it's fair to say this thesis would not exist if I'd never figured that part out. I also thank him for many memorable and informative conversations.

I thank Michael Ramsey-Musolf for his counsel, collaboration, and support over the last few years. I thank him for serving on my defense and candidacy committees.

I thank John Preskill for serving on my defense and candidacy committees, Brad Filippone for serving on my defense committee, and Robert McKeown for serving on my candidacy committee.

I thank Jiunn-Wei Chen and Andre Walker-Loud for an especially fruitful collaboration and for their friendship.

I thank Alejandro Jenkins for collaboration but mainly for many bad conversations in dubious bars. I thank him for continued patience as my time has been absorbed by the completion of this thesis. I claim that, contrary to suggestions in his thesis, it is he who is the real quack. Despite all of these issues, I nevertheless learned a great deal from Alejandro, and I thank him for his sharing his wit, and his knowledge, and also for his friendship.

I thank my collaborators Ben Grinstein and Ruth van de Water, who both taught me me a great deal of useful physics.

I thank current and former members of my group, Lotty Ackermann, Christian Bauer, Vincenzo Cirigliano, Matt Dorsten, Rebecca Erwin, Misha Gorshteyn, Michael Graesser,

Moira Gresham, Jennifer Kile, Christopher Lee, Keith Lee, Sonny Mantry, Stefano Profumo, Michael Salem, Sean Tulin, Peng Wang, and Margaret Wessling. I am especially grateful to Michael Graesser, Chris Lee, Sonny Mantry and Michael Salem for helping me out with various aspects of my work over the last few years. But most of all, I thank Lotty for being such a tolerant office mate for several years now.

I thank Jie Yang, who has had the misfortune of teaching with me in my last terms at Caltech, for cheerfully bearing more than her fair share of the teaching load.

I thank Kris Sigurdson for many memorable times in my early years in Caltech. I fondly remember many trips to the cinema, evenings in bars, and various board games enjoyed in his company; the occasion when Kris upstaged the President of Caltech in the Athenaeum is especially memorable. I thank him, too, for advice on how to make progress in academia.

I thank Robert Hodyss, Tristan McLoughlin, Paul O'Gorman, and Christophe Basset for providing excellent company on a great many occasions, without which it would have been difficult to keep at my work when the challenges seemed too great.

I thank my apartment mates Jonathan Pritchard, Asa Hopkins, and Ben Toner for not complaining about my antisocial habits too loudly.

I thank my friends Igor Bargatin, Michael Boyle, Paul Cook, Patrick Dondl, Michael Edgar, Jeff Fingler, Lisa Goggin, Rosie Jones, Ramon van Handel, Hannes Helgason, Vala Hjörleifsdóttir, Ilya Mandel, Tony Miller, Carlos Mochon, Paige Randall, Nikoo Saber, Paul Skerritt, Graeme Smith, Tristan Smith, Ian Swanson, Tasos Vayonakis, Ketan Vyas and Daniel Wagenaar for many good times.

I thank Brega Howley for organizing an excellent Christmas dinner every year, and especially for always making sure to choose a date which suited me.

I thank my family: my mother, Jane, Tim, Eoin, Lise, Tadhg, Hilda, Eva, and Sadhbh for putting up with my long absences. I particularly thank Tadhg for awakening my interest in science when I was small.

I especially thank Árdís Elíasdóttir for all her help and support over the last several years.

Abstract

Quantum field theory is by now a mature field. Nevertheless, certain physical phenomena remain difficult to understand. This occurs in some cases because well-established quantum field theories are strongly coupled and therefore difficult to solve; in other cases, our current understanding of quantum field theory seems to be inadequate. In this thesis, we will discuss various modifications of quantum field theory which can help to alleviate certain of these problems, either in their own right or as a component of a greater computational scheme. The modified theories we will consider all include unusual signs in some aspect of the theory. We will also discuss limitations on what we might expect to see in experiments, imposed by sign constraints in the customary formulation of quantum field theory.

Contents

List of Figures

List of Tables

Chapter 1

Introduction

The standard model of particle physics describes a wide variety of phenomena. In this thesis, we will examine what the standard model has to teach us about certain topics of current research interest. The topics we will examine will be disparate, but one thing which will emerge from our discussion is the utility of modifying quantum field theory to allow for unusual signs.

The thesis could be divided into two broad sections. In the first section, we will devote our attention to QCD applied to the understanding of nuclei. QCD is a very well established theory, and is known to describe the behaviour of quarks at energies greater than the QCD scale accurately. At lower energies, the theory becomes strongly coupled and consequently perturbation theory breaks down. Thus, it becomes difficult to say anything quantitative about the dynamics of the theory. Nevertheless, there are a variety of tools at our disposal. The technique of effective field theory has been very fruitful in allowing a quantitative understanding of the interactions of the light mesons and baryons, for example. But a detailed understanding of nuclei and their properties eludes us. The best tool at our disposal in this area is known as lattice QCD. One begins by discretizing a finite volume of spacetime. The variables of the quantum field—the quarks and the gluons—are now associated with the lattice points of the spacetime, or with the links between these lattice points. In particular,

this discretization results in a finite number of degrees of freedom. Consequently, some of the properties of the quantum field theory can be calculated using computers.

Unfortunately, lattice QCD computations are very difficult. Large amounts of supercomputer time are required to compute physically interesting quantities accurately. At the current level of development of the subject, it is impossible to simulate QCD using the known physical values of the quark masses—larger quark masses must be used in order to allow the simulation to complete in a reasonable period of time. This circumstance requires us to understand how physical quantities depend on quark masses. Effective field theory, in particular chiral perturbation theory, provides such a tool. The combination of lattice data, computed at various unphysical quark masses, and analytic formulae computed in chiral perturbation theory, have recently allowed us to quantitatively understand several interesting properties of the simplest nuclear systems; for example, the neutron-proton mass difference due to strong isospin violation [1], and hyperon-nucleon scattering [2].

In the previous paragraph, we simplified slightly. It is not enough to simply compute formulae in the usual continuum chiral perturbation theory because lattice simulations include various unphysical effects not present in the continuum. For example, the finite size of the lattice spacing has important effects. In addition, lattice simulations are typically performed using different masses for quarks which appear in loops ("sea quarks") and for quarks which are parts of in or out states ("valence quarks.") This procedure, known as partial quenching, results in a violation of unitarity in lattice simulations and has considerable practical consequences. The version of chiral perturbation theory used to describe lattice simulations incorporates this lack of unitarity by violating the spin-statistics theorem. Anticommuting scalars are present in the theory. The extra sign coming from closed loops of these unphysical scalars allows them to cancel loops of ordinary scalars associated

with valence mesons. Additional mesonic fields are then included in the theory to act as mesons composed of sea quarks. These sea-sea mesons can be taken to have masses larger than valence-valence mesons, reproducing the loop structure of partially quenched lattice simulations. This well-known technique has been extensively discussed in the literature (see, for example, Refs. [3, 4, 5, 6, 7, 8]). In the first three chapters of this thesis, we will discuss the neutron electric dipole moment, pion scattering, and then, more generally, meson scattering, in partially quenched chiral perturbation theory and its extensions. The results of the computations are being used in conjunction with lattice computations to deepen our knowledge of these physical quantities and processes.

The second broad section of this thesis deals with extensions of the standard model, and constraints on such speculative physics. We open with a brief discussion of the Higgs sector of the standard model. We describe the simplest extension of the Higgs sector and some of the consequences of this extension for physics at the LHC. Next, we turn to the topic of sign constraints on operators in any effective field theory. Based on our customary understanding of quantum field theory, one can prove quite generally that certain signs of Wilson coefficients of operators in effective Lagrangians must have a definite sign [9]. We describe briefly an intuitive picture of the underlying physics which leads to these sign constraints. In the next chapter, we show using a lattice regulator how an attempt to induce an unusual sign in a quantum field theory via a loop correction [10] must depend on the regulator used.

In the final two chapters of the thesis, we turn to a different topic — namely, the hierarchy problem in the standard model. We describe a speculative solution to the hierarchy problem, which can be understood as an explicit violation of the sign constraints we usually expect. The ideas of these chapters are based on work of Lee and Wick [11, 12] who showed

how one can make sense of this class of quantum field theories. In Chapter 8, we extend the standard model to include new Lee-Wick degrees of freedom which have the effect of canceling large corrections to the Higgs mass occurring in loops.[1] In Chapter 9, we show that very heavy right-handed neutrinos can be coupled to the theory without destabilizing the Higgs mass. These heavy neutrinos, at low energy, induce small masses for the left-handed neutrinos of the standard model, as we observe. Lee-Wick quantum field theory, if realized physically, would constitute a violation of several of our basic physical principles; but nevertheless, it appears to be self-consistent and parameters can be chosen which allow it to pass current experimental tests. The theory, however, is unusual and may not be well-defined nonperturbatively. Even so, this work shows that higher dimensional operators can resolve the hierarchy problem if they are summed up to all orders.

In summary, this thesis is an attempt to demonstrate that it is interesting to consider quantum field theories which have been modified in various ways. These theories may just be computational tools, as in the case of chiral perturbation theory applied to the lattice, or they may be speculative theories of new physics, such as Lee-Wick quantum field theory. In both cases there are many interesting physical phenomena still to be explored.

The body of this thesis consists of work performed in collaboration with various physicists. The work of Chapter 2 was performed in collaboration with Martin Savage, and was previously published in Ref. [14]. Chapter 3 is the fruit of collaboration with Jiunn-Wei Chen, Ruth van de Water, and André Walker-Loud; it was previously published in Ref. [15]. Meanwhile, the research discussed in Chapter 4 was performed in conjunction with Jiunn-Wei Chen and André Walker-Loud and appeared in Ref. [16]. Chapter 5 appeared previously in Ref. [17]; the work discussed in that chapter was performed with

[1] The LHC phenomenology of this extension has recently been discussed in [13].

Michael Ramsey-Musolf and Mark B. Wise. The discussion presented in Chapter 6 has previously appeared in Ref. [18], coauthored with Alejandro Jenkins. The work of Chapter 7 has appeared in Ref. [19]. Finally, the work of Chapters 8 and 9 was performed in collaboration with Benjamín Grinstein and Mark B. Wise. Chapter 8 has appeared previously in Ref. [20].

Chapter 2

Extrapolation Formulas for Neutron EDM Calculations in Lattice QCD

2.1 Introduction

CP-violation is still a mystery, and so it seems appropriate to open the discussion of QCD in this thesis by examining a fascinating CP-violating observable: the electric dipole moment (edm) of the neutron. Current measurements of CP-violating processes in the kaon and B-meson sectors would suggest that the single phase in the CKM matrix provides a complete description. However, the baryon asymmetry of the universe cannot be described by this phase alone, and there are additional sources of CP-violation that await discovery. The recent revelation that neutrinos have non-zero masses has presented us with the possibility of CP-violation in the lepton sector. With both Dirac and Majorana type masses possible, CP-violation in the neutrino sector is likely to be far more intricate than in the quark sector. The significant number of experiments operating in, and planned to explore the neutrino sector will greatly improve our knowledge in this area in the not-so-distant future. It has been a puzzle for many years that there is the possibility of strong CP-violation arising from the θ term in the strong interaction sector, but that there is no evidence at this point in time

for such an interaction. The naive estimate for the size of observables, such as the neutron edm, induced by such an interaction is orders of magnitude larger than current experimental upper bounds, thereby placing a stringent upper bound on the coefficient of the interaction, $\overline{\theta}$. An anthropic argument that compels $\overline{\theta}$ to be small does not yet exist and so it is likely that there is an underlying mechanism, such as the Peccei-Quinn mechanism and associated axion, that eliminates this operator. With the increasingly precise experimental efforts to observe the neutron edm [21, 33], it is important to have a rigorous calculation directly from QCD.

Lattice calculations of the neutron edm [22, 23, 24, 25, 26, 27] in terms of the strong CP-violating parameter are continually evolving toward a reliable estimate that can be directly compared with experimental limits and possible future observations. The latest generation of lattice calculations respect chiral symmetry, and lattice spacing effects have been relegated to $\mathcal{O}(a^2)$. However, the calculations are performed in modest finite volumes and at quark masses that are larger than those of nature. In this chapter we explore the impact of finite volume on such calculations and also examine the quark mass dependence of partially-quenched calculations.

The QCD Lagrange density in the presence of the CP-violating θ-term is

$$\mathcal{L} = \overline{q} i \not{D} q - \overline{q}_L m_q q_R - \overline{q}_R m_q^\dagger q_L - \frac{1}{4} G^{(A)\mu\nu} G^{(A)}_{\mu\nu} + \theta \frac{g^2}{32\pi^2} G^{(A)}_{\mu\nu} \tilde{G}^{(A)\mu\nu}, \tag{2.1}$$

where $\tilde{G}^{(A)\mu\nu} = \frac{1}{2}\varepsilon^{\mu\nu\alpha\beta} G^{(A)}_{\alpha\beta}$, $\varepsilon^{0123} = +1$, and where $q = (u, d)^T$ for two-flavor QCD. Chiral redefinitions of the quark fields modify the coefficient of the $G\tilde{G}$ operator through the strong anomaly, and as a consequence it is the quantity $\overline{\theta} = \theta - \arg(\det(m_q))$ that has physical meaning. For our purposes it is convenient to start with a Lagrange density where m_q is

real and diagonal, and θ in eq. (2.1) is equal to $\overline{\theta}$. One can then remove the $G\tilde{G}$ operator by a chiral transformation, $q_{jR} \to e^{i\phi_j/2} q_{jR}$, and $q_{jL} \to e^{-i\phi_j/2} q_{jL}$ subject to the constraint that $\overline{\theta} = -\sum \phi_j$. Under this transformation the elements of the quark mass matrix become $m_j \to m_j e^{i\phi_j}$.

The low-energy effective field theory (EFT) describing the behavior of the pseudo-Goldstone bosons associated with the breaking of chiral symmetry is, at leading order,

$$\mathcal{L} \;=\; \frac{f^2}{8}\mathrm{Tr}\left[\, D^\mu \Sigma \; D_\mu \Sigma^\dagger \,\right] \;+\; \lambda \; \frac{f^2}{4} \; \mathrm{Tr}\left[\, m_q \Sigma^\dagger \;+\; m_q^\dagger \Sigma \,\right] \quad , \tag{2.2}$$

where $f \sim 132$ MeV is the pion decay constant, the covariant derivative describing the coupling of the pions to the electromagnetic field $\mathcal{A}_\mu$ is $D_\mu \Sigma = \partial_\mu \Sigma + ie[Q, \Sigma]\mathcal{A}_\mu$ with $e > 0$, and $\Sigma \to L \Sigma R^\dagger$ under chiral transformations,

$$\Sigma \;=\; e^{\frac{2iM}{f}} \quad , \quad M \;=\; \begin{pmatrix} \pi^0/\sqrt{2} & \pi^+ \\ \pi^- & -\pi^0/\sqrt{2} \end{pmatrix} \quad . \tag{2.3}$$

We are restricting ourselves to the two-flavor case, but the arguments are general. In order for the pion field in eq. (2.3) to be a fluctuation about the true strong interaction ground state, the phases ϕ_j are constrained so that in the expansion of eq. (2.2), terms linear in the pion field are absent. The two constraints on the phases lead to the well-known relations

$$\phi_u \;=\; -\frac{\overline{\theta}\; m_d}{m_u + m_d} \quad , \quad \phi_d \;=\; -\frac{\overline{\theta}\; m_u}{m_u + m_d} \quad , \tag{2.4}$$

where we have used the fact that $\overline{\theta} \ll 1$.

2.2 Strong CP-Violation in Chiral Perturbation Theory

At leading order in the heavy baryon expansion, the nucleon dynamics are described by a Lagrange density of the form

$$\mathcal{L} \;=\; \overline{N}\; iv\cdot D N \;+\; 2g_A \overline{N}\; S^\mu A_\mu\; N \quad , \tag{2.5}$$

where v_μ is the nucleon four-velocity and S_μ is the covariant spin operator. The chiral covariant derivative is given in terms of the meson vector field $D_\mu N = \partial_\mu N + V_\mu N$, where $V_\mu = \frac{1}{2}\left(\xi^\dagger \partial_\mu \xi + \xi \partial_\mu \xi^\dagger\right)$. The field ξ is related to the Σ-field in eq.(2.3) by $\Sigma = \xi^2$, and $\xi \to L\xi U^\dagger = U\xi R^\dagger$ under chiral transformations. The leading order interaction between nucleons and the pions is characterized by the axial coupling constant $g_A \sim 1.26$ in eq. (2.5), where $A_\mu = \frac{i}{2}\left(\xi \partial_\mu \xi^\dagger - \xi^\dagger \partial_\mu \xi\right)$. The light quark masses contribute to the dynamics of nucleons through the Lagrange density

$$\mathcal{L}_m \;=\; -\,2\alpha\; \overline{N}\; m_{q\xi+}\; N \;-2\;\sigma\; \overline{N}\; N\; \mathrm{Tr}\left(\; m_{q\xi+}\;\right) \quad , \tag{2.6}$$

where $m_{q\xi+} = \frac{1}{2}\left(\xi^\dagger m_q \xi^\dagger + \xi m_q^\dagger \xi\;\right)$, $m_q \to L m_q R^\dagger$, and $m_{q\xi+} \to U m_{q\xi+} U^\dagger$. The quantities α and σ are constants that must be determined experimentally. Upon removing the $G\tilde{G}$ term by a chiral transformation, the mass matrix becomes $m_q = \mathrm{diag}\left(m_u e^{i\phi_u}, m_d e^{i\phi_d}\right)$, where $\phi_{u,d}$ are given in eq. (2.4). Neglecting electromagnetic contributions to the nucleon mass splitting, and using light quark masses of $m_u = 5$ MeV and $m_d = 10$ MeV, we find

that [1]

$$2\alpha = \frac{M_p - M_n}{m_u - m_d} \sim 0.26 \quad . \tag{2.9}$$

The sigma term is defined to be

$$\sigma_N = \sum_{u,d} m_q \frac{\partial M_N}{\partial m_q} \quad , \tag{2.10}$$

where M_N is the nucleon mass in the isospin limit $m_u, m_d \to \overline{m}$, and is related to the quantities α and σ by

$$\sigma_N = 2(\alpha + 2\sigma)\overline{m}. \tag{2.11}$$

The value of σ_N is somewhat uncertain, with values ranging between 45 ± 8 MeV [28] and 64 ± 7 MeV [29]. Partially-quenched lattice computations are currently underway to evaluate both α and σ_N.

Expanding out the interaction in eq. (2.6) to linear order in the pion field gives rise to the CP-violating, momentum independent $NN\pi$ vertex

$$\mathcal{L} = -\frac{4\ \alpha\ \overline{\theta}}{f}\ \frac{m_u\ m_d}{m_u + m_d}\ \overline{N} \begin{pmatrix} \pi^0/\sqrt{2} & \pi^+ \\ \pi^- & -\pi^0/\sqrt{2} \end{pmatrix} N + \ldots \quad . \tag{2.12}$$

It is well known that a single insertion of this interaction into a one-loop diagram gives rise

[1] The standard analysis usually invokes the approximate flavor $SU(3)$ symmetry, e.g. Ref. [32]. The light quark contribution to the baryon masses arises from

$$\mathcal{L}_m = -b_0\ \mathrm{Tr}\left[\ m_{q\xi+}\ \right] \mathrm{Tr}\left[\ \overline{B}\ B\ \right] - b_1\ \mathrm{Tr}\left[\ \overline{B}\ m_{q\xi+}\ B\right] - b_2\ \mathrm{Tr}\left[\ \overline{B}\ B\ m_{q\xi+}\ \right] \quad , \tag{2.7}$$

from which one finds that, neglecting electromagnetic corrections,

$$b_1 = \frac{M_{\Xi^0} - M_{\Sigma^+}}{m_s - m_u} \sim 1.1 \ , \ b_2 = \frac{M_p - M_{\Sigma^+}}{m_s - m_d} \sim -2.3 \quad , \tag{2.8}$$

where we have used $m_s \sim 120$ MeV.

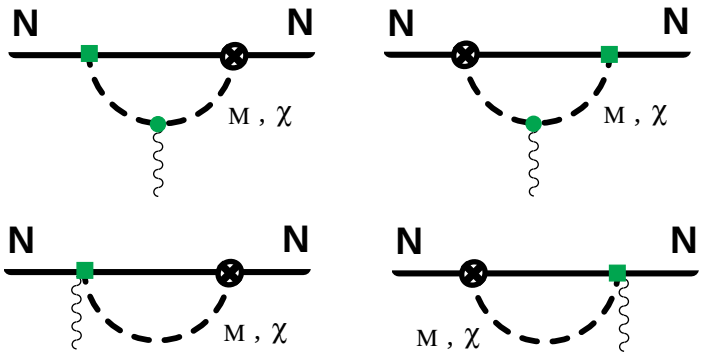

Figure 2.1: The one-loop diagrams that contribute to the neutron edm in chiral perturbation theory. In QCD only πs participate in the loop diagram, while in partially-quenched QCD there are contributions from the bosonic mesons, M, and the fermionic mesons, χ. The crossed circle denotes an insertion of the CP-violating vertex in eq. (2.12), the square denotes an insertion of the strong πNN or $\pi\gamma$NN interaction from eq. (2.5) with derivatives promoted to covariant derivatives, and the small circle denotes an electromagnetic interaction with the meson from eq. (2.2).

to an electric dipole moment (edm) of the nucleon [30] [2].

The electric dipole moment of the neutron, d_n, is defined by the Lagrange density describing the interaction between a neutron and an external electric field,

$$\mathcal{L} \;=\; d_n \, \overline{n} \, \boldsymbol{\sigma} \cdot \mathbf{E} \, n \quad , \tag{2.13}$$

where $\boldsymbol{\sigma}$ are the Pauli spin matrices, and $\mathbf{E}$ is an external electric field. A calculation of the one-loop diagrams shown in Fig. 2.1 leads to

$$d_n = \frac{g_A \alpha \; e \; \overline{\theta}}{2\pi^2 f^2} \frac{m_u m_d}{m_u + m_d} \log\left(\frac{m_\pi^2}{\mu^2}\right) + \overline{\theta} \frac{m_u m_d}{m_u + m_d} \; \frac{e}{\Lambda_\chi^2} c(\mu). \tag{2.14}$$

We have only kept the logarithmic contribution from the loop diagram, which depends upon the renormalization scale μ. This scale dependence is exactly compensated by the contributions from local counterterms, which we have combined into $c(\mu)$. There are ten

[2] This set of diagrams also dominates the nucleon edm form-factor, as recently computed in Ref. [31].

local counterterms that contribute to the nucleon edm, as presented in Ref. [32], and setting $\mu \sim \Lambda_\chi$ we anticipate that $c(\Lambda_\chi) \sim 1$, where $\Lambda_\chi \sim 1$ GeV is the scale of chiral symmetry breaking.

Numerically, using the value of α in eq. (2.9), we find the one-loop contribution to be

$$d_n \quad \sim \quad -1.2 \times 10^{-16}\, \overline{\theta} \quad \text{e cm} \quad , \tag{2.15}$$

which is consistent with previous estimates [30, 32] of the one-loop diagram[3]. The current experimental upper limit is $|d_n| < 6.3 \times 10^{-26}$ e cm, from which one concludes that $|\overline{\theta}| \lesssim 5 \times 10^{-10}$.

2.3 Neutron EDM at Finite Volume

Lattice calculations of the neutron edm are performed on finite lattices, and therefore one must consider finite volume corrections in translating the lattice results to physical predictions. For large enough lattices, of course, these finite volume effects will be exponentially small [36, 37, 52]. There has been a fair amount of work on finite volume corrections to quantities calculated in lattice QCD [34, 35, 37, 38, 39, 40, 41, 5, 42, 43, 44, 45, 46, 47, 48, 49, 50, 51, 52, 53, 54, 55], but it is only recently that the properties of baryons, and in particular the nucleon, have been considered [52, 53, 54, 55].

In the calculations that follow, we will assume that the time direction of the lattice is infinite. Clearly, this can only be an approximation, but in most simulations, the time direction is considerably larger than the spatial directions, usually by more than a factor of two. By assuming that it is infinitely long, we are able to analytically perform the integral

[3] In Refs. [30, 32] the electronic charge e is negative.

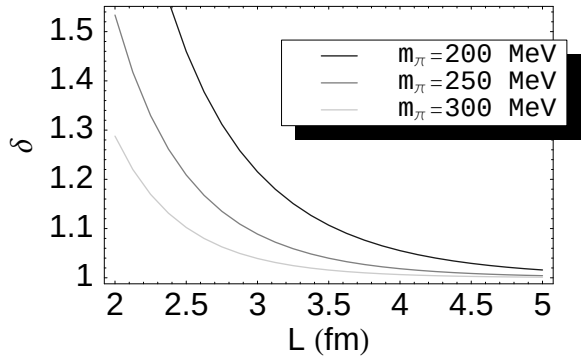

Figure 2.2: The ratio, $\delta = d_n^{(L)}/d_n^{(\infty)}$, of the neutron edm at finite volume to its value at infinite volume as a function of spatial lattice size L, for $c(\mu) = 0$.

over energy in the loop diagrams that contribute to the observable of interest, leaving sums over the allowed three-momentum modes on the lattice. Details of this procedure can be found in Refs. [52, 53], and we will not elaborate further here. By computing the one-loop diagrams in Fig. 2.1 in a finite spatial volume for which the spatial dimension, L, is much greater than the pion Compton wavelength, $m_\pi L \gg 1$, and for which the power counting rules are those of the p-regime at infinite volume, we find that

$$d_n^{(L)} \;=\; d_n^{(\infty)} \;-\; \frac{g_A\;\alpha\;e\;\overline{\theta}}{\pi^2 f^2}\frac{m_u\;m_d}{m_u+m_d}\sum_{\mathbf{n}\neq\mathbf{0}} K_0\left(m_\pi L|\mathbf{n}|\right) \quad , \tag{2.16}$$

where $d_n^{(L)}$ is the neutron edm at finite volume, and $d_n^{(\infty)}$ is its value at infinite volume. $K_0(x)$ is a modified Bessel function. In Fig. 2.2 we show the ratio $d_n^{(L)}/d_n^{(\infty)}$ for $c(\mu) = 0$, as an example. The finite volume corrections are found to be quite large, primarily due to the fact that the leading order contribution to the edm is at the one-loop level, and not from a lower dimension operator. In the case of the nucleon properties previously considered [52, 53], such as the nucleon mass, magnetic moment, and matrix elements of the axial current, the loop contributions are subleading, and hence the finite volume corrections are subleading in the effective field theory.

As one moves into smaller volumes, where $m_\pi L \lesssim 1$, the p-regime power counting is no longer applicable, and we move into the ϵ'-regime [56]. In this regime, the spatial zero-modes are enhanced relative to the non-zero-modes, and a power counting in terms of the small parameter $\epsilon' = m_\pi L$ is appropriate. For the neutron edm calculation, the same one-loop diagram shown in Fig. 2.1 makes the leading contribution in $\epsilon' = m_\pi L$, and the neutron edm is found to be

$$d_n^{(L)} = \frac{-2\ g_A\ \alpha\ e\ \overline{\theta}}{f^2\ m_\pi^3\ L^3} \frac{m_u\ m_d}{m_u + m_d} + \cdots \quad , \tag{2.17}$$

where the ellipses denote terms higher order in the ϵ'-expansion. The classic exponential behavior of the p-regime becomes power law, $1/L^3$, behavior as the spatial volume decreases.

2.4 Neutron EDM in Partially-Quenched QCD

While partially-quenched QCD (PQQCD) [3, 4, 5, 6, 57, 7, 58] is not a theory that describes nature, it is a theory that can be used to describe unphysical lattice calculations, and allows the direct extraction of QCD observables via an extrapolation in quark-masses. In calculating quantities in lattice QCD, the quark masses used in the generation of gauge field configurations does not have to be the same as the quark masses of the propagators computed on those configurations. The reason why this is a useful concept is that the computer time required to generate a dynamical configuration grows rapidly as the quark mass is reduced, while the time to compute a propagator grows more slowly. Currently, lattice calculations cannot be performed at the physical quark masses, but we wish to be as "close as possible" to the physical values in order to minimize the impact of quark mass extrapolations.

The Lagrange density describing the quark sector of PQQCD is

$$\mathcal{L} = \sum_{k,n=u,d,\tilde{u},\tilde{d},j,l} \overline{Q}^k \left[i\not{D} - m_Q \right]_k^n Q_n - \frac{1}{4} G^{(A)\mu\nu} G^{(A)}_{\mu\nu} + \theta \frac{g^2}{32\pi^2} G^{(A)}_{\mu\nu} \tilde{G}^{(A)\mu\nu} \quad , \tag{2.18}$$

where the left- and right-handed valence, sea, and ghost quarks are combined into column vectors

$$Q_L \;=\; \left(u, d, j, l, \tilde{u}, \tilde{d}\right)^T_L \quad , \quad Q_R \;=\; \left(u, d, j, l, \tilde{u}, \tilde{d}\right)^T_R \quad . \tag{2.19}$$

The objects η_k correspond to the parity of the component of Q_k, with $\eta_k = +1$ for $k = 1, 2, 3, 4$, and $\eta_k = 0$ for $k = 5, 6$. The $Q_{L,R}$ in eq. (2.19) transform in the fundamental representation of $SU(4|2)_{L,R}$, respectively. The ground floor of Q_L transforms as a $(\mathbf{4}, \mathbf{1})$ of $SU(4)_{qL} \otimes SU(2)_{\tilde{q}L}$ while the first floor transforms as $(\mathbf{1}, \mathbf{2})$, and the right handed field Q_R transforms analogously. In the absence of quark masses, $m_Q = 0$, the Lagrange density in eq. (2.18) has a graded symmetry $U(4|2)_L \otimes U(4|2)_R$, where the left- and right-handed quark fields transform as $Q_L \rightarrow U_L Q_L$ and $Q_R \rightarrow U_R Q_R$, respectively. The strong anomaly reduces the symmetry of the theory, which can be taken to be $SU(4|2)_L \otimes SU(4|2)_R \otimes U(1)_V$ [58]. It is assumed that this symmetry is spontaneously broken $SU(4|2)_L \otimes SU(4|2)_R \otimes U(1)_V \rightarrow SU(4|2)_V \otimes U(1)_V$ so that an identification with QCD can be made. The mass matrix, m_Q, has entries $m_Q = \mathrm{diag}(m_u, m_d, m_j, m_l, m_u, m_d)$, (i.e., the valence quarks and ghosts are degenerate) so that the contribution to the determinant in the path integral from the valence quarks and ghosts exactly cancel, leaving the contribution from the sea quarks alone. This makes clear why the partially-quenched theory describes lattice calculations with sea quarks and valence quarks of differing mass. The details concerning the construction of partially-quenched chiral perturbation theory

(PQχPT) are well known and can be found in several works, e.g. Ref. [8, 59]. The quantity that has "physical" impact for lattice calculations of strong CP-violating quantities is[4] $\overline{\theta} = \theta - \arg\left(\mathrm{sdet}\left(m_Q\right)\right)$.

The strong interaction dynamics of the pseudo-Goldstone bosons are described at leading order (LO) in PQχPT by a Lagrange density of the form,

$$\mathcal{L} = \frac{f^2}{8}\mathrm{str}\left[\partial^\mu \Sigma^\dagger \partial_\mu \Sigma\right] + \lambda\frac{f^2}{4}\mathrm{str}\left[m_Q\Sigma^\dagger + m_Q^\dagger\Sigma\right] + \alpha_\Phi \partial^\mu\Phi_0\partial_\mu\Phi_0 - \ m_0^2\Phi_0^2, \tag{2.21}$$

where α_Φ and m_0 are quantities that do not vanish in the chiral limit. In order to simply project out the singlet of the graded group one takes the limit $m_0 \to \infty$ [58]. The meson field is incorporated in Σ via

$$\Sigma \ = \ \exp\left(\frac{2\ i\ \Phi}{f}\right) \ = \ \xi^2 \quad , \quad \Phi \ = \ \begin{pmatrix} M & \chi^\dagger \\ \chi & \tilde{M} \end{pmatrix} \quad , \tag{2.22}$$

where M and $\tilde{M}$ are matrices containing bosonic mesons while χ and $\chi^\dagger$ are matrices containing fermionic mesons, with

$$M = \begin{pmatrix} \eta_u & \pi^+ & J^0 & L^+ \\ \pi^- & \eta_d & J^- & L^0 \\ \overline{J}^0 & J^+ & \eta_j & Y_{jl}^+ \\ L^- & \overline{L}^0 & Y_{jl}^- & \eta_l \end{pmatrix}, \tilde{M} = \begin{pmatrix} \tilde{\eta}_u & \tilde{\pi}^+ \\ \tilde{\pi}^- & \tilde{\eta}_d \end{pmatrix}, \chi = \begin{pmatrix} \chi_{\eta_u} & \chi_{\pi^+} & \chi_{J^0} & \chi_{L^+} \\ \chi_{\pi^-} & \chi_{\eta_d} & \chi_{J^-} & \chi_{L^0} \end{pmatrix}, \tag{2.23}$$

where the upper 2×2 block of M is the usual triplet plus singlet of pseudo-scalar mesons

[4]
$$\mathrm{sdet}\begin{pmatrix} A & B \\ C & D \end{pmatrix} \ = \ \frac{\det\left(A - BD^{-1}C\right)}{\det\left(D\right)} \quad . \tag{2.20}$$

while the remaining entries correspond to mesons formed from the sea quarks. The convention we use corresponds to $f \sim 132$ MeV, and the charge assignments have been made using an electromagnetic charge matrix of $\mathcal{Q}^{(PQ)} = \frac{1}{3}\mathrm{diag}\,(2,-1,2,-1,2,-1)$. For the calculations we will be performing, the flavor singlet pseudo-Goldstone boson does not contribute, and so we do not discuss it and its associated hairpin interactions.

The free Lagrange density describing the interactions of the nucleon and its superpartners which are embedded in the **70** dimensional irreducible representation of $SU(4|2)$ $\mathcal{B}_{ijk}$ is, at LO in the heavy baryon expansion [60, 61, 62, 63],

$$\mathcal{L} = i\left(\overline{\mathcal{B}} v\cdot\mathcal{D}\mathcal{B}\right) - 2\alpha_M^{(\mathrm{PQ})}\left(\overline{\mathcal{B}}\mathcal{B}\mathcal{M}_+\right) - 2\beta_M^{(\mathrm{PQ})}\left(\overline{\mathcal{B}}\mathcal{M}_+\mathcal{B}\right) - 2\sigma_M^{(\mathrm{PQ})}\left(\overline{\mathcal{B}}\mathcal{B}\right)\ \mathrm{str}\left(\mathcal{M}_+\right), \quad (2.24)$$

where $\mathcal{M}_+ = \frac{1}{2}\left(\xi^\dagger m_Q \xi^\dagger + \xi m_Q^\dagger \xi\right)$. The brackets (...) denote contraction of Lorentz and flavor indices as defined in Ref. [7].

The Lagrange density describing the interactions of the **70** with the pseudo-Goldstone bosons at LO in the chiral expansion is [7],

$$\mathcal{L} \;=\; 2\rho\ \left(\overline{\mathcal{B}} S^\mu \mathcal{B} A_\mu\right)\ +\ 2\beta\ \left(\overline{\mathcal{B}} S^\mu A_\mu \mathcal{B}\right)\ , \quad (2.25)$$

where S^μ is the covariant spin vector [60, 61, 62]. Restricting ourselves to the valence sector, we can compare eq. (2.25) with the LO interaction Lagrange density of QCD,

$$\mathcal{L} \;=\; 2g_A\ \overline{N} S^\mu A_\mu N\ +\ g_1 \overline{N} S^\mu N\ \mathrm{tr}\left[\ A_\mu\ \right]\ , \quad (2.26)$$

and find that at tree level

$$\rho \;=\; \frac{4}{3}g_A \;+\; \frac{1}{3}g_1 \quad , \quad \beta \;=\; \frac{2}{3}g_1 - \frac{1}{3}g_A \quad . \tag{2.27}$$

The contribution to the strong anomaly from the valence quarks is exactly cancelled by the contribution from the ghosts. Therefore, chiral transformations of the sea quarks alone remove the θ-term from the Lagrange density in eq. (2.18). Upon a chiral transformation of the valence quark, sea quark, and ghost fields, the quark super-mass matrix becomes $m_Q = \mathrm{diag}(m_u e^{i\phi_u}, m_d e^{i\phi_d}, m_j e^{i\phi_j}, m_l e^{i\phi_l}, m_u e^{i\phi_u}, m_d e^{i\phi_d})$ subject to the constraint that $\overline{\theta} = -\sum\,(-)^{\eta_k+1}\,\phi_k$. The vacuum stability condition for small $\overline{\theta}$ further provides the constraint $m_u\phi_u = m_d\phi_d = m_j\phi_j = m_l\phi_l$. Therefore, we have

$$\phi_j = -\frac{\overline{\theta}m_l}{m_j+m_l}, \;\; \phi_l = -\frac{\overline{\theta}m_j}{m_j+m_l}, \;\; \phi_u = -\frac{\overline{\theta}m_j m_l}{m_j+m_l}\frac{1}{m_u}, \;\; \phi_d = -\frac{\overline{\theta}m_j m_l}{m_j+m_l}\frac{1}{m_d}. \tag{2.28}$$

By using this phase-rotated mass matrix in the Lagrange density of eq. (2.24), one induces a CP-violating interaction between the pseudo-Goldstone bosons and the baryons of the partially-quenched theory, in precisely the same way as in QCD. Further, this vertex generates the leading contribution to the neutron edm through the one-loop diagrams analogous to those in Fig. 2.1. One further slight complication that can be considered is that the electric charge matrix in the partially-quenched theory is not specified by nature; all that is required is that one reproduces QCD in the limit that the sea and valence quarks become degenerate[5] [64, 65, 8, 59]. In our computations, we use an electric charge matrix of the form $\mathcal{Q}^{(\mathcal{PQ})} = \mathrm{diag}\left(\frac{2}{3}, -\frac{1}{3}, q_j, q_l, q_j, q_l\right)$.

Working in the isospin limit where $m_j = m_l = m_{\mathrm{sea}}$, and defining $q_{jl} = q_j + q_l$, we find

[5] Even this constraint is excessive. It is sufficient to determine matrix elements of operators transforming in the singlet and adjoint representations of the graded group.

that the leading order contribution to the neutron edm is

$$\begin{aligned} d_n^{(PQ)} &= \frac{e\ \overline{\theta}\ m_{\rm sea}}{4\pi^2 f^2}\left[\ F_\pi\ \log\left(\frac{m_\pi^2}{\mu^2}\right)\ +\ F_J\ \log\left(\frac{m_J^2}{\mu^2}\right)\ \right] \\ &\quad + \overline{\theta}\ \frac{e}{\Lambda_\chi^2}\ \left[\ \frac{m_{\rm sea}}{2}\ c(\mu)\ +\ d\,(m_{\rm sea}-m_{\rm val})\ +\ f q_{jl}\ (m_{\rm sea}-m_{\rm val})\right]\ , \end{aligned} \tag{2.29}$$

where m_J is the mass of the Goldstone boson composed of a sea quark and a valence quark, and

$$\begin{aligned} F_\pi &= g_A\left(\frac{2\alpha_M^{(\rm PQ)}-\beta_M^{(\rm PQ)}}{3}\right) - g_A\alpha_M^{(\rm PQ)}\left(\frac{1}{3}+\frac{q_{jl}}{2}\right) + g_1\left(\frac{\beta_M^{(\rm PQ)}}{3} - \left(\frac{\alpha_M^{(\rm PQ)}+2\beta_M^{(\rm PQ)}}{4}\right)q_{jl}\right) \\ F_J &= g_A\alpha_M^{(\rm PQ)}\left(\frac{1}{3}+\frac{q_{jl}}{2}\right)\ -\ g_1\left(\frac{\beta_M^{(\rm PQ)}}{3}\ -\ \left(\frac{\alpha_M^{(\rm PQ)}+2\beta_M^{(\rm PQ)}}{4}\right)q_{jl}\right)\quad . \end{aligned} \tag{2.30}$$

As we can make the tree level identification $\alpha = (2\alpha_M^{(\rm PQ)} - \beta_M^{(\rm PQ)})/3$, the expression in eq. (2.29) reduces to the QCD result in eq. (2.14) when $m_{\rm sea} \to m_{\rm valence}$ and $m_J \to m_\pi$, since $F_\pi + F_J = g_A\alpha$. It is important to notice that the counterterm that contributes in the partially-quenched case, $c(\mu)$, is the same as in the QCD case, while the other two counterterms, d and f, make a vanishing contribution in QCD. The expression in eq. (2.29) exhibits one of the well known pathologies of the partially quenched theory. One sees that this expression behaves as $\sim m_{\rm sea}\log(m_{\rm valence})$. For a fixed sea quark mass, the one-loop contribution diverges as the valence quarks move toward the chiral limit, in contrast to the case of QCD where the diagram diminishes as $\sim m_\pi^2\log\left(m_\pi^2\right)$.

The finite volume corrections resulting from a partially-quenched calculation are obviously more complicated than in QCD. In the limit where the volume is large compared to the Compton wavelength of both the valence and sea mesons, one can use the power

counting of the p-regime to find that

$$d_n^{(PQ)(L)} \;=\; d_n^{(PQ)(\infty)} \;-\; \frac{e\;\overline{\theta}\;m_{\rm sea}}{2\pi^2 f^2}\,[\;F_J\;S_J\;+\;F_\pi\;S_\pi]$$
$$S_\pi \;=\; \sum_{\mathbf{n}\neq\mathbf{0}} K_0\left(m_\pi L|\mathbf{n}|\right) \quad , \quad S_J \;=\; \sum_{\mathbf{n}\neq\mathbf{0}} K_0\left(m_J L|\mathbf{n}|\right) \quad . \tag{2.31}$$

One can imagine performing a calculation of the neutron edm for lattice parameters such that $m_\pi L \ll 1$ but $m_J L \gtrsim 1$. Parametrically, we could arrange for $m_\pi/\Lambda_\chi \sim \epsilon'^2$, $\Lambda_\chi L \sim 1/\epsilon'$, and $m_J/\Lambda_\chi \gtrsim \epsilon'$. In such a scenario, the finite volume correction would become

$$d_n^{(PQ)(L)} = -\frac{e\;\overline{\theta}\;m_{\rm sea}}{f^2\;m_\pi^3\;L^3}\;F_\pi\;+\cdots\quad . \tag{2.32}$$

This somewhat bizarre computational set-up allows one to quite dramatically separate the contributions to the neutron edm, as the leading contribution results from one-loop graphs involving pions, and the contribution from mesons involving the sea quarks is suppressed. However, the sea quarks play a central role via the CP-violating pion-nucleon coupling. In the more symmetric scenario in which $m_\pi L, m_J L \lesssim 1$, the finite volume expression becomes

$$d_n^{(PQ)(L)} \;=\; -\frac{e\;\overline{\theta}\;m_{\rm sea}}{f^2\;L^3}\left[\;\frac{F_\pi}{m_\pi^3}\;+\;\frac{F_J}{m_J^3}\;\right]\;+\cdots\quad . \tag{2.33}$$

2.5 Conclusions

A non-zero electric dipole moment of the neutron would provide direct evidence for time-reversal violation in nature. It continues to be the focus of ever more precise experimental measurements, and the fact that it has not been observed at the present limits of exper-

imental resolution provides one of the more intriguing puzzles in modern physics. In this chapter we have considered how lattice QCD calculations of the neutron edm originating from the QCD θ-term, performed in a finite volume and at unphysical quark masses, are related to its value in nature. We have provided explicit formulas that allow for the extrapolation from finite volume calculations to the infinite volume limit and for the chiral extrapolation of partially-quenched calculations. In order for these formulas to be useful, lattice QCD calculations of both the light quark mass dependence of the nucleon mass, α, and the neutron edm are required. With the lattice value of α known with a given precision, the lattice determination of the neutron edm will then allow for the counterterm $c(\mu)$ to be determined. Once these constants are computed, the chiral extrapolation of the neutron edm to the physical quark masses, and to infinite volume, is possible.

Chapter 3

Ginsparg-Wilson Pions Scattering in a Sea of Staggered Quarks

3.1 Introduction

Lattice QCD can, in principle, be used to calculate precisely low-energy quantities including hadron masses, decay constants, and form factors. In practice, however, limited computing resources make it currently impossible to calculate processes with dynamical quark masses as light as those in the real world. Thus one performs simulations with quark masses that are as light as possible and then extrapolates the lattice calculations to the physical values using expressions calculated in chiral perturbation theory (χPT). This, of course, relies on the assumption that the quark masses are light enough that one is in the chiral regime and can trust χPT to be a good effective theory of QCD [66, 67].

Lattice simulations with staggered fermions [68] can at present reach significantly lighter quark masses than other fermion discretizations and have proven extremely successful in accurately reproducing experimentally measurable quantities [69, 70]. Staggered fermions, however, have the disadvantage that each quark flavor comes in four tastes. Because these species are degenerate in the continuum, one can formally remove them by taking the fourth root of the quark determinant. In practice, however, the fourth root must be taken before

the continuum limit; thus it is an open theoretical question whether or not this fourth-rooted theory becomes QCD in the continuum limit.[1] Even if one assumes the validity of the fourth-root trick, which we do in the rest of this chapter, staggered fermions have other drawbacks. On the lattice, the four tastes of each quark flavor are no longer degenerate, and this taste symmetry breaking is numerically significant in current simulations [70]. Thus one must use staggered chiral perturbation theory (SχPT), which accounts for taste-breaking discretization effects, to extrapolate correctly staggered lattice calculations to the continuum [72, 73, 74, 75]. Fits of SχPT expressions for meson masses and decay constants have been remarkably successful. Nevertheless, the large number of operators in the next-to-leading order (NLO) staggered chiral Lagrangian [75] and the complicated form of the kaon B-parameter in SχPT [76] both show that SχPT expressions for many physical quantities will contain a daunting number of undetermined fit parameters. Another practical hindrance to the use of staggered fermions as valence quarks is the construction of lattice interpolating fields. Although the construction of a staggered interpolating field is straightforward for mesons since they are spin 0 objects [77, 78], this is not in general the case for vector mesons, baryons or multi-hadron states since the lattice rotation operators mix the spin, angular momentum and taste of a given interpolating field [79, 80, 81].

The use of Ginsparg-Wilson (GW) fermions [82] evades both the practical and theoretical issues associated with staggered fermions. Because GW fermions are tasteless, one can simply construct interpolating operators with the right quantum numbers for the desired meson or baryon. Moreover, massless GW fermions possess an exact chiral symmetry on the lattice [83] which protects expressions in χPT from becoming unwieldy.[2] Unfortunately,

[1] See Ref. [71] for a recent review of staggered fermions and the fourth-root trick.

[2] In practice, the degree of chiral symmetry is limited by how well the domain-wall fermion [84, 85, 86] is realized or the overlap operator [87, 88, 89] is approximated.

simulations with dynamical GW quarks are approximately 10 to 100 times slower than those with staggered quarks [90] and thus are not presently practical for realizing light quark masses.

A practical compromise is therefore the use of GW valence quarks and staggered sea quarks. This so-called "mixed action" theory is particularly appealing because the MILC improved staggered field configurations are publicly available. Thus one only needs to calculate correlation functions on top of these background configurations, making the numerical cost comparable to that of quenched GW simulations. Several lattice calculations using domain-wall or overlap valence quarks with the MILC configurations are underway [91, 92, 93], including a determination of the isospin 2 ($I = 2$) $\pi\pi$ scattering length [94]. Although this is not the first $I = 2$ $\pi\pi$ scattering lattice simulation [95, 96, 97, 98, 99], it is the only one with pions light enough to be in the chiral regime [66, 67]. Its precision is limited, however, without the appropriate mixed action χPT expression for use in continuum and chiral extrapolation of the lattice data. With this motivation we calculate the $I = 2$ $\pi\pi$ scattering length in chiral perturbation theory for a mixed action theory with GW valence quarks and staggered sea quarks.

Mixed action chiral perturbation theory (MAχPT) was first introduced in Refs. [100, 101, 102] and was extended to include GW valence quarks on staggered sea quarks for both mesons and baryons in Refs. [103] and [104], respectively. $\pi\pi$ scattering is well understood in continuum, infinite-volume χPT [105, 106, 107, 108, 109, 110, 111], and is the simplest two-hadron process that one can study numerically with LQCD. We extend the NLO χPT calculations of Refs. [106, 107] to MAχPT. A mixed action simulation necessarily involves partially quenched QCD (PQQCD) [3, 4, 5, 6, 58, 112], in which the valence and sea quarks are treated differently. Consequently, we provide the PQχPT $\pi\pi$ scattering amplitude by

taking an appropriate limit of our MAχPT expressions. In all of our computations, we work in the isospin limit both in the sea and valence sectors.

This chapter is organized as follows. We first comment on the determination of infinite volume scattering parameters from lattice simulations in Section 3.2, focusing on the applicability of Lüscher's method [113, 114] to mixed action lattice simulations. We then review mixed action LQCD and MAχPT in Section 3.3. In Section 3.4 we calculate the $I = 2$ $\pi\pi$ scattering amplitude in MAχPT, first by reviewing $\pi\pi$ scattering in continuum $SU(2)$ χPT and then by extending to partially quenched mixed action theories with $N_f = 2$ and $N_f = 2 + 1$ sea quarks. We discuss the role of the double poles in this process [115] and parameterize the partial quenching effects in a particularly useful way for taking various interesting and important limits. Next, in Section 3.5, we present results for the pion scattering length in both 2 and $2 + 1$ flavor MAχPT. These expressions show that it is advantageous to fit to partially quenched lattice data using the lattice pion mass and pion decay constant measured on the lattice rather than the LO parameters in the chiral Lagrangian. We also give expressions for the corresponding continuum PQχPT scattering amplitudes, which do not already appear in the literature. Finally, in Section 3.6 we briefly discuss how to use our MAχPT formulae to determine the physical scattering length in QCD from mixed action lattice data, and conclude.

3.2 Determination of Scattering Parameters from Mixed Action Lattice Simulations

Lattice QCD calculations are performed in Euclidean spacetime, thereby precluding the extraction of S-matrix elements from infinite volume [116]. Lüscher, however, developed a

method to extract the scattering phase shifts of two particle scattering states in quantum field theory by studying the volume dependence of two-point correlation functions in Euclidean spacetime [113, 114]. In particular, for two particles of equal mass m in an s-wave state with zero total 3-momentum in a finite volume, the difference between the energy of the two particles and twice their rest mass is related to the s-wave scattering length:[3]

$$\Delta E_0 = -\frac{4\pi a_0}{m\mathrm{L}^3}\left[1 + c_1\frac{a_0}{\mathrm{L}} + c_2\left(\frac{a_0}{\mathrm{L}}\right)^2 + \mathcal{O}\left(\frac{1}{\mathrm{L}^3}\right)\right]. \tag{3.1}$$

In the above expression, a_0 is the scattering length (not to be confused with the lattice spacing, a), L is the length of one side of the spatially symmetric lattice, and c_1 and c_2 are known geometric coefficients.[4] Thus, even though one cannot directly calculate scattering amplitudes with lattice simulations, Eq. (3.1), which we will refer to as Lüscher's formula, allows one to determine the infinite volume scattering length. One can then use the expression for the scattering length computed in infinite volume χPT to extrapolate the lattice data to the physical quark masses.

Because Lüscher's method requires the extraction of energy levels, it relies upon the existence of a Hamiltonian for the theory being studied. This has not been demonstrated (and is likely false) for partially quenched and mixed action QCD, both of which are nonunitary. Nevertheless, one can calculate the ratio of the two-pion correlator to the square of the single-pion correlator in lattice simulations of these theories and extract the coefficient of the term which is linear in time, which becomes the energy shift in the QCD (and continuum) limit. We claim that in certain scattering channels, despite the inherent sicknesses

[3] Here we use the "particle physics" definition of the scattering length which is opposite in sign to the "nuclear physics" definition.

[4] This expression generalizes to scattering parameters of higher partial waves and non-stationary particles [113, 114, 117, 118].

of partially quenched and mixed action QCD, this quantity is still related to the infinite volume scattering length via Eq. (3.1), i.e., the volume dependence is identical to Eq. (3.1) up to exponentially suppressed corrections.[5] This is what we mean by "Lüscher's method" for nonunitary theories. We will expand upon this point in the following paragraphs.

It is well known that Lüscher's formula does not hold for many scattering channels in quenched theories because unitarity-violating diagrams give rise to enhanced finite volume effects [119]. For certain scattering channels, however, quenched χPT calculations in finite volume show that, at one-loop order, the volume dependence is identical in form to Lüscher's formula [119, 120, 121]. Chiral perturbation theory calculations additionally show that the same sicknesses that generate enhanced finite volume effects in quenched QCD also do so in partially quenched and mixed action theories [6, 58, 122, 100, 101, 123, 103, 124]. It then follows that if a given scattering channel has the same volume dependence as Eq. (3.1) in quenched QCD, the corresponding partially quenched (and mixed action) two-particle process will also obey Eq. (3.1). Correspondingly, scattering channels which have enhanced volume dependence in quenched QCD also have enhanced volume dependence in partially quenched and mixed action theories. We now proceed to discuss in some detail why Lüscher's formula does or does not hold for various $2\to2$ scattering channels.

Finite volume effects in lattice simulations come from the ability of particles to propagate over long distances and feel the finite extent of the box through boundary conditions. Generically, they are proportional either to inverse powers of L or to $\exp(-m\mathrm{L})$, but Lüscher's formula neglects exponentially suppressed corrections. Calculations of scattering processes in effective field theories at finite volume show that the power-law corrections only arise from s-channel diagrams [119, 43, 121, 123, 125]. This is because all of the intermediate

[5] Here, and in the following discussion, we restrict ourselves to a perturbative analysis.

particles can go on-shell simultaneously, and thus are most sensitive to boundary effects. Consequently, when there are no unitarity-violating effects in the s-channel diagrams for a particular scattering process, the volume dependence will be identical to Eq. (3.1), up to exponential corrections. Unitarity-violating *hairpin* propagators in s-channel diagrams, however, give rise to enhanced volume corrections because they contain double poles which are more sensitive to boundary effects [119].[6] Thus all violations of Lüscher's formula come from on-shell hairpins in the s-channel.

Let us now consider $I = 2$ $\pi\pi$ scattering in the mixed action theory. All intermediate states must have isospin 2 and $s \geq 4m^2$. If one cuts an arbitrary graph connecting the incoming and outgoing pions, there is only enough energy for two of the internal pions to be on-shell, and, by conservation of isospin, they must be valence π^+s.[7] Thus no hairpin diagrams ever go on-shell in the s-channel, and the structure of the integrals which contribute to the power-law volume dependence in the partially quenched and mixed action theories is identical to that in continuum χPT. This insures that Lüscher's formula is correctly reproduced to all orders in 1/L with the correct ratios between coefficients of the various terms. Moreover, this holds to all orders in χPT, PQχPT, MAχPT, and even quenched χPT. The sicknesses of the partially quenched and mixed action theories only alter the exponential volume dependence of the $I = 2$ scattering amplitude.[8] This is in contrast to the $I = 0$ $\pi\pi$ amplitude, which suffers from enhanced volume corrections away from the QCD limit. In general, the argument which protects Lüscher's formula from enhanced power-like volume

[6] We note that, while the enhanced volume corrections in quenched QCD invalidate the extraction of scattering parameters from certain scattering channels, e.g., $I = 0$ [119, 121], this is not the case in principle for partially quenched QCD, since QCD is a subset of the theory. Because the enhanced volume contributions must vanish in the QCD limit, they provide a "handle" on the enhanced volume terms. In practice, however, these enhanced volume terms may dominate the correlation function, making the extraction of the desired (non-enhanced) volume dependence impractical.

[7] We restrict the incoming pions to be below the inelastic threshold; this is necessary for the validity of Lüscher's formula even in QCD.

[8] In fact, hairpin propagators will give larger exponential dependence than standard propagators because they are more chirally sensitive.

corrections holds for all "maximally stretched" states at threshold in the meson sector, i.e., those with the maximal values of all conserved quantum numbers; other examples include K^+K^+ and $K^+\pi^+$ scattering. We expect that a similar argument will hold for certain scattering channels in the baryon sector.

Therefore the s-wave $I = 2$ $\pi\pi$ scattering length can be extracted from mixed action lattice simulations using Lüscher's formula and then extrapolated to the physical quark masses and to the continuum using the infinite volume MAχPT expression for the scattering length.[9]

3.3 Mixed Action Lagrangian and Partial Quenching

Mixed action theories use different discretization techniques in the valence and sea sectors and are therefore a natural extension of partially quenched theories. We consider a theory with N_f staggered sea quarks and N_v valence quarks (with N_v corresponding ghost quarks) which satisfy the Ginsparg-Wilson relation [82, 83]. In particular we are interested in theories with two light dynamical quarks ($N_f = 2$) and with three dynamical quarks where the two light quarks are degenerate (commonly referred to as $N_f = 2 + 1$). To construct the continuum effective Lagrangian which includes lattice artifacts one follows the two-step procedure outlined in Ref. [127]. First one constructs the Symanzik continuum effective Lagrangian at the quark level [128, 129] up to a given order in the lattice spacing, a:

$$\mathcal{L}_{Sym} = \mathcal{L} + a\mathcal{L}^{(5)} + a^2\mathcal{L}^{(6)} + \ldots, \tag{3.2}$$

[9] For a related discussion, see Ref. [126]

where $\mathcal{L}^{(4+n)}$ contains higher dimensional operators of dimension $4+n$. Next one uses the method of spurion analysis to map the Symanzik action onto a chiral Lagrangian, in terms of pseudo-Goldstone mesons, which now incorporates the lattice spacing effects. This has been done in detail for a mixed GW-staggered theory in Ref. [103]; here we only describe the results.

The leading quark level Lagrangian is given by

$$\mathcal{L} = \sum_{a,b=1}^{4N_f+2N_v} \bar{Q}^a \left[i\not{D} - m_Q \right]_a^{\ b} Q_b, \tag{3.3}$$

where the quark fields are collected in the vectors

$$Q^{N_f=2} = (\underbrace{u, d}_{\text{valence}}, \underbrace{j_1, j_2, j_3, j_4, l_1, l_2, l_3, l_4}_{\text{sea}}, \underbrace{\tilde{u}, \tilde{d}}_{\text{ghost}})^T, \tag{3.4}$$

$$Q^{N_f=2+1} = (\underbrace{u, d, s}_{\text{valence}}, \underbrace{j_1, j_2, j_3, j_4, l_1, l_2, l_3, l_4, r_1, r_2, r_3, r_4}_{\text{sea}}, \underbrace{\tilde{u}, \tilde{d}, \tilde{s}}_{\text{ghost}})^T \tag{3.5}$$

for the two theories. There are 4 tastes for each flavor of sea quark, j, l, r.[10] We work in the isospin limit in both the valence and sea sectors so the quark mass matrix in the 2+1 sea flavor theory is given by

$$m_Q = \text{diag}(\underbrace{m_u, m_u, m_s}_{\text{valence}}, \underbrace{m_j, m_j, m_j, m_j, m_j, m_j, m_j, m_j, m_r, m_r, m_r, m_r}_{\text{sea}}, \underbrace{m_u, m_u, m_s}_{\text{ghost}}). \tag{3.6}$$

The quark mass matrix in the two-flavor theory is analogous but without strange valence, sea, and ghost quark masses. The leading order mixed action Lagrangian, Eq. (3.3), has an approximate graded chiral symmetry, $SU(4N_f + N_v|N_v)_L \otimes SU(4N_f + N_v|N_v)_R$, which is

[10] Note that we use different labels for the valence and sea quarks than Ref. [103]. Instead we use the "nuclear physics" labeling convention, which is consistent with Ref. [104].

exact in the massless limit. [11] In analogy to QCD, we assume that the vacuum spontaneously breaks this symmetry down to its vector subgroup, $SU(4N_f + N_v|N_v)_V$, giving rise to $(4N_f + 2N_v)^2 - 1$ pseudo-Goldstone mesons. These mesons are contained in the field

$$\Sigma = \exp\left(\frac{2i\Phi}{f}\right), \quad \Phi = \begin{pmatrix} M & \chi^\dagger \\ \chi & \tilde{M} \end{pmatrix}. \tag{3.7}$$

The matrices M and $\tilde{M}$ contain bosonic mesons while χ and $\chi^\dagger$ contain fermionic mesons. Specifically,

$$M = \begin{pmatrix} \eta_u & \pi^+ & \dots & \phi_{uj} & \phi_{ul} & \dots \\ \pi^- & \eta_d & \dots & \phi_{dj} & \phi_{dl} & \dots \\ \vdots & \vdots & \ddots & \dots & \dots & \dots \\ \phi_{ju} & \phi_{jd} & \vdots & \eta_j & \phi_{jl} & \dots \\ \phi_{lu} & \phi_{ld} & \vdots & \phi_{lj} & \eta_l & \dots \\ \vdots & \vdots & \vdots & \vdots & \vdots & \ddots \end{pmatrix}, \quad \tilde{M} = \begin{pmatrix} \tilde{\eta}_u & \tilde{\pi}^+ & \dots \\ \tilde{\pi}^- & \tilde{\eta}_d & \dots \\ \vdots & \vdots & \ddots \end{pmatrix}$$

$$\chi = \begin{pmatrix} \phi_{\tilde{u}u} & \phi_{\tilde{u}d} & \dots & \phi_{\tilde{u}j} & \phi_{\tilde{u}l} & \dots \\ \phi_{\tilde{d}u} & \phi_{\tilde{d}d} & \dots & \phi_{\tilde{d}j} & \phi_{\tilde{d}l} & \dots \\ \vdots & \vdots & \vdots & \vdots & \vdots & \ddots \end{pmatrix}. \tag{3.8}$$

In Eq. (3.8) we only explicitly show the mesons needed in the two-flavor theory. The ellipses indicate mesons containing strange quarks in the 2+1 theory. The upper $N_v \times N_v$ block of M contains the usual mesons composed of a valence quark and anti-quark. The fields composed of one valence quark and one sea anti-quark, such as ϕ_{uj}, are 1×4 matrices of

[11] This is a "fake" symmetry of PQQCD. However, it gives the correct Ward identities and thus can be used to understand the symmetries and symmetry breaking of PQQCD [58].

fields where we have suppressed the taste index on the sea quarks. Likewise, the sea-sea mesons such as ϕ_{jl} are 4×4 matrix-fields. Under chiral transformations, Σ transforms as

$$\Sigma \longrightarrow L\ \Sigma\ R^\dagger \quad , \quad L, R \in SU(4N_f + N_v|N_v)_{L,R}. \tag{3.9}$$

In order to construct the chiral Lagrangian it is useful to first define a power-counting scheme. Continuum χPT is an expansion in powers of the pseudo-Goldstone meson momentum and mass squared [106, 107]:

$$\varepsilon^2 \sim p_\pi^2/\Lambda_\chi^2 \sim m_\pi^2/\Lambda_\chi^2\,, \tag{3.10}$$

where $m_\pi^2 \propto m_Q$ and Λ_χ is the cutoff of χPT. In a mixed theory (or any theory which incorporates lattice spacing artifacts) one must also include the lattice spacing in the power counting. Both the chiral symmetry of the Ginsparg-Wilson valence quarks and the remnant $U(1)_A$ symmetry of the staggered sea quarks forbid operators of dimension five; therefore the leading lattice spacing correction for this mixed action theory arises at $\mathcal{O}(a^2)$. Moreover, current staggered lattice simulations indicate that taste-breaking effects (which are of $\mathcal{O}(a^2)$) are numerically of the same size as the lightest staggered meson mass [70]. We therefore adopt the following power-counting scheme:

$$\varepsilon^2 \sim p_\pi^2/\Lambda_\chi^2 \sim m_Q/\Lambda_{\rm QCD} \sim a^2\Lambda_{\rm QCD}^2\,. \tag{3.11}$$

The leading order (LO), $\mathcal{O}(\varepsilon^2)$, Lagrangian is then given in Minkowski space by [103]

$$\mathcal{L} = \frac{f^2}{8}\mathrm{str}\left(\partial_\mu\Sigma\,\partial^\mu\Sigma^\dagger\right) + \frac{f^2B}{4}\mathrm{str}\left(\Sigma m_Q^\dagger + m_Q\Sigma^\dagger\right) - a^2\left(\mathcal{U}_S + \mathcal{U}_S' + \mathcal{U}_V\right), \tag{3.12}$$

where we use the normalization $f \sim 132$ MeV and have already integrated out the taste singlet Φ_0 field, which is proportional to str(Φ) [58]. $\mathcal{U}_S$ and $\mathcal{U}'_S$ are the well-known taste breaking potential arising from the staggered sea quarks [72, 73]. The staggered potential only enters into our calculation through an additive shift to the sea-sea meson masses; we therefore do not write out its explicit form. The enhanced chiral properties of the mixed action theory are illustrated by the fact that only one new potential term arises at this order:

$$\mathcal{U}_V = -C_{\text{Mix}} \text{ str} \left(T_3 \Sigma T_3 \Sigma^\dagger \right), \tag{3.13}$$

where

$$T_3 = \mathcal{P}_S - \mathcal{P}_V = \text{diag}(-I_V, I_t \otimes I_S, -I_V). \tag{3.14}$$

The projectors, $\mathcal{P}_S$ and $\mathcal{P}_V$, project onto the sea and valence-ghost sectors of the theory, I_V and I_S are the valence and sea flavor identities, and I_t is the taste identity matrix. From this Lagrangian, one can compute the LO masses of the various pseudo-Goldstone mesons in Eq. (3.8). For mesons composed of only valence (ghost) quarks of flavors a and b,

$$m_{ab}^2 = B(m_a + m_b). \tag{3.15}$$

This is identical to the continuum LO meson mass because the chiral properties of Ginsparg-Wilson quarks protect mesons composed of only valence (ghost) quarks from receiving mass corrections proportional to the lattice spacing. However, mesons composed of only sea quarks of flavors s_1 and s_2 and taste t, or mixed mesons with one valence (v) and one sea

(s) quark both receive lattice spacing mass shifts. Their LO masses are given by

$$\tilde{m}^2_{s_1 s_2,t} = B(m_{s_1} + m_{s_2}) + a^2\Delta(\xi_t), \tag{3.16}$$

$$\tilde{m}^2_{vs} = B(m_v + m_s) + a^2\Delta_{\text{Mix}}. \tag{3.17}$$

From now on we use tildes to indicate masses that include lattice spacing shifts. The only sea-sea mesons that enter $\pi\pi$ scattering to the order at which we are working are the taste-singlet mesons (this is because the valence-valence pions that are being scattered are tasteless), which are the heaviest; we therefore drop the taste label, t. The splittings between meson masses of different tastes have been determined numerically on the MILC configurations [70], so $\Delta(\xi_I)$ should be considered an input rather than a fit parameter. The mixed mesons all receive the same a^2 shift given by

$$\Delta_{\text{Mix}} = \frac{16 C_{\text{Mix}}}{f^2}\,, \tag{3.18}$$

which has yet to be determined numerically.

After integrating out the Φ_0 field, the two-point correlation functions for the flavor-neutral states deviate from the simple single-pole form. The momentum space propagator between two flavor neutral states is found to be at leading order [58]

$$\mathcal{G}_{\eta_a\eta_b}(p^2) = \frac{i\epsilon_a\delta_{ab}}{p^2 - m^2_{\eta_a} + i\epsilon} - \frac{i}{N_f}\frac{\prod_{k=1}^{N_f}(p^2 - \tilde{m}^2_k + i\epsilon)}{(p^2 - m^2_{\eta_a} + i\epsilon)(p^2 - m^2_{\eta_b} + i\epsilon)\prod_{k'=1}^{N_f-1}(p^2 - \tilde{m}^2_{k'} + i\epsilon)}, \tag{3.19}$$

where

$$\epsilon_a = \begin{cases} +1 & \text{for a = valence or sea quarks} \\ -1 & \text{for a = ghost quarks}\,. \end{cases} \tag{3.20}$$

In Eq. (3.19), k runs over the flavor neutral states $(\phi_{jj}, \phi_{ll}, \phi_{rr})$ and k' runs over the mass eigenstates of the sea sector. For $\pi\pi$ scattering, it will be useful to work with linear combinations of these η_a fields. In particular we form the linear combinations

$$\pi^0 = \frac{1}{\sqrt{2}}\left(\eta_u - \eta_d\right) \quad , \quad \bar{\eta} = \frac{1}{\sqrt{2}}\left(\eta_u + \eta_d\right), \tag{3.21}$$

for which the propagators are

$$\mathcal{G}_{\pi^0}(p^2) = \frac{i}{p^2 - m_\pi^2 + i\epsilon}, \tag{3.22}$$

$$\mathcal{G}_{\bar{\eta}}(p^2) = \frac{i}{p^2 - m_\pi^2 + i\epsilon} - \frac{2i}{N_f}\frac{\prod_{k=1}^{N_f}(p^2 - \tilde{m}_k^2 + i\epsilon)}{(p^2 - m_\pi^2 + i\epsilon)^2 \prod_{k'=1}^{N_f-1}(p^2 - \tilde{m}_{k'}^2 + i\epsilon)}. \tag{3.23}$$

Specifically,

$$\mathcal{G}_{\bar{\eta}}(p^2) = \frac{i}{p^2 - m_\pi^2} - i\frac{p^2 - \tilde{m}_{jj}^2}{(p^2 - m_\pi^2)^2}, \qquad \text{for } N_f = 2, \tag{3.24}$$

$$= \frac{i}{p^2 - m_\pi^2} - \frac{2i}{3}\frac{(p^2 - \tilde{m}_{jj}^2)(p^2 - \tilde{m}_{rr}^2)}{(p^2 - m_\pi^2)^2\,(p^2 - \tilde{m}_\eta^2)}, \qquad \text{for } N_f = 2+1, \tag{3.25}$$

where $\tilde{m}_\eta^2 = \frac{1}{3}(\tilde{m}_{jj}^2 + 2\tilde{m}_{rr}^2)$.

3.4 Calculation of the $I = 2$ Pion Scattering Amplitude

Our goal in this chapter is to calculate the $I = 2$ $\pi\pi$ scattering length in chiral perturbation theory for a partially quenched, mixed action theory with GW valence quarks and staggered sea quarks, in order to allow correct continuum and chiral extrapolation of mixed action lattice data. We begin, however, by reviewing the pion scattering amplitude in continuum $SU(2)$ chiral perturbation theory. We next calculate the scattering amplitude in $N_f = 2$

PQχPT and MAχPT, and finally in $N_f = 2+1$ PQχPT and MAχPT. When renormalizing divergent 1-loop integrals, we use dimensional regularization and a modified minimal subtraction scheme where we consistently subtract all terms proportional to [106]:

$$\frac{2}{4-d} - \gamma_E + \log 4\pi + 1,$$

where d is the number of space-time dimensions. The scattering amplitude can be related to the scattering length and other scattering parameters, as we discuss in Section 3.5.

3.4.1 Continuum $SU(2)$

The tree-level $I = 2$ pion scattering amplitude at threshold is well known to be [105]

$$i\mathcal{A} = -\frac{4im_\pi^2}{f_\pi^2}. \tag{3.26}$$

It is corrected at $\mathcal{O}(\varepsilon^4)$ by loop diagrams and also by tree level terms from the NLO (or Gasser-Leutwyler) chiral Lagrangian [106].[12] The diagrams that contribute at one loop order are shown in Figure 3.1; they lead to the following NLO expression for the scattering amplitude:

$$i\mathcal{A}_{\vec{p}_i=0} = -\frac{4im_{uu}^2}{f^2}\left\{1 + \frac{m_{uu}^2}{(4\pi f)^2}\left[8\ln\left(\frac{m_{uu}^2}{\mu^2}\right) - 1 + l'_{\pi\pi}(\mu)\right]\right\}, \tag{3.27}$$

where m_{uu} is the tree-level expression given in Eq. (3.15) and f is the LO pion decay constant which appears in Eq. (3.7). The coefficient $l'_{\pi\pi}$ is a linear combination of low-energy constants appearing in the Gasser-Leutwyler Lagrangian whose scale dependence exactly cancels the scale dependence of the logarithmic term. One can re-express the amplitude,

[12] The continuum $\pi\pi$ scattering amplitude is known to two loops [108, 109, 110, 111].

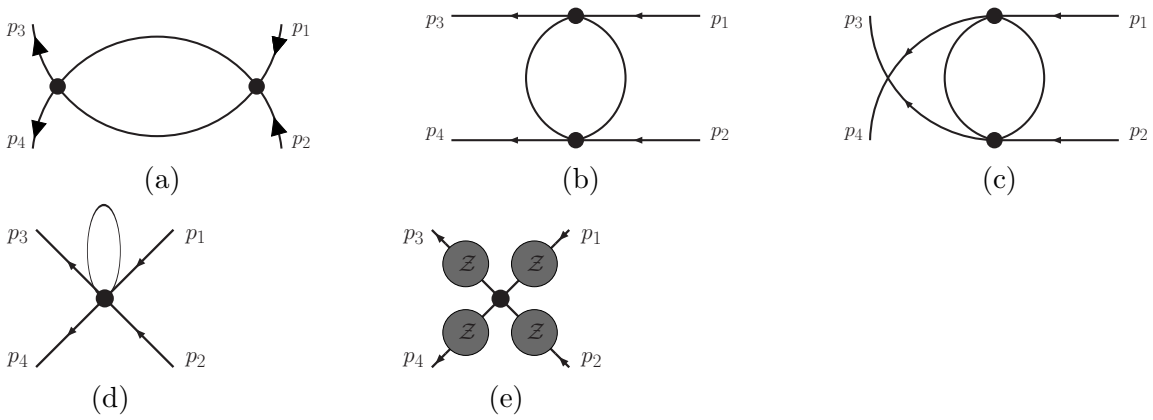

Figure 3.1: One-loop diagrams contributing to the $\pi\pi$ scattering amplitude. Diagrams (a)–(c) are the s-, t-, and u-channel diagrams, respectively, while diagram (e) represents wavefunction renormalization.

however, in terms of the physical pion mass and decay constant using the NLO formulae for m_π and f_π to find:

$$i\mathcal{A}_{\vec{p_i}=0} = -\frac{4im_\pi^2}{f_\pi^2}\left\{1 + \frac{m_\pi^2}{(4\pi f_\pi)^2}\left[3\ln\left(\frac{m_\pi^2}{\mu^2}\right) - 1 + l_{\pi\pi}(\mu)\right]\right\}, \tag{3.28}$$

where $l_{\pi\pi}$ is a different linear combination of low energy constants. The expression for $l_{\pi\pi}$ can be found in Ref. [110]. We do not, however, include it here because we do not envision either using the known values of the Gasser-Leutwyler parameters in the the fit of the scattering length or using the fit to determine them. The simple expression (3.28) has already been used in extrapolation of lattice data from mixed action simulations [94], but it neglects lattice spacing effects from the staggered sea quarks which are known from other simulations to be of the same order as the leading order terms in the chiral expansion of some observables [70]. We therefore proceed to calculate the scattering amplitude in a partially quenched, mixed action theory relevant to simulations.

3.4.2 Mixed GW-Staggered Theory with 2 Sea Quarks

The scattering amplitude in the partially quenched theory differs from the unquenched theory in three important respects. First, more mesons propagate in the loop diagrams. Second, some of the mesons have more complicated propagators due to hairpin diagrams at the quark level [115, 58]. Third, there are additional terms in the NLO Lagrangian which arise from partial quenching [112], and lattice spacing effects [103, 75].

At the level of quark flow, there are diagrams such as Figure 3.2, which route the valence quarks through the diagram in a way which has no ghostly counterpart. Consequently, the ghosts do not exactly cancel the valence quarks in loops. Of course, this is simply a reflection of the fact that the initial and final states—valence pions—are themselves not symmetric under the interchange of ghost and valence quarks, and therefore the graded symmetry between the valence and ghost pions has already been violated. This is well known in quenched and partially quenched heavy baryon χPT [7, 8, 59]. This fact also partly explains the success of quenched $\pi\pi$ scattering in the $I = 2$ channel [95, 96]; quenching does not eliminate *all* loop graphs like it does in many other processes, and in particular, the s-channel diagram is not modified by (partial) quenching effects. As a consequence, it is necessary to compute all the graphs contributing to this process in order to determine the scattering amplitude.

Quark level disconnected (hairpin) diagrams lead to higher order poles in the propagator of any particle which has the quantum numbers of the vacuum [115, 58]. In the isospin limit of the $N_f = 2$ partially quenched theory, conservation of isospin prevents the π^0 from suffering any hairpin effects. Hence only the $\bar{\eta}$ acquires a disconnected propagator. Moreover, in the $m_0 \to \infty$ limit, the $\bar{\eta}$ propagator (given for a general PQ theory in

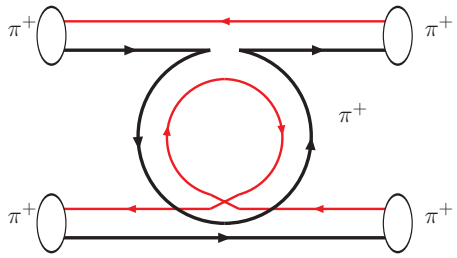

Figure 3.2: Example quark flow for a one-loop t-channel graph. This diagram illustrates the presence of meson loops composed of purely valence-valence mesons which are not cancelled by valence-ghost loops. Different colors (shades of grey) represent different quark flavors.

Eq. (3.23)) is given by the simple expression

$$\begin{aligned} G_{\bar{\eta}}(p^2) &= \frac{i}{p^2 - m_\pi^2} - i\frac{p^2 - \tilde{m}_{jj}^2}{(p^2 - m_\pi^2)^2} \\ &= \frac{i\tilde{\Delta}_{PQ}^2}{(p^2 - m_\pi^2)^2}, \end{aligned} \tag{3.29}$$

where the parameter

$$\tilde{\Delta}_{PQ}^2 = \tilde{m}_{jj}^2 - m_\pi^2 \tag{3.30}$$

quantifies the partial quenching. (Recall that $\tilde{m}_{jj}$ is the physical mass of a taste *singlet* sea-sea meson.) Notice that when $\tilde{\Delta}_{PQ} \to 0$ the propagator (3.29) also goes to zero; this is what we expect since, in the $SU(2)$ theory, the only neutral propagating state is the π^0. The propagator in Eq. (3.29) can appear in loops, thereby producing new diagrams such as those in Fig. 3.3.[13] After adding all such hairpin diagrams, one finds that the contribution

[13]We note that there are also similar contributions to the four particle vertex with a loop and to the mass correction. We do not show them, however, because they cancel against one another in the amplitude expressed in lattice-physical parameters, which we will show in the following pages.

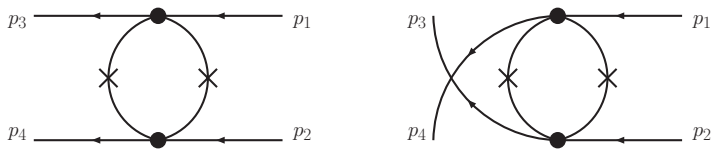

Figure 3.3: Example hairpin diagrams contributing to pion scattering. The propagator with a cross through it indicates the quark-disconnected piece of the $\bar{\eta}$ propagator, Eq. (3.29).

of the $\bar{\eta}$ to the amplitude is[14]

$$i\mathcal{A}_{\bar{\eta}} = \frac{4i}{(4\pi f_\pi)^2}\frac{\tilde{\Delta}^4_{PQ}}{6f_\pi^2}. \tag{3.31}$$

In addition to 1-loop contributions, the NLO scattering amplitude receives tree-level analytic contributions from operators of $\mathcal{O}(\epsilon^4)$ in the chiral Lagrangian. At this order, the mixed action Lagrangian contains the same $\mathcal{O}(p^4)$, $\mathcal{O}(p^2 m_q)$, and $\mathcal{O}(m_q^2)$ operators as in the continuum partially quenched chiral Lagrangian, plus additional $\mathcal{O}(a^4)$, $\mathcal{O}(a^2 m_q)$, and $\mathcal{O}(a^2 p^2)$ operators arising from discretization effects. We can now enumerate the generic forms of analytic contributions from these NLO operators. Because of the chiral symmetry of the GW valence sector, all tree-level contributions to the scattering length must vanish in the limit of vanishing valence quark mass.[15] Thus there are only three possible forms, each of which must be multiplied by an undetermined coefficient: m_{uu}^4, $m_{uu}^2 m_{jj}^2$, and $m_{uu}^2 a^2$. It may, at first, seem surprising that operators of $\mathcal{O}(a^2 m_q)$, which come from taste-symmetry breaking and contain projectors onto the sea sector, can contribute at tree-level to a purely valence quantity. Nevertheless, this turns out to be the case. These $\mathcal{O}(a^2 m_q)$ mixed action operators can be determined by first starting with the NLO staggered chiral Lagrangian [75],

[14] We note that this contribution does not vanish in the limit that $m_\pi^2 \to 0$ with $\tilde{m}_{jj}^2 \neq 0$. Similar effects have been observed in quenched computations of pion scattering amplitudes [120, 119]. This non-vanishing contribution is the $I = 2$ remnant of the divergences that are known to occur in the $I = 0$ amplitude at threshold. These divergences give rise to enhanced volume corrections to the $I = 0$ amplitude with respect to the one-loop $I = 2$ amplitude and prevent the use of Lüscher's formula. Moreover, it is known [4, 6] that PQχPT is singular in the limit $m_u \to 0$ with nonzero sea quark masses, so the behavior of the amplitude in this limit is meaningless.

[15] As we discussed in the previous footnote, this condition need not hold for loop contributions to the scattering amplitude.

and then inserting a sea projector, $\mathcal{P}_S$, next to every taste matrix. One example of such an operator is $\left[\mathrm{str}\left(\Sigma m_Q^\dagger\right)\mathrm{str}\left(\mathcal{P}_S\xi_5\Sigma\xi_5\Sigma^\dagger\right)+\mathrm{p.c.}\right]$, where, ξ_5 is the γ_5 matrix acting in taste-space and p.c. indicates parity-conjugate. This double-trace operator will contribute to the lattice pion mass, decay constant, and 4-point function at tree level because one can place all of the valence pions inside the first supertrace, and the second supertrace containing the projector $\mathcal{P}_S$ will just reduce to the identity.

Putting everything together, the total mixed action scattering amplitude to NLO is

$$\begin{aligned} i\mathcal{A}_{\vec{p_i}=0} = -\frac{4im_{uu}^2}{f^2}\Bigg\{1+\frac{m_{uu}^2}{(4\pi f)^2}\left[4\ln\left(\frac{m_{uu}^2}{\mu^2}\right)+4\frac{\tilde{m}_{ju}^2}{m_{uu}^2}\ln\left(\frac{\tilde{m}_{ju}^2}{\mu^2}\right)-1+l'_{\pi\pi}(\mu)\right] \\ -\frac{m_{uu}^2}{(4\pi f)^2}\left[\frac{\tilde{\Delta}_{PQ}^4}{6m_{uu}^4}+\frac{\tilde{\Delta}_{PQ}^2}{m_{uu}^2}\left[\ln\left(\frac{m_{uu}^2}{\mu^2}\right)+1\right]\right]+\frac{\tilde{\Delta}_{PQ}^2}{(4\pi f)^2}l'_{PQ}(\mu)+\frac{a^2}{(4\pi f)^2}l'_{a^2}(\mu)\Bigg\}. \end{aligned} \quad (3.32)$$

The first line of Eq. (3.32) contains those terms which remain in the continuum and full QCD limit, Eq. (3.27), while the second line accounts for the effects of partial quenching and of the nonzero lattice spacing. Note that, for consistency with the 1-loop terms, we chose to re-express the analytic contribution proportional to the sea quark mass as $m_{uu}^2\tilde{\Delta}_{PQ}^2$. In Eq. (3.32) we have multiplied every contribution from diagrams which contain a sea quark loop by 1/4, thus making our expression applicable to lattice simulations in which the fourth root of the staggered sea quark determinant is taken.

It is useful, however, to re-express the scattering amplitude in terms of the quantities that one measures in a lattice simulation: m_π and f_π. Throughout this chapter, we will refer to these renormalized measured quantities as the lattice-physical pion mass and decay constant.[16] Because we are working consistently to second order in chiral perturbation

[16]Notice that once the lattice spacing a has been determined, the lattice-physical pion mass can be unambiguously determined by measuring the exponential decay of a pion-pion correlator. We assume that the lattice spacing a has been determined, for example, by studying the heavy quark potential or quarkonium spectrum.

theory, we can equate the lattice-physical pion mass to the 1-loop chiral perturbation theory expression for the pion mass, and likewise for the lattice-physical decay constant. Thus, in terms of lattice-physical parameters, the mixed action $I = 2$ $\pi\pi$ scattering amplitude is

$$i\mathcal{A}^{MA\chi PT}_{\vec{p}_i=0} = -\frac{4im_\pi^2}{f_\pi^2}\left\{1 + \frac{m_\pi^2}{(4\pi f_\pi)^2}\left[3\ln\left(\frac{m_\pi^2}{\mu^2}\right) - 1 + l_{\pi\pi}(\mu)\right] - \frac{m_\pi^2}{(4\pi f_\pi)^2}\frac{\tilde{\Delta}^4_{PQ}}{6\,m_\pi^4}\right\}, \quad (3.33)$$

where the first few terms are identical in form to the full QCD amplitude, Eq. (3.28). This expression for the scattering amplitude is vastly simpler than the one in terms of the bare parameters. First, the hairpin contributions from all diagrams except those in Fig. 3.3 have exactly cancelled, removing the enhanced chiral logs and leaving the last term in Eq. (3.33) as the only explicit modification arising from the partial quenching and discretization effects. Second, all contributions from mixed valence-sea mesons in loops have cancelled, thereby removing the new mixed action parameter, $C_{\rm Mix}$, completely.[17] Third, all tree-level contributions proportional to the sea quark mass have also cancelled from this expression. And finally, most striking is the fact that an explicit computation of the $\mathcal{O}(a^2 m_q)$ contributions to the amplitude arising from the NLO mixed action Lagrangian show that these effects exactly cancel when the amplitude is expressed in lattice-physical parameters. This result will be discussed in detail in Chapter 4. Thus to reiterate, the only partial quenching and lattice spacing dependence in the amplitude comes from the hairpin diagrams of Fig. 3.3, which produce contributions proportional to $\tilde{\Delta}^4_{PQ} = (m^2_{jj} + a^2\Delta(\xi_I) - m_\pi^2)^2$, where $m^2_{jj} + a^2\Delta(\xi_1)$ is the mass-squared of the taste-singlet sea-sea meson. Moreover, we presume that anyone performing a mixed action lattice simulation will separately measure the taste-singlet sea-sea meson mass and use it as an input to fits of other quantities such as

[17] Another consequence of the exact cancellation of the loops with mixed valence-sea quarks is that one does not have to implement the "fourth-root trick" through this order.

the $\pi\pi$ scattering length. Thus we do not consider it to be an undetermined parameter.

It is now clear that one should fit $\pi\pi$ scattering lattice data in terms of the lattice-physical pion mass and decay constant rather than in terms of the LO pion mass and LO decay constant. By doing this, one eliminates three undetermined fit parameters: C_{Mix}, l'_{PQ}, and l'_{a^2}, as well as the enhanced chiral logs.

3.4.3 Mixed GW-Staggered Theory with $2+1$ Sea Quarks

The $2+1$ flavor theory has three additional quarks—the strange valence and ghost and strange sea quarks—which can lead to new contributions to the scattering amplitude. Because we only consider the scattering of valence pions, however, strange valence quarks cannot appear in this process. Thus all new contributions to the scattering amplitude necessarily come only from the sea strange quark, r. Because the r quark is heavier than the other sea quarks there is $SU(3)$ symmetry breaking in the sea. This symmetry breaking only affects the pion scattering amplitude, expressed in lattice-physical quantities, through the graphs with internal $\bar{\eta}$ propagators because the masses of the mixed valence-sea mesons cancel in the final amplitude as they did in the earlier two-flavor case. In addition, the only signature of partial quenching in the amplitude comes from these same diagrams. It is therefore worthwhile to investigate the physics of the neutral meson propagators further.

There are more hairpin graphs in the $2+1$ flavor theory since the η_s may propagate as well as the η_u and the η_d. Because these mesons mix with one another, the flavor basis is not the most convenient basis for the computation. Rather, a useful basis of states is π^0, $\bar{\eta} = (\eta_u + \eta_d)/\sqrt{2}$ and η_s. Since we work in the isospin limit, the π^0 cannot mix with $\bar{\eta}$ or η_s; in addition, there is no vertex between the η_s and $\pi^+\pi^-$ at this order, so we never encounter a propagating η_s. Thus all the PQ effects are absorbed into the $\bar{\eta}$ propagator,

which is given by

$$G_{\bar{\eta}}(p^2) = \frac{i}{p^2 - m_\pi^2} - \frac{2i}{3}\frac{(p^2 - \tilde{m}_{jj}^2)(p^2 - \tilde{m}_{rr}^2)}{(p^2 - m_\pi^2)^2\,(p^2 - \tilde{m}_\eta^2)}. \tag{3.34}$$

In $SU(3)$ chiral perturbation theory, the neutral mesons are the π^0 and the η_8. Therefore, in the PQ theory, we know that there will be a contribution from the $\bar{\eta}$ graphs that does not result from partial quenching or $SU(3)$ symmetry breaking. Therefore the extra PQ graphs arising from the internal $\bar{\eta}$ fields must not vanish in the $\tilde{\Delta}_{PQ} \to 0$ limit, in contrast to the two-flavor case of Eq. (3.31).

To make this clear, we can re-express the propagator of Eq. (3.34) in terms of $\tilde{\Delta}_{PQ}$ as

$$G_{\bar{\eta}}(p^2) = i\left[\frac{\tilde{\Delta}_{PQ}^2}{(p^2 - m_\pi^2)^2} + \frac{1}{3}\frac{1}{p^2 - \tilde{m}_\eta^2}\left(1 - \frac{\tilde{\Delta}_{PQ}^2}{p^2 - m_\pi^2}\right)^2\right]. \tag{3.35}$$

This propagator has a single pole which is independent of $\tilde{\Delta}_{PQ}$, as well as higher-order poles that are at least quadratic in $\tilde{\Delta}_{PQ}$. It is interesting to consider the large m_r limit of this propagator. In this limit, $\tilde{m}_\eta^2 \approx \frac{4}{3}Bm_r$ is also large. For momenta that are small compared to $\tilde{m}_\eta$, the second term of this equation goes to zero in the large m_r limit, and the $2+1$ flavor propagator reduces to the two-flavor propagator, Eq. (3.29), as expected.

While the above expression clarifies the $\tilde{\Delta}_{PQ}$ dependence of the propagator and the large m_r limit, it obscures the $SU(3)_{sea}$ limit. An equivalent form of the propagator is

$$G_{\bar{\eta}}(p^2) = i\left[\frac{\tilde{\Delta}_{PQ}^2}{(p^2 - m_\pi^2)^2} + \frac{1}{3}\left(1 + \frac{\tilde{\Delta}_3^2}{p^2 - \tilde{m}_\eta^2}\right)\frac{1}{p^2 - m_\pi^2}\left(1 - \frac{\tilde{\Delta}_{PQ}^2}{p^2 - m_\pi^2}\right)\right], \tag{3.36}$$

where the quantity $\tilde{\Delta}_3 = \sqrt{\tilde{m}_\eta^2 - \tilde{m}_{jj}^2}$ parametrizes the $SU(3)_{sea}$ breaking. When $\tilde{\Delta}_3 = 0$ this propagator is similar in form to the corresponding 2 flavor propagator, Eq. (3.29), but it has an additional single pole due to the extra neutral meson in the $SU(3)$ theory.

Having considered the new physics of the hairpin propagator, we can now calculate the scattering amplitude. For our purposes here, it is most convenient to express the total $I = 2$ $\pi\pi$ scattering amplitude in terms of $\tilde{\Delta}_{PQ}$. Just as in the 2-flavor computation, the NLO analytic contributions due to partial quenching and finite lattice spacing effects exactly cancel when the amplitude is expressed in lattice-physical parameters. All sea quark mass and lattice spacing dependence comes from the hairpin diagrams, which produce terms proportional to powers of $\tilde{\Delta}_{PQ}$ with known coefficients. The amplitude is

$$i\mathcal{A}^{MA\chi PT}_{\vec{p}_i=0} = -\frac{4im_\pi^2}{f_\pi^2}\Bigg\{1 + \frac{m_\pi^2}{(4\pi f_\pi)^2}\left[3\ln\left(\frac{m_\pi^2}{\mu^2}\right) - 1 + \frac{1}{9}\left[\ln\left(\frac{\tilde{m}_\eta^2}{\mu^2}\right) + 1\right] + \bar{l}_{\pi\pi}(\mu)\right] + \frac{1}{(4\pi f_\pi)^2}\left[-\frac{\tilde{\Delta}_{PQ}^4}{6m_\pi^2} + m_\pi^2\sum_{n=1}^{4}\left(\frac{\tilde{\Delta}_{PQ}^2}{m_\pi^2}\right)^n \mathcal{F}_n\left(\tilde{m}_\eta^2/m_\pi^2\right)\right]\Bigg\}, \quad (3.37)$$

where $\tilde{\Delta}_{PQ}^2 = m_{jj}^2 + a^2\Delta(\xi_I) - m_\pi^2$ and

$$\mathcal{F}_1(x) = -\frac{2}{9(x-1)^2}\left[5(x-1) - (3x+2)\ln(x)\right], \quad (3.38a)$$

$$\mathcal{F}_2(x) = \frac{2}{3(x-1)^3}\left[(x-1)(x+3) - (3x+1)\ln(x)\right], \quad (3.38b)$$

$$\mathcal{F}_3(x) = \frac{1}{9(x-1)^4}\left[(x-1)(x^2-7x-12) + 2(7x+2)\ln(x)\right], \quad (3.38c)$$

$$\mathcal{F}_4(x) = -\frac{1}{54(x-1)^5}\left[(x-1)(x^2-8x-17) + 6(3x+1)\ln(x)\right]. \quad (3.38d)$$

The functions $\mathcal{F}_i$ have the property that $\mathcal{F}_i(x) \to 0$ in the limit that $x \to \infty$. Therefore, when the strange sea quark mass is very large, i.e., $\tilde{m}_\eta^2/m_\pi^2 \gg 1$, the $2+1$ flavor amplitude reduces to the two-flavor amplitude, Eq. (3.33), with the exception of terms that can be absorbed into the analytic terms. The low energy constants have a scale dependence which exactly cancels the scale dependence in the logarithms. The coefficient $\bar{l}_{\pi\pi}$ is the same linear

combination of Gasser-Leutwyler coefficients that appear in the $SU(3)$ scattering amplitude expressed in terms of the physical pion mass and decay constant [108, 111].

Because the functions $\mathcal{F}_i$ depend logarithmically on x, the $2+1$ flavor scattering amplitude features enhanced chiral logarithms [4] that are absent from the two-flavor amplitude. This is a useful observation, as we will now explain. Because there is a strange quark in nature and its mass is less than the QCD scale, Λ_{QCD}, lattice simulations must use $2+1$ quark flavors. It is often practical to fix the strange quark mass at a constant value near its physical value in these simulations. This circumstance is helpful because, just as $SU(2)$ chiral perturbation theory is useful to describe nature at scales smaller than the strange quark mass, the two-flavor amplitude given in Eq. (3.33) can be used to extrapolate $2+1$ flavor lattice data at energy scales smaller than the strange sea quark mass used in the simulation (provided, of course, there are no strange valence quarks) [130]. This is valid because, at energy scales smaller than the strange quark mass (or actually twice the strange quark mass, since the purely pionic systems have no valence strange quarks), one can integrate out the strange quark. This is not an approximation, because all of the effects of the strange quark are absorbed into a renormalization of the parameters of the chiral Lagrangian. Moreover, since the two-flavor amplitude does not exhibit enhanced chiral logarithms, signatures of partial quenching can be reduced by extrapolating lattice data with the two-flavor, rather than the $2+1$ flavor, expression. We note that in this case the effects of the strange quark are absorbed in the coefficients of the analytic terms appearing in Eq. (3.33), and thus they are not constant, but rather depend logarithmically upon the strange sea quark mass.

3.5 $I = 2$ Pion Scattering Length Results

In this section we present our results for the s-wave $I = 2$ $\pi\pi$ scattering length in the two theories most relevant to current mixed action lattice simulations: those with GW valence quarks and either $N_f = 2$ or $N_f = 2 + 1$ staggered sea quarks. We only present results for the scattering length expressed in lattice-physical parameters. The s-wave scattering length is trivially related to the full scattering amplitude at threshold by an overall prefactor:

$$a_{l=0}^{(I=2)} = \frac{1}{32\pi m_\pi} \mathcal{A}^{I=2}\Big|_{\vec{p_i}=0}. \tag{3.39}$$

3.5.1 Scattering Length with 2 Sea Quarks

The $I = 2$ $\pi\pi$ s-wave scattering length in a MAχPT theory with 2 sea quarks is given by

$$a_0^{(2)^{MA\chi PT}} = -\frac{m_\pi}{8\pi f_\pi^2}\left\{1 + \frac{m_\pi^2}{(4\pi f_\pi)^2}\left[3\ln\left(\frac{m_\pi^2}{\mu^2}\right) - 1 + l_{\pi\pi}(\mu)\right] - \frac{m_\pi^2}{(4\pi f_\pi)^2}\frac{\tilde{\Delta}_{PQ}^4}{6\, m_\pi^4}\right\}, \tag{3.40}$$

where $\tilde{\Delta}_{PQ}^2 = m_{jj}^2 + a^2\Delta(\xi_I) - m_\pi^2$. The first two terms are the result one obtains in $SU(2)$ χPT [110] and the last term is the only new effect arising from the partial quenching and mixed action. All other possible partial quenching terms, enhanced chiral logs and additional linear combinations of the $\mathcal{O}(p^4)$ Gasser-Leutwyler coefficients, exactly cancel when the scattering length is expressed in terms of lattice-physical parameters. And, most strikingly, the pion mass, decay constant and the 4-point function all receive $\mathcal{O}(a^2 m_q)$ corrections from the lattice, but they exactly cancel in the scattering length expressed in terms of the lattice-physical parameters. It is remarkable that the only artifact of the nonzero lattice spacing, $m_{jj}^2 + a^2\Delta_I$, can be separately determined simply by measuring the exponential fall-off of the taste-singlet sea-sea meson 2-point function. Thus there are no

undetermined fit parameters in the mixed action scattering length expression from either partial quenching or lattice discretization effects; there is only the unknown continuum coefficient, $l_{\pi\pi}$.

One can trivially deduce the continuum PQ scattering length from Eq. (3.40): simply let $a \to 0$, reducing $\tilde{m}_{jj} \to m_{jj} = 2Bm_j$ in $\tilde{\Delta}_{PQ}$, resulting in

$$a_0^{(2)\,PQ\chi PT} = -\frac{m_\pi}{8\pi f_\pi^2}\left\{1 + \frac{m_\pi^2}{(4\pi f_\pi)^2}\left[3\ln\left(\frac{m_\pi^2}{\mu^2}\right) - 1 + l_{\pi\pi}(\mu)\right] - \frac{\Delta_{PQ}^4}{6(4\pi m_\pi f_\pi)^2}\right\}. \quad (3.41)$$

3.5.2 Scattering Length with 2+1 Sea Quarks

The $I = 2$ $\pi\pi$ s-wave scattering length in a MAχPT theory with 2+1 sea quarks is given by

$$a_0^{(2)\,MA\chi PT} = -\frac{m_\pi}{8\pi f_\pi^2}\left\{1 + \frac{m_\pi^2}{(4\pi f_\pi)^2}\left[3\ln\left(\frac{m_\pi^2}{\mu^2}\right) - 1 + \frac{1}{9}\left[\ln\left(\frac{\tilde{m}_\eta^2}{\mu^2}\right) + 1\right] + \bar{l}_{\pi\pi}(\mu)\right]\right.$$
$$\left. + \frac{1}{(4\pi f_\pi)^2}\left[-\frac{\tilde{\Delta}_{PQ}^4}{6m_\pi^2} + m_\pi^2\sum_{n=1}^{4}\left(\frac{\tilde{\Delta}_{PQ}^2}{m_\pi^2}\right)^n \mathcal{F}_n\left(\tilde{m}_\eta^2/m_\pi^2\right)\right]\right\}, \quad (3.42)$$

where the functions $\mathcal{F}_i$ are defined in Eq. (3.38). As in the 2-flavor MAχPT expression, Eq. (3.40), the only undetermined parameter is the linear combination of Gasser-Leutwyler coefficients, $\bar{l}_{\pi\pi}$, which also appears in the continuum χPT expression.

We note as an aside that this suppression of lattice spacing counterterms is in contrast to the larger number of terms that one would need in order to correctly fit data from simulations with Wilson valence quarks on Wilson sea quarks. Because the Wilson action breaks chiral symmetry at $\mathcal{O}(a)$, even for massless quarks, there will be terms proportional to all powers of the lattice spacing in the expression for the scattering length in Wilson χPT [131, 132]; this will be discussed further in the next Chapter. Moreover, such lattice spacing corrections begin at $\mathcal{O}(a)$, rather than $\mathcal{O}(a^2)$. If one uses $\mathcal{O}(a)$ improved Wilson

quarks, then the leading discretization effects are of $\mathcal{O}(a^2)$, as for staggered quarks; however, this does not remove the additional chiral symmetry-breaking operators. Another practical issue is whether or not one can perform simulations with Wilson sea quarks that are light enough to be in the chiral regime.

3.6 Discussion

Considerable progress has recently been made in fully dynamical simulations of pion scattering in the $I = 2$ channel [98, 94]. We have considered $I = 2$ scattering of pions composed of Ginsparg-Wilson quarks on a staggered sea. We have calculated the scattering length in both this mixed action theory and in continuum PQχPT for theories with either 2 or $2+1$ dynamical quarks. These expressions are necessary for the correct continuum and chiral extrapolation of PQ and mixed action lattice data to the physical pion mass.

Our formulae, Eqs. (3.40) and (3.42), not only provide the form for the mixed action scattering length, but also contain two predictions relevant to the recent work of Ref. [94]. Beane et al. calculated the $I = 2$ $s-$wave $\pi\pi$ scattering length using domain wall valence quarks and staggered sea quarks, but used the continuum χPT expression to extrapolate to the physical quark masses. In Figure 2 of Ref. [94], which plots $m_\pi a_2^{(0)}$ versus m_π/f_π, the fit of the χPT expression to the lattice data overshoots the lightest pion mass point but fits the heavier two points quite well. This is interesting because Eq. (3.40) predicts a *known*, positive shift to $m_\pi a_2^{(0)}$ of size $\tilde{\Delta}_{PQ}^4/(768 f_\pi^4 \pi^3)$. Accounting for this positive shift is equivalent to lowering the entire curve, and could therefore move the fit such that it goes between the data points. This turns out, however, not to be the case. In Ref. [94], the valence and sea quark masses are tuned to be equal, so $\tilde{\Delta}_{PQ}^2 = a^2\Delta_I \simeq (446 \text{ MeV})^2$ [70]. Despite the large value of $\tilde{\Delta}_{PQ}$, the predicted shift is insignificant, being an order of mag-

Table 3.1: Predicted shifts to the scattering length computed in Ref. [94] arising from finite lattice spacing effects in the mixed action theory. The first two rows show the approximate values of m_π and f_π, while the third shows $m_\pi a_2^{(0)}$ plus the statistical error calculated in [94]. In the fourth row, we give the predicted shifts in the scattering length (times m_π) and, in the fifth row, we give the ratio of the predicted shift to the leading order contribution to the scattering length.

m_π (MeV)	294	348	484
f_π (MeV)	145	149	158
$m_\pi a_2^{(0)}$	-0.212 ± 0.024	-0.222 ± 0.014	-0.38 ± 0.03
$\frac{\tilde{\Delta}_{PQ}^4}{768\pi^3 f_\pi^4}$	0.00374	0.00336	0.00266
$\frac{\tilde{\Delta}_{PQ}^4}{6(4\pi f_\pi m_\pi)^2}$	0.0229	0.0155	0.00711

nitude less than the statistical error. In Table 3.1, we collect the predicted shifts to $m_\pi a_2^{(0)}$ at the three pion masses used in Ref. [94]. We also list the magnitude of the ratio of these predicted shifts to the leading contribution to the scattering length, which turn out to be small, lending confidence to the power counting we have used, Eq. (3.11). The other more important prediction is that there are no unknown corrections to the χPT formula for the scattering length arising from lattice spacing corrections or partial quenching through the order $\mathcal{O}(m_q^2)$, $\mathcal{O}(a^2 m_q)$ and $\mathcal{O}(a^4)$. Therefore, to within statistical and systematic errors, the continuum χPT expression used by Beane et al. to fit their numerical $\pi\pi$ scattering data [94] receives no corrections through the 1-loop level.

The central result of this chapter is that the appropriate way to extrapolate lattice $\pi\pi$ scattering data is in terms of the lattice-physical pion mass and decay constant rather than in terms of the LO parameters which appear in the chiral Lagrangian. When expressed in terms of the LO parameters, the scattering length depends upon 4 undetermined parameters, $l'_{\pi\pi}$, l'_{PQ}, l'_{a^2}, and C_{Mix}. In contrast, the scattering length expressed in terms of the lattice-physical parameters depends upon only one unknown parameter, $l_{\pi\pi}$, the same linear combination of Gasser-Leutwyler coefficients which contributes to the scattering length in continuum χPT. In the next chapter, we will build on these results.

Chapter 4

Two Meson Systems with Ginsparg-Wilson Valence Quarks

4.1 Introduction

There is currently a tension in lattice simulations of QCD phenomena between the need for quarks obeying chiral symmetry on the lattice, and the need for quark masses light enough that one is in the chiral regime. This tension occurs because quark discretization schemes which obey chiral symmetry on the lattice, such as domain wall fermions [84, 85, 86] or overlap fermions [87, 88, 89], both of which satisfy the Ginsparg-Wilson relation [82, 83], are numerically expensive to simulate. On the other hand, Wilson fermions [133] or staggered fermions [134, 68] are faster but violate chiral symmetry at non-zero lattice spacing.

One way of resolving this tension is to recognize that the most computationally intensive stage of a fully dynamical simulation is the evaluation of the quark determinant. This determinant is associated with the sea quarks and is a component of the probability measure on the space of gauge field configurations. This observation has long been the motivation for partial quenching (PQ) [3, 4]: sea quark masses are taken to be larger than valence quark masses so that the sea quarks are more localized and the determinant is easier to compute. The notion of a "mixed action" (MA) simulation takes this line of reasoning

one step farther [100, 101]. A mixed action simulation uses different quark discretizations in the sea and valence sectors. In this case, the valence quarks can be chosen to obey the Ginsparg-Wilson relation so that they enjoy chiral symmetry at finite lattice spacing. The numerically expensive sea quarks, on the other hand, can be chosen to be inexpensive Wilson or (rooted) staggered sea quarks, for example.

There have recently been a significant number of mixed action lattice QCD simulations, [92, 93, 135, 94, 136, 137, 1, 138, 139, 140, 141], the majority of which have employed domain wall valence fermions on the publicly available MILC lattices [142].[1] The effective theories appropriate for mixed action simulations were originally developed in Refs. [100, 101] for Ginsparg-Wilson (GW) valence fermions on Wilson sea fermions, and later for GW valence fermions on staggered sea fermions [103]; these theories have received considerable theoretical attention recently [102, 124, 104, 145, 146] in response to the numerical interest.

In this chapter, we study aspects of the chiral perturbation theories appropriate for mesonic processes in mixed action simulations with Ginsparg-Wilson valence quarks. This chapter builds on the results of Chapter 3, extends certain of the results of that chapter to more general mesonic systems, and explains some of the surprising features noted during our study of the $\pi\pi$ system in Chapter 3. The chiral properties of the Ginsparg-Wilson valence quarks are central to our work, so we adopt the convention that when we refer to a mixed action simulation, we imply that the valence quarks are Ginsparg-Wilson. We work consistently at next-to-leading order (NLO) in the effective field theory expansion, which is a dual expansion in powers of the quark mass, m_q and the lattice spacing, a. At this order, one can view current lattice simulations as being methods of computing the values of certain coefficients in the NLO chiral Lagrangian, which for mesonic quantities is

[1] The MILC lattices themselves utilize asqtad-improved [143, 144], staggered sea fermions.

known as the Gasser-Leutwyler Lagrangian [106, 147]. This is because lattice simulations are performed at quark masses larger than the physical quark mass, so that lattice data must be fit to formulae computed in chiral perturbation theory. These fits determine the unknown coefficients occurring in the chiral formulae, known as low energy constants (LEC)s, so that the chiral expression can then be used at the physical values of the meson masses and decay constants to predict the results of physical experiments. Frequently there are non-physical operators in the NLO chiral Lagrangians describing discretized fermions. For example, there are of order 100 operators in the NLO staggered chiral Lagrangian [75] compared to order 10 in the Gasser-Leutwyler Lagrangian. These unphysical operators lead to unphysical terms in chiral extrapolation formulae which must somehow be removed to make physical predictions. One might think that this will also be an issue in mixed action chiral perturbation theory (MAχPT), since there are certainly many additional operators at NLO. However, we show that mixed action lattice simulations of mesonic scattering lengths do not depend on any unphysical operators at NLO, if these scattering lengths are expressed in terms of the pion mass measured on the lattice and the decay constant measured on the lattice [148]. For linguistic brevity, we will refer to the pion mass measured on the lattice as the lattice-physical pion mass and similarly for the decay constant.

Each choice of sea quark discretization leads to a different MAχPT. For example, tree-level shifts of the masses of mesons composed of two sea quarks, or of one valence and one sea quark, are different for staggered sea quarks and for Wilson sea quarks. Therefore, one may think that the chiral extrapolation formulae depend on the nature of the sea quark discretization. We show that, at NLO, the only difference between the extrapolation formulae is in the leading order mass shifts of the mesons composed of two sea quarks. Thus, once these mass shifts are known, one can use the same extrapolation formulae for

different sea quark discretizations.[2] In fact, any sea quark discretization will do provided,[3] firstly, that QCD is recovered in the continuum limit, and secondly, that the sea-sea mesons may be described at leading order by chiral perturbation theory with the usual kinetic and mass terms, or that the non-locality of the appropriate chiral perturbation theory is correctly captured by the replica method [149].[4] In addition, we have assumed that the quarks of the sea sector are only distinguished by their masses, so that, for example, the same discretization scheme has been used for all sea quarks, and we assume that chiral perturbation theory itself is a valid approximation.

There are still various challenges facing mixed action simulations. Mixed action simulations always violate unitarity at finite lattice spacing.[5] In MAχPT and PQχPT, the most severe unitarity violations are encoded in hairpin propagators of flavor neutral mesons. We point out a simple parametrization which allows a convenient bookkeeping of these unitarity violating effects. Additionally, the value of the new constant, $C_{\rm Mix}$, that appears in the LO mixed action Lagrangian, is currently unknown. This term leads to an additive lattice spacing dependent mass shift of "mixed" mesons consisting of one valence and one sea quark. This causes a mismatch of the meson masses composed of different quarks but does not play a role in the well-known enhanced chiral logarithms [151, 40, 4] or the enhanced power-law volume dependence of two-hadron states [119].[6] In addition, the value of

[2]For staggered fermions, these mass corrections to the mesons are well known [70]. However, these effects are less well determined for Wilson fermions.

[3]In this chapter, we restrict ourselves to isospin symmetric masses in the valence and sea sectors.

[4]We have in mind the current discussion regarding whether rooted staggered fermions become QCD in the continuum limit. There is growing numerical and formal evidence lending support to the hope that rooted staggered fermions are in the same universality class as QCD. We refer the reader to Ref. [150] for current summary of the issues.

[5]For arbitrarily small lattice spacings, the differences arising from the different lattice actions will become negligible, which practically means smaller than the statistical and systematic uncertainties for a given observable, and these unitarity violating terms will no longer be important (assuming the quark masses are tuned equal). This of course, also implies that a MA effective field theory description will no longer be necessary, however for MA lattice simulations today and the foreseeable future, MAχPT is the necessary tool for controlling extrapolations to the physical point.

[6]In this chapter we do not discuss the observed negative norm issues involving scalar meson correla-

this constant is presumably different for each sea quark discretization. However, we show that under favorable circumstances physical quantities such as scattering lengths do not depend on this constant, first we have already discussed in the context of the $\pi\pi$ system in Chapter 3.

Finally, to demonstrate our arguments, we determine various NLO formulae for use in chiral extrapolation of certain mesonic quantities. We have computed the KK and $K\pi$ scattering lengths in $SU(6|3)$ MAχPT. We conclude with a discussion of our results, and in particular show that among the three meson scattering lengths mentioned above and the quantity f_K/f_π there are only two linearly independent counterterms at NLO, which are the corresponding physical counterterms of χPT. Therefore, these four processes provide a means to test the MA formalism with only one lattice spacing. In the appendix we collect the various formulae which are necessary for the chiral extrapolations of the quantities we discuss in this chapter. In addition, for completeness, we present the $\pi\pi$ scattering length in $SU(4|2)$ and $SU(6|3)$ MAχPT, which were computed in Chapter 3 as well as the π and K meson masses and decay constants, which were first computed in Refs. [100, 101, 103], but we express these quantities in terms of the useful PQ parameters we introduce in Section 4.2.1.

4.2 Mixed Action Effective Field Theory

We will not give a thorough introduction to mixed action or partially quenched theories here. We will simply give a brief review to remind the reader of our notation and power counting. For a good introduction to MA theories we refer the reader to Refs. [100, 101, 103], and for PQ theories to Refs. [6, 58].

tors [70, 152], but these can at least be qualitatively understood with the appropriate effective field theory methods [153, 154].

4.2.1 Mixed Actions at Lowest Order

To construct the appropriate Lagrangian to a given order, one must specify a power counting. As mentioned above, χPT is a systematic expansion about the zero momentum, zero quark mass limit, for which the small expansion parameter is

$$\varepsilon_m^2 \sim \frac{p^2}{\Lambda_\chi^2} \sim \frac{m_\pi^2}{\Lambda_\chi^2}, \tag{4.1}$$

where $m_\pi^2 \propto m_q$. For effective theories extended to include lattice spacing artifacts, one must include an additional small parameter.[7] We will be interested in theories for which the leading sea quark lattice spacing dependence is $\mathcal{O}(a^2)$, such as staggered, $\mathcal{O}(a)$-improved Wilson [155], twisted-mass at maximal twist [156], or chiral fermions. Therefore, we shall denote the small parameter counting lattice spacing artifacts to be

$$\varepsilon_a^2 \sim a^2\,\Lambda_{QCD}^2\,, \tag{4.2}$$

and we shall work consistently in the dual expansion to

$$\mathcal{O}(\varepsilon_m^4) \quad , \quad \mathcal{O}(\varepsilon_m^2\,\varepsilon_a^2) \quad , \quad \mathcal{O}(\varepsilon_a^4)\,. \tag{4.3}$$

At leading order (LO) in the quark mass expansion, the mixed action Lagrangian is simply given by the partially quenched Lagrangian [100],

$$\mathcal{L} = \frac{f^2}{8}\mathrm{str}\left(\partial_\mu\Sigma\partial^\mu\Sigma^\dagger\right) + \frac{f^2 B_0}{4}\mathrm{str}\left(m_q\Sigma^\dagger + \Sigma m_q^\dagger\right)\,, \tag{4.4}$$

[7] The general procedure [127] is to construct the continuum Symanzik quark level effective theory for a given lattice action [128, 129] and then build the low energy effective theory with spurion analysis on this continuum lattice action.

where we use the normalization $f \simeq 132$ MeV, and

$$\Sigma = \exp\left(\frac{2i\Phi}{f}\right), \quad \Phi = \begin{pmatrix} M & \chi^\dagger \\ \chi & \tilde{M} \end{pmatrix}. \tag{4.5}$$

The matrices M and $\tilde{M}$ contain bosonic mesons while χ and $\chi^\dagger$ contain fermionic mesons with one ghost quark or antiquark. To be specific, we will discuss the theory with 3 valence (and ghost) quarks and 3 sea quarks, for which[8]

$$M = \begin{pmatrix} \eta_u & \pi^+ & K^+ & \phi_{uj} & \phi_{ul} & \phi_{ur} \\ \pi^- & \eta_d & K^0 & \phi_{dj} & \phi_{dl} & \phi_{dr} \\ K^- & \overline{K}^0 & \eta_s & \phi_{sj} & \phi_{sl} & \phi_{sr} \\ \phi_{ju} & \phi_{jd} & \phi_{js} & \eta_j & \phi_{jl} & \phi_{jr} \\ \phi_{lu} & \phi_{ld} & \phi_{ls} & \phi_{lj} & \eta_l & \phi_{lr} \\ \phi_{ru} & \phi_{rd} & \phi_{rs} & \phi_{rj} & \phi_{rl} & \eta_r \end{pmatrix},$$

$$\tilde{M} = \begin{pmatrix} \tilde{\eta}_u & \tilde{\pi}^+ & \tilde{K}^+ \\ \tilde{\pi}^- & \tilde{\eta}_d & \tilde{K}^0 \\ \tilde{K}^- & \tilde{\overline{K}}^0 & \tilde{\eta}_s \end{pmatrix}, \quad \chi^\dagger = \begin{pmatrix} \phi_{u\tilde{u}} & \phi_{u\tilde{d}} & \phi_{u\tilde{s}} \\ \phi_{d\tilde{u}} & \phi_{d\tilde{d}} & \phi_{d\tilde{s}} \\ \phi_{s\tilde{u}} & \phi_{s\tilde{d}} & \phi_{s\tilde{s}} \\ \phi_{j\tilde{u}} & \phi_{j\tilde{d}} & \phi_{j\tilde{s}} \\ \phi_{l\tilde{u}} & \phi_{l\tilde{d}} & \phi_{l\tilde{s}} \\ \phi_{r\tilde{u}} & \phi_{r\tilde{d}} & \phi_{r\tilde{s}} \end{pmatrix}. \tag{4.6}$$

The upper $N_v \times N_v$ block of M contains the usual mesons composed of a valence quark and anti-quark. The lower $N_s \times N_s$ block of M contains the sea quark-antiquark mesons and

[8]For staggered sea quarks, each sea quark label implicitly includes a taste label as well. For example, ϕ_{uj} is a 1×4 vector in taste-space.

the off-diagonal block elements of M contain bosonic mesons of mixed valence-sea type.

For MA theories there are two types of operators we need to consider at LO in ε_a^2. There are those which modify the sea-sea sector meson potential, which we shall denote as $\mathcal{U}_{sea}$, and those which modify the mixed meson potential, which we shall denote as $\mathcal{U}_{VS}$, such that the Lagrangian, Eq. (4.4) is modified by the additional terms (following the sign conventions of Ref. [103]),

$$\mathcal{L}_{MA} = -a^2\Big(\mathcal{U}_{sea} - \mathcal{U}_{VS}\Big)\,. \tag{4.7}$$

We shall not specify the form of the sea-sea meson potential, $\mathcal{U}_{sea}$, but only note again that at the order we are concerned with, we only need to know how the masses of the sea-sea mesons are modified at LO in ε_a^2 which have been discussed, for example, in Refs. [100, 103]. The other important thing to know is that the structure of $\mathcal{U}_{VS}$ is independent of the type of sea quark and is given by [100, 103]

$$\mathcal{U}_{VS} = C_{\text{Mix}}\,\text{str}\Big(T_3\,\Sigma\,T_3\,\Sigma^\dagger\Big)\,, \tag{4.8}$$

where the flavor matrix T_3 is a difference in projectors onto the valence and sea sectors of the theory,

$$T_3 = \mathcal{P}_S - \mathcal{P}_V = \text{diag}(-I_V, I_S, -I_V)\,. \tag{4.9}$$

This operator leads to an additive shift of the valence-sea meson masses, such that all the pseudo-Goldstone mesons composed of either valence quarks, v, sea quarks, s, or both have

LO masses given by[9]

$$\begin{aligned} m^2_{v_1 v_2} &= B_0(m_{v_1} + m_{v_2})\,, \\ \tilde{m}^2_{vs} &= B_0(m_v + m_s) + a^2\Delta_{\rm Mix}\,, \\ \tilde{m}^2_{s_1 s_2} &= B_0(m_{s_1} + m_{s_2}) + a^2\Delta_{sea}\,, \end{aligned} \tag{4.10}$$

with Δ_{sea} determined by $\mathcal{U}_{sea}$ and[10]

$$\Delta_{\rm Mix} = \frac{16\,C_{\rm Mix}}{f^2}\,. \tag{4.11}$$

The most severe and well known unitarity violating feature of PQ and MA theories is the presence of double pole propagators in the flavor neutral mesons [3]. In particular the momentum space propagators between two mesons composed of valence quarks of flavors a and b respectively are given by[11]

$$\mathcal{G}_{ab}(p^2) = \frac{i\delta_{ab}}{p^2 - m^2_{aa}} - \frac{i}{3}\frac{(p^2 - \tilde{m}^2_{jj})(p^2 - \tilde{m}^2_{rr})}{(p^2 - m^2_{aa})(p^2 - m^2_{bb})(p^2 - \tilde{m}^2_X)} \tag{4.12}$$

where $\tilde{m}_X$ is the mass of the η_{sea}-field,

$$\tilde{m}^2_X = \frac{1}{3}\tilde{m}^2_{jj} + \frac{2}{3}\tilde{m}^2_{rr}\,. \tag{4.13}$$

[9]Here and throughout this chapter, we use tildes over the masses to indicate additive lattice spacing corrections to the meson masses.

[10]For a twisted mass sea [156], one must keep separate track of the neutral and charged mesons as they receive a relative $\mathcal{O}(a^2)$ splitting [157], similar to the various taste mesons for staggered fermions.

[11]In mixed action theories, there are additional hairpin interactions proportional to the lattice spacing which arise from unphysical operators in the theory, similar to the lattice spacing dependent hairpin interactions in staggered χPT [73]. For $\mathcal{O}(a)$ improved Wilson fermions and staggered fermions, these effects are higher order than we are concerned with in this chapter [124], which is also true for twisted mass fermions at maximal twist. For Wilson and twisted mass fermions (away from maximal twist), these effects appear at the order we are working, and must be included. We assume for the rest of the chapter that the sea quark scaling violations are $\mathcal{O}(a^2)$ or higher.

When the valence quark masses are equal, either in the isospin limit of light quarks or for the same flavor, $a = b$, the above propagator acquires a double pole. It is these double poles which lead to the well-known sicknesses of PQχPT, such as the enhanced chiral logs [151, 40, 4], and enhanced power-law volume dependence of two-particle states [119]. Here, we introduce what we call "partial quenching parameters," which are a difference in the quark masses for PQ theories and, more generally for MA theories, a difference in the masses of mesons composed of two sea quarks and two valence quarks. For PQ theories, when these quantities are zero, the theory reduces to an unquenched theory. For MA theories, when one tunes these parameters to zero, one tunes the double pole structure of the flavor-neutral meson propagators to zero up to higher order corrections, and thus has the most QCD-like scenario for a MA theory (we note that there is still a mismatch in the mass of the mixed meson, composed of one valence and one sea quark, Eq. (4.10), from the others). We therefore introduce the partial quenching parameters,[12]

$$\begin{aligned} \tilde{\Delta}_{ju}^2 &\equiv \tilde{m}_{jj}^2 - m_{uu}^2 = 2B_0(m_j - m_u) + a^2\Delta_{sea} + \dots , \\ \tilde{\Delta}_{rs}^2 &\equiv \tilde{m}_{rr}^2 - m_{ss}^2 = 2B_0(m_r - m_s) + a^2\Delta_{sea} + \dots , \end{aligned} \tag{4.14}$$

where the dots denote higher order corrections to the meson masses. We will now move on to discuss the general structure of mixed action theories for arbitrary sea quarks at the next order.

[12] For a staggered sea it is the taste-identity meson masses which enter these PQ parameters [103] (which have been measured [70]), while for a twisted mass sea, it is the neutral pion mass.

4.2.2 Mixed Action χPT at NLO

In Chapter 3, we showed that the $I = 2$ $\pi\pi$ scattering length at NLO, expressed in terms of the bare parameters of the chiral Lagrangian, is[13]

$$m_\pi a_{\pi\pi}^{I=2} = -\frac{m_{uu}^2}{8\pi f^2}\left\{1 + \frac{m_{uu}^2}{(4\pi f)^2}\left[4\ln\left(\frac{m_{uu}^2}{\mu^2}\right) + 4\frac{\tilde{m}_{ju}^2}{m_{uu}^2}\ln\left(\frac{\tilde{m}_{ju}^2}{\mu^2}\right) - 1 + \ell'_{\pi\pi}(\mu)\right]\right.$$
$$\left. - \frac{m_{uu}^2}{(4\pi f)^2}\left[\frac{\tilde{\Delta}_{ju}^4}{6m_{uu}^4} + \frac{\tilde{\Delta}_{ju}^2}{m_{uu}^2}\left[\ln\left(\frac{m_{uu}^2}{\mu^2}\right) + 1\right]\right] + \frac{\tilde{\Delta}_{ju}^2}{(4\pi f)^2}\,\ell'_{PQ}(\mu) + \frac{a^2}{(4\pi f)^2}\ell'_{a^2}(\mu)\right\}. \quad (4.15)$$

Let us remind the reader of some features of this expression which are relevant from the point of view of chiral extrapolations. Eq. (4.15) depends on the mass $\tilde{m}_{ju}$ of a mixed valence-sea meson and consequently the expression depends on the value of the parameter $C_{\rm Mix}$. In addition, there is a dependence on the unphysical unknowns $\ell'_{PQ}(\mu)$ and $\ell'_{a^2}(\mu)$, as well as the decay constant and chiral condensate in the chiral limit, f, and B_0. Thus, Eq. (4.15) depends on three unphysical unknown parameters and three physical unknown parameters, $\ell'_{\pi\pi}(\mu)$, f, and B_0. One must fit all unknown parameters to extrapolate lattice data but only three are of intrinsic interest.

In terms of lattice-physical parameters, the same scattering length becomes

$$m_\pi a_{\pi\pi}^{I=2} = -\frac{m_\pi^2}{8\pi f_\pi^2}\left\{1 + \frac{m_\pi^2}{(4\pi f_\pi)^2}\left[3\ln\left(\frac{m_\pi^2}{\mu^2}\right) - 1 - l_{\pi\pi}^{I=2}(\mu) - \frac{\tilde{\Delta}_{ju}^4}{6\,m_\pi^4}\right]\right\}. \quad (4.16)$$

Notice that this expression does not depend on the mixed valence-sea mesons, and, in fact, the only unknown terms in the expression are the physical parameter $\ell_{\pi\pi}(\mu)$, and the sea-sea meson mass shift in $\tilde{\Delta}_{ju}^2$, Eq. (4.10), which is already determined for staggered sea-quarks.

[13] Here, we show the scattering length for a two-sea flavor theory. In the appendix, we also list the result for the three-sea flavor theory. However, the following discussion of the counterterm structure of the NLO Lagrangian is independent of the number of sea flavors.

Thus, chiral extrapolations using the formula Eq. (4.16) require fitting only one parameter (two for non-staggered sea quarks), in contrast to chiral extrapolations using the scattering length expressed in terms of the bare parameters, Eq. (4.15). Our goal in this section is to understand the origin of this simplification, and under what circumstances we may expect similar simplifications to occur in other processes. To do so, we must discuss the structure of the NLO terms of the MAχPT Lagrangian.

The symmetry structure of the underlying mixed action form of QCD determines the NLO operators in the mixed action chiral Lagrangian through a spurion analysis. However, the symmetries enjoyed by the valence quarks are different to the symmetries of the sea quarks in a mixed action theory. In particular, we only consider GW valence quarks which have a chiral symmetry; the numerically cheaper sea quarks typically violate chiral symmetry. Thus, it is helpful to consider spurions arising from the valence sector separately to the spurions of the sea sector.

The valence sector only violates chiral symmetry explicitly through the quark mass. Therefore, at NLO,[14] the purely valence spurions are identical to the spurions in continuum, unquenched chiral perturbation theory, and so the valence-valence sector of the NLO mixed action chiral Lagrangian is the Gasser-Leutwyler Lagrangian. The sea sector is different. At finite lattice spacing, the sea sector has enhanced sources of chiral symmetry violation—for example, there are additional spurions associated with taste violation if the sea quarks are staggered, or in the case of a Wilson sea, the Wilson term violates chiral symmetry. Consequently, there are additional spurions in the sea sector. Of course, these spurions must involve the sea quarks and must vanish when the sea quark fields vanish.[15] Nevertheless,

[14]Lattice artifacts such as Lorentz symmetry violation lead to the presence of unphysical operators in the chiral Lagrangian. These operators will not be important in the following, as they are higher order in the chiral expansion for mesons [101] (however they are relevant at $\mathcal{O}(\varepsilon_a^2)$ for baryons [102]).

[15]Not all the lattice spacing dependence may be captured with spurion analysis. There are $\mathcal{O}(a^2)$ operators at the quark level which do not break chiral symmetry, for example, $\mathcal{O}^{(6)} = a^2\,\overline{Q}\,\not{D}^3\,Q$. This operator leads

scattering amplitudes expressed in terms of lattice-physical parameters do not explicitly depend on the lattice spacing a, as we will now discuss.

In this chapter, we work consistently to NLO in the MAχPT power counting which we have defined in Eq. (4.3). At this order, the NLO operators in the Lagrangian are only used as counterterms; that is, at NLO one only computes at tree level with the NLO operators. Since the in/out states used in lattice simulations involve purely valence quarks, we must project the NLO operators onto the purely valence quark sector of the theory. Consequently, all of the spurions which involve the sea quark fields vanish. Since the remaining spurions involve the valence quarks alone, we only encounter the symmetry structure of the valence quarks as far as the NLO operators are concerned. These spurions only depend on quark masses and the quark condensate itself, and so there can be no dependence on lattice discretization effects arising in this way. The exception to this argument arises in the case of double trace operators in the NLO chiral Lagrangian; in these cases the valence and sea sectors interact in a flavor-disconnected manner, unlike the operator in Eq. (4.8). If one trace involves a valence-valence spurion while the other involves a sea-sea spurion, then the trace over the sea may still contribute to a physical quantity, for example the meson masses and decay constants (see Appendix A.1–A.3 for explicit examples). Note that the valence-valence operators which occur in these double trace operators must be proportional to one of the two operators present in the LO chiral Lagrangian, Eq. (4.4). Thus for meson scattering processes, the dependence upon the sea quarks from these double trace operators can only involve a renormalization of the leading order quantities f and B_0. Both

to an a^2 renormalization of all the low energy constants (LEC)s of the low energy theory. Because this operator does not break any of the continuum QCD symmetries, it can not be distinguished through spurion analysis [101]. Of course, an operator of this form is present when the QCD Lagrangian is run from a high scale (say, the weak scale) down to the scale of the lattice, so its effects could in principle be accounted for by performing a perturbative matching computation between the QCD effective Lagrangian at the scale $\mu = a^{-1}$ and the lattice action.

the explicit sea quark mass dependence and the explicit lattice spacing dependence are removed from the scattering processes expressed in terms of the lattice-physical parameters since they are eliminated in favor of the decay constants and meson masses which can simply be measured on the lattice. We therefore conclude that when expressed in lattice-physical parameters, there can be no dependence upon the sea quark masses leading to unphysical PQ counterterms and similarly there can be no dependence upon an unphysical lattice-spacing counterterm.

Let us present another, more physically intuitive argument concerning the absence of sea quark mass dependence in meson scattering processes. To do so, we must digress briefly on $\pi\pi$ scattering in $SU(3)$ chiral perturbation theory. The strange quark mass m_s is a parameter of $SU(3)$ χPT, and so one would expect that the $\pi\pi$ scattering length includes analytic terms involving m_s. However, we can consider a theory in which the strange quark is heavy, so that we may integrate it out; we must then recover $SU(2)$ χPT. Chiral symmetry forces any m_s dependence in the analytic terms of the $\pi\pi$ amplitude to occur in the form $m_\pi^2 m_K^2$. But the only counterterm in the on-shell $SU(2)$ scattering amplitude (Eq. (4.16) with $\tilde{\Delta}_{ju} = 0$) is proportional to m_π^4. It is not possible to absorb $m_\pi^2 m_K^2$ into m_π^4, so there can be no m_s dependence in the $SU(3)$ $\pi\pi$ scattering amplitude. This is indeed the case, as was observed in Ref. [108].

Now, let us return to the PQ and MA theories. For the purposes of this discussion, we can ignore the flavor-neutral and ghost sectors, reducing our theory from an $SU(6|3)$ theory to an $SU(6)$ theory. The sea quark dependence of this $SU(6)$ chiral perturbation theory is analogous to the m_s dependence of $SU(3)$ χPT in our $\pi\pi$ scattering example (as in this process the strange quark of $SU(3)$ only participates as a sea quark). A similar decoupling argument tells us that the sea quark masses cannot affect processes involving the valence

sector provided one uses the analogues of on-shell parameters which are the lattice-physical parameters. We conclude that there can be no analytic dependence on the sea quark masses in a mesonic scattering amplitude. Further, these arguments only depend upon the chiral symmetry of the valence quarks and thus also apply to the lattice spacing dependence.

Now, we shall make these arguments concrete by explicit computations. The NLO Lagrangian describing the valence and sea quark mass dependence is the Gasser-Leutwyler Lagrangian with traces replaced by supertraces:

$$\begin{aligned}\mathcal{L}_{GL} = {} & L_1 \left[\mathrm{str}\left(\partial_\mu \Sigma \partial^\mu \Sigma^\dagger\right)\right]^2 + L_2 \,\mathrm{str}\left(\partial_\mu \Sigma \partial_\nu \Sigma^\dagger\right) \mathrm{str}\left(\partial^\mu \Sigma \partial^\nu \Sigma^\dagger\right) \\ & + L_3 \,\mathrm{str}\left(\partial_\mu \Sigma \partial^\mu \Sigma^\dagger \partial_\nu \Sigma \partial^\nu \Sigma^\dagger\right) + 2B_0 L_4 \,\mathrm{str}\left(\partial_\mu \Sigma \partial^\mu \Sigma^\dagger\right) \mathrm{str}\left(m_q \Sigma^\dagger + \Sigma m_q^\dagger\right) \\ & + 2B_0 L_5 \,\mathrm{str}\left[\partial_\mu \Sigma \partial^\mu \Sigma^\dagger \left(m_q \Sigma^\dagger + \Sigma m_q^\dagger\right)\right] + 4B_0^2 L_6 \left[\mathrm{str}\left(m_q \Sigma^\dagger + \Sigma m_q^\dagger\right)\right]^2 \\ & + 4B_0^2 L_7 \left[\mathrm{str}\left(m_q^\dagger \Sigma - \Sigma^\dagger m_q\right)\right]^2 + 4B_0^2 L_8 \,\mathrm{str}\left(m_q \Sigma^\dagger m_q \Sigma^\dagger + \Sigma m_q^\dagger \Sigma m_q^\dagger\right). \end{aligned} \tag{4.17}$$

Having a concrete expression for the Lagrangian,[16] we can easily show explicitly how the sea quark mass dependence disappears. The key is that when constructing NLO correlation functions of purely valence quarks, we can replace the mesonic matrix Φ in the NLO Lagrangian by a projected matrix

$$\Phi \to P_V \Phi P_V \tag{4.18}$$

where P_V is the projector onto the valence subspace. Therefore the matrix Σ has an

[16]The generators of the PQ and MA theories form graded groups and therefore lack the Cayley-Hamilton identities of $SU(N)$ theories. Therefore, PQ and MA theories have additional operators compared to their χPT counterparts. For example, the $\mathcal{O}(p^4)$ Lagrangian has one additional operator as compared to the Gasser-Leutwyler Lagrangian. However, we do not need to consider the effects of this operator in our analysis as it has been shown that it can be constructed such that it does not contribute to valence quantities until $\mathcal{O}(p^6)$ [112]. This is not generally the case, as is demonstrated by various examples in the baryon sector [8, 59, 122, 158, 159, 160, 161, 14, 162, 163].

expansion of the form

$$\Sigma = 1 + P_V \Phi P_V + \cdots \tag{4.19}$$

Now, insert this expression into Eq. (4.17), and consider only the terms involving non-zero powers of Φ. In the single trace operators, the projectors remove any dependence on the sea quark masses. There is still sea quark mass dependence remaining in the double trace operators proportional to L_4 and L_6 given by

$$\delta\mathcal{L}_{GL} = 4B_0\, L_4\, \mathrm{str}\left(\partial_\mu \Sigma P_V\, \partial^\mu \Sigma^\dagger P_V\right) \mathrm{str}(m_q) + 16 B_0^2\, L_6\, \mathrm{str}\left(m_q \Sigma^\dagger P_V + P_V \Sigma m_q^\dagger\right) \mathrm{str}(m_q). \tag{4.20}$$

However, these operators simply shift f and B_0

$$f^2 \to f^2 + 32 L_4\, B_0\, \mathrm{str}(m_q) \tag{4.21}$$

$$f^2 B_0 \to f^2 B_0 + 64 L_6\, B_0^2\, \mathrm{str}(m_q). \tag{4.22}$$

Since the parameters f and B_0 are eliminated in lattice-physical parameters in favor of the measured decay constants and meson masses, we can remove the dependence of scattering lengths on the sea quark masses by working in lattice-physical parameters. In an analogous way, we can remove all the explicit lattice spacing dependence. The general MA Lagrangian involving valence-valence external states at $\mathcal{O}(\varepsilon_m^2 \varepsilon_a^2)$ can be reduced to the following form

$$\begin{aligned}\delta\mathcal{L}_{MA} = {} & a^2 L_{a^2}^{\partial}\, \mathrm{str}\left(\partial_\mu \Sigma P_V\, \partial^\mu \Sigma^\dagger P_V\right) \mathrm{str}\left(f(P_S \Sigma P_S)\, f'(P_S \Sigma^\dagger P_S)\right) \\ & + a^2\, L_{a^2}^{m_q}\, \mathrm{str}\left(m_q P_V \Sigma^\dagger P_V + P_V \Sigma P_V m_q^\dagger\right) \mathrm{str}\left(g(P_S \Sigma P_S)\, g'(P_S \Sigma^\dagger P_S)\right) + h.c.,\end{aligned} \tag{4.23}$$

where the fs and gs are functions dependent upon the sea-quark lattice action. These then

lead to renormalizations of the LO constants,

$$f^2 \to f^2 + 8a^2\, L^{\partial}_{a^2}\, \mathrm{str}\left(f(P_S\Sigma P_S)\, f'(P_S\Sigma^\dagger P_S)\right)\,,$$
$$f^2 B_0 \to f^2 B_0 + 4a^2\, L^{m_q}_{a^2}\, \mathrm{str}\left(g(P_S\Sigma P_S) g'(P_S\Sigma^\dagger P_S)\right)\,, \tag{4.24}$$

and just as with the sea quark mass dependence, expressing physical quantities in terms of the lattice-physical parameters removes any explicit dependence upon the lattice spacing in mesonic scattering processes.

Together, these results show that at NLO, the only counterterms entering into the extrapolation formulae for mesonic scattering lengths are the same as the counterterms entering into the physical scattering length at NLO. This lack of unphysical counterterms is desirable from the point of view of chiral extrapolations, but it also has another consequence. Loop graphs in quantum field theories are frequently divergent; there must be a counterterm to absorb these divergences in a consistent field theory. Since there is no counterterm proportional to a^2 or the sea quark masses, loop graphs involving these quantities are constrained so that they have no divergence proportional to a^2 or the sea quark masses. This further reduces the possible sources of sea quark or lattice spacing dependence. For example, mixed valence-sea meson masses have lattice spacing shifts, so there can be no divergence involving the valence-sea meson masses. In some cases this constraint is strong enough to force the entire valence-sea mass dependence to cancel from scattering lengths expressed in lattice-physical parameters. If this occurs, then the scattering length will not depend on the unknown constant C_{Mix}.

4.2.2.1 Dependence upon sea quarks

Now, let us move on to discuss how the NLO extrapolation formulae depend on the particular sea quark discretization in use. At NLO in the effective field theory expansion, mesons composed of one or two sea quarks only arise in loop graphs. In particular, the valence-sea mesons can propagate between vertices where they interact with valence-valence mesons; these interactions involve the LO chiral Lagrangian augmented with the mixing term $a^2\mathcal{U}_{VS}$. Because the mixing term is universal, these interaction vertices are the same for all discretization schemes provided LO chiral perturbation theory is applicable. The sea-sea mesons only arise at NLO in hairpins; therefore, they are only sensitive to the quadratic part of the appropriate LO chiral Lagrangian on the sea-sea sector. Thus, we see that our NLO extrapolation formulae only depend on the LO chiral Lagrangian to quadratic order in the sea-sea sector and the LO chiral Lagrangian (with the mixing term) in the valence-sea sector. Together, we see that the condition we require on the sea quark discretization is that the sea-sea sector alone should be described by chiral perturbation theory at LO, and that the constant C_{Mix} should not be so large that its explicit violation of chiral symmetry overwhelms the dynamical violation of chiral symmetry. Non-locality which is described by the replica trick does not present a problem since at the level of perturbation theory the analytic continuation required by the replica method is trivial.

Note that the impact of using different sea quark discretizations in our work is only at the level of the quadratic Lagrangian. Therefore, the same NLO extrapolation formulae can be used to describe simulations with different sea quark discretizations, provided that the appropriate mass shifts are taken into account. In the case of staggered sea quarks, the sea-sea mass splitting which occurs in the MA formulae is that of the taste-identity, which

has been measured [70], and for the coarse MILC lattices is given by

$$a^2\Delta_{sea} = a^2\Delta_I \simeq (450 \text{ MeV})^2 \,, \tag{4.25}$$

for $a \simeq 0.125$ fm. These mass shifts can only appear through the hairpin interactions at this order. These terms will generally be associated with unphysical MA/PQ effects which give rise to the enhanced chiral logarithms as well as additional finite analytic dependence upon the sea-sea as well as valence-valence meson masses (and their associated lattice spacing dependent mass corrections). The exception to this is the dependence upon the η-mass. As can be seen in Eq. (4.12), the only way the η-mass dynamically enters processes involving external pions and kaons through $\mathcal{O}(\varepsilon_m^2\varepsilon_a^2)$ is via the mass of the sea-sea η, Eq. (4.13). The other way these discretization effects enter MA formulae is through the mixed valence-sea meson masses, Eq. (4.10). Currently, this mass shift, $a^2\Delta_{\text{Mix}}$, is not known for any type of sea quark discretization. This is one of the more important MA effects, because it enters many quantities of interest at the one-loop level, for both mesons and baryons, and thus to perform chiral extrapolations properly this mass splitting must be taken into account.

4.2.2.2 Mixed actions at NNLO

It is important to note that these conclusions will not hold at NNLO in the effective field theory expansion. At this order, NNLO terms in the effective Lagrangian will introduce a^2 shifts of the Gasser-Leutwyler parameters themselves. In simulations which are precise enough to be sensitive to NNLO effects in chiral perturbation theory, these effects would have to be removed. In addition, there will be new effects which can not be absorbed into the Gasser-Leutwyler parameters, but are truly new lattice spacing artifacts. The simplest

example to understand is to consider how the pion mass is modified at $\mathcal{O}(\varepsilon_m^4 \varepsilon_a^2)$ in a MA theory with staggered sea quarks [163].

Briefly, there will be contributions to the pion mass which break taste, arising for example from the Gasser-Leutwyler operator in Eq. (4.17) with coefficient L_6. The taste-breaking contributions to the pion mass arise when the valence pion is contracted with the meson fields in one of the super-traces while the other super-trace is taken over sea-sea mesons which form a loop at this order,

$$\delta m_\pi^2(NNLO) = -\frac{64 m_\pi^2}{f^2} L_6 N_s^2 \sum_{F,t} n_t \frac{B_0(m_{s_1} + m_{s_2})}{(4\pi f)^2} \tilde{m}^2_{s_1 s_2, t} \ln\left(\frac{\tilde{m}^2_{s_1 s_2, t}}{\mu^2}\right) , \tag{4.26}$$

where $N_s = 1/4$ is the factor one inserts according to the replica method to account for the 4^{th}-root of the sea quark determinant, and n_t counts the weighting of the mesons of various taste propagating in the loop. The staggered meson mass of flavor F, and taste t, is given at LO by [72, 73, 70]

$$\tilde{m}^2_{s_1 s_2, t} = B_0(m_{s_1} + m_{s_2}) + a^2 \Delta(\xi_t) . \tag{4.27}$$

These taste-breaking effects are unphysical and their associated μ-dependence can only be absorbed by the appropriate unphysical lattice spacing dependent operators arising in the mixed action Lagrangian. This is simply one of many possible examples of how the continuum–like behavior of mixed action theories will break down.

4.3 Applications

In this section, we discuss applications of these results to some specific quantities of physical interest. There have been a number of recent lattice computations [93, 94, 135, 136, 137,

1, 138, 140, 139] utilizing the scheme first developed by the LHP collaboration [91, 164] of employing domain wall valence quarks with the publicly available MILC configurations. In particular, the NPLQCD collaboration has computed the $I = 2$ $\pi\pi$ scattering length [94],[17] f_K/f_π [138] and determined both the $I = 3/2$ and $I = 1/2$ $K\pi$ scattering lengths through a direct determination of the $I = 3/2$ $K\pi$ scattering length [140]. As we will demonstrate by explicit computation, the $I = 1$ KK scattering length, together with the above three systems share only two linearly independent sets of counterterms, which are the physical counterterms of interest. Therefore, these four quantities provide a means to test the mixed action formalism with only one lattice spacing.[18]

4.3.1 f_K/f_π

The pion and kaon decay constants were computed in a mixed action theory with staggered sea quarks in Ref. [103]. In Appendix A.3, we include the general form of these results for arbitrary sea quarks to NLO, which we express in terms of the PQ parameters we introduced in Eq. (4.14). We use these formulae to estimate the error arising from the finite lattice spacing in the recent determination of f_K/f_π in Ref. [138], in which the continuum χPT form of this quantity was used to extrapolate the lattice data to the physical point. The MA functional form of this quantity depends upon the mixed valence-sea meson masses, and so we can not make a concrete prediction of the error made in this approximation,

[17] In addition to the lattice spacing modifications of the $I = 2$ $\pi\pi$ scattering length computed in Chapter 3, the exponential finite volume corrections to this quantity were also computed in Ref. [165]. It was found that for the pion masses in use today, these effects were not significant, being on the order of 1%. It is expected that the exponential volume dependence in the other scattering processes will be similar to that of the two-pion system, as in all cases the pion is the lightest particle and will dominate the long range (finite volume) effects.

[18] Recall that in Chapter 3, we argued that to all orders in perturbation theory, the unitarity violating features of MA and PQ theories do not invalidate the known method of extracting infinite volume scattering parameters from finite volume correlation functions [166, 113, 114] for all "maximally stretched" two-meson states (i.e., the $I = 2$ $\pi\pi$, $I = 3/2$ $K\pi$, and $I = 1$ KK systems).

as the mixed meson mass depends upon $C_{\rm Mix}$, Eq. (4.10), which is currently unknown.[19] Consequently we form the ratio,

$$\Delta\left(\frac{f_K}{f_\pi}\right) = \frac{\left.\frac{f_K}{f_\pi}\right|_{MA} - \left.\frac{f_K}{f_\pi}\right|_{QCD}}{\left.\frac{f_K}{f_\pi}\right|_{QCD}}\,, \tag{4.28}$$

and in Eq. (A.8), we provide the explicit formula for this quantity, with the mass tuning used in Ref. [138] ($m_{q_s} = m_{q_v} \Longrightarrow \tilde{\Delta}^2_{rs} = \tilde{\Delta}^2_{ju} = a^2\Delta_I \simeq (450\text{ MeV})^2$). In Fig. 4.1, we plot this ratio as a function of the mixed meson splitting in the range $-(600\text{ MeV})^2 \lesssim a^2\Delta_{\rm Mix} \lesssim (800\text{ MeV})^2$. We take the value of $L_5(\mu)$ from Ref. [138], as their various fitting procedures produced little variation in the extraction of $L_5(\mu)$. This provides us with an indirect means at estimating the error in the extrapolation of the quantity f_K/f_π. As can be seen from Fig. 4.1, reasonable values of $a^2\Delta_{\rm Mix}$ can produce deviations in f_K/f_π on the order of 5%. These deviations are important enough to include in the fitting procedure (although still within the confidence levels in Ref. [138, 167]), but not significant enough to determine $a^2\Delta_{\rm Mix}$ directly from the data in Ref. [138]. One can also determine the size of the hairpin contributions alone by setting $a^2\Delta_{\rm Mix} = 0$, and, as can be seen in Fig. 4.1, these effects are a fraction of a percent for all values of the pion mass.

It is important to note that at this order, the counterterm structure of f_K/f_π in a MA theory is identical to the counterterm structure of f_K/f_π in χPT, as can be verified by examining Eqs. (A.5) and (A.6),

$$\left.\frac{f_K}{f_\pi}\right|_{MA} \propto \frac{8(m_K^2 - m_\pi^2)}{f^2}\, L_5(\mu)\,. \tag{4.29}$$

[19] In Ref. [145], this quantity was recently estimated by comparing the MA form of the pion form-factor to a MA simulation [93]. Unfortunately, only one of the lattice data points was in the chiral regime, so a precise determination of this quantity was not possible.

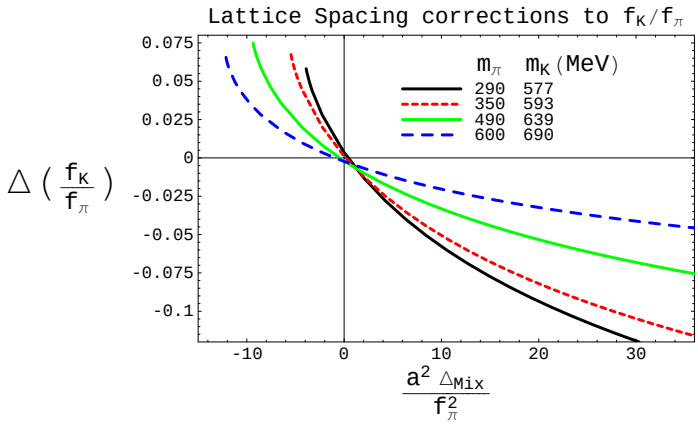

Figure 4.1: We plot the ratio, $\Delta(f_K/f_\pi)$, defined in Eq. (4.28) as a function of the unknown mixed meson mass splitting, $-(600\text{ MeV})^2 \lesssim a^2\Delta_{\text{Mix}} \lesssim (800\text{ MeV})^2$. The observed deviation from the continuum χPT formulae is on the order of 5%, which is important, but not significant enough to directly determine this unknown mass splitting from the MA lattice data of f_K/f_π [138] alone.

This can be understood with the arguments presented in Section 4.2.2, and the knowledge that the lattice spacing artifacts are flavor-blind.

4.3.2 KK $I = 1$ scattering length, $a_{KK}^{I=1}$

Next, we discuss the form of the $I = 1$ KK scattering length, for a MA theory with arbitrary sea quarks, for which the full functional form is provided in Appendix A.5. The two-Kaon system is theoretically ideal for testing the convergence of $SU(3)$ χPT, however experimentally much more difficult to study. But recent progress with lattice QCD simulations has allowed the $I = 1$ KK system to be explored within the MA framework. Thus one can use lattice QCD in combination with the appropriate MA effective field theory to explore the convergence of $SU(3)$ χPT [147], or whether a generalized version of χPT is a more appropriate description of nature [168]. In fact it has only recently been confirmed that the standard $SU(2)$ χPT power counting is phenomenologically correct [169, 170, 171], by comparing our theoretical knowledge of the two-loop $\pi\pi$ scattering [109, 110], the pion

scalar form-factor [172], and the Roy equation analysis [173] with the recent experimental determination of the pion scattering lengths [174, 175].

The $I = 1$ KK system has several features in common with the $I = 2$ $\pi\pi$ system we discussed in Chapter 3. Firstly, the $I = 1$ KK system does not have on-shell hairpins in the s-channel loops. Secondly, the scattering length does not depend upon the mixed valence-sea mesons when expressed in terms of the lattice-physical parameters, and, finally, the only counterterm at NLO is the physical counterterm of interest. The form of the $I = 1$ KK scattering length is given by

$$m_K a_{KK}^{I=1} = -\frac{m_K^2}{8\pi f_K^2}\left\{1 + \frac{m_K^2}{(4\pi f_K)^2}\left[C_\pi \ln\left(\frac{m_\pi^2}{\mu^2}\right) + C_K \ln\left(\frac{m_K^2}{\mu^2}\right) + C_X \ln\left(\frac{\tilde{m}_X^2}{\mu^2}\right) + C_{ss} \ln\left(\frac{m_{ss}^2}{\mu^2}\right) + C_0 - 32(4\pi)^2 L_{KK}^{I=1}(\mu)\right]\right\}, \quad (4.30)$$

where the various coefficients, C_ϕ, are provided in Eqs. (A.15)–(A.18).

One important point is that the counterterm for the $I = 1$ scattering length, $L_{KK}^{I=1}$, is identical to the $I = 2$ $\pi\pi$ scattering length counterterm,

$$L_{KK}^{I=1} = L_{\pi\pi}^{I=2} = 2L_1 + 2L_2 + L_3 - 2L_4 - L_5 + 2L_6 + L_8\,. \quad (4.31)$$

Before discussing this scattering length in more detail, we first give the result in χPT, as this has not been presented in the literature to the authors' knowledge.

$$m_K a_{KK}^{I=1} = -\frac{m_K^2}{8\pi f_K^2}\left\{1 + \frac{m_K^2}{(4\pi f_K)^2}\left[2\ln\left(\frac{m_K^2}{\mu^2}\right) - \frac{2m_\pi^2}{3(m_\eta^2 - m_\pi^2)} \ln\left(\frac{m_\pi^2}{\mu^2}\right) + \frac{2(20m_K^2 - 11m_\pi^2)}{27(m_\eta^2 - m_\pi^2)} \ln\left(\frac{m_\eta^2}{\mu^2}\right) - \frac{14}{9} - 32(4\pi)^2 L_{KK}^{I=1}(\mu)\right]\right\}, \quad (4.32)$$

Table 4.1: Hairpin contributions to $m_\pi a_{\pi\pi}^{I=2}$. We provide the various hairpin contributions to the $I = 2$ $\pi\pi$ scattering length for both the 2-sea flavor, (b), and 3-sea flavor theory, (d), which we compare to the χPT NLO contribution, (a), and LO contribution, top row. In row (c), we give the new hairpin effects which arise in the 3-flavor theory, and in (d) we provide the total 3-sea flavor hairpin effects.

	m_π (MeV)	293	354	493	592
	$-\frac{m_\pi^2}{8\pi f_\pi^2}$	-0.156	-0.218	-0.372	-0.483
(a)	$-\frac{2\pi m_\pi^4}{(4\pi f_\pi)^4}\left[3\ln\left(\frac{m_\pi^2}{\mu^2}\right) - 1 - l_{\pi\pi}^{I=2}(\mu)\right]$	0.00460	0.00140	-0.0314	-0.0818
(b)	$-\frac{2\pi m_\pi^4}{(4\pi f_\pi)^4}\left[-\frac{\tilde{\Delta}_{ju}^4}{6m_\pi^4}\right]$	0.00359	0.00327	0.00254	0.00207
(c)	$-\frac{2\pi m_\pi^4}{(4\pi f_\pi)^4}\left[\sum_{n=1}^4\left(\frac{\tilde{\Delta}_{ju}}{m_\pi^2}\right)^n \mathcal{F}_n(m_\pi^2/\tilde{m}_X^2)\right]$	-0.00243	-0.00289	-0.00371	-0.00396
(d)	$-\frac{2\pi m_\pi^4}{(4\pi f_\pi)^4}\left[-\frac{\tilde{\Delta}_{ju}^4}{6m_\pi^4} + \sum_{n=1}^4\left(\frac{\tilde{\Delta}_{ju}}{m_\pi^2}\right)^n \mathcal{F}_n(m_\pi^2/\tilde{m}_X^2)\right]$	0.00116	0.00040	-0.00117	-0.00188

with $L_{KK}^{I=1}$ given in Eq. (4.31), and we have used the leading order meson mass relations to simplify the form of this expression.

The equality of the $I = 2$ $\pi\pi$ and $I = 1$ KK scattering length counterterms allows us to make a prediction for the numerical values of $m_K a_{KK}^{I=1}$ one should obtain in a simulation of this system with domain-wall valence quarks on the MILC configurations. To do this, we must first convert the counterterm, $l_{\pi\pi}(\mu)$ obtained by NPLQCD in Ref. [94] from the effective theory with two sea flavors to the theory with three sea flavors. For PQ and MA theories, there is an additional subtlety which arises in this matching. If we match the χPT forms of $m_\pi a_{\pi\pi}^{I=2}$ in $SU(2)$ to $SU(3)$, then we arrive at the equality (with the conventions defined in Appendix A.4)

$$l_{\pi\pi}^{I=2}(\mu) = 32(4\pi)^2\, L_{\pi\pi}^{I=2}(\mu) - \frac{1}{9}\,\ln\left(\frac{m_\eta^2}{\mu^2}\right) - \frac{1}{9}\,. \tag{4.33}$$

This leads to an exact matching between the $SU(2)$ and $SU(3)$ theories, in which all of the strange quark mass dependence at this order, which is purely logarithmic, is absorbed in the $SU(2)$ Gasser-Leutwyler coefficients [147]. If we naively attempt to match the $SU(4|2)$ to $SU(6|3)$ MA/PQ expressions for $m_\pi a_{\pi\pi}^{I=2}$, using Eqs. (A.9) and (A.10), one arrives at the

relation

$$l_{\pi\pi}^{I=2}(\mu) = \; 32(4\pi)^2\, L_{\pi\pi}^{I=2}(\mu) - \frac{1}{9}\,\ln\left(\frac{\tilde{m}_X^2}{\mu^2}\right) - \frac{1}{9} \; - \sum_{n=1}^{4}\left(\frac{\tilde{\Delta}_{ju}^2}{m_\pi^2}\right)^n \mathcal{F}_n(m_\pi^2/\tilde{m}_X^2)\,, \qquad (4.34)$$

where the functions, $\mathcal{F}_n(y)$ were determined in Chapter 3 and are given in Eqs. (3.38). All of the new terms in this matching arise from the extra hairpin interactions present in the $SU(6|3)$ theory which are not present in $SU(4|2)$. One can show that these terms are formally higher order in the $SU(4|2)$ chiral expansion, but nevertheless we will see that they are not negligible.

The NPLQCD collaboration has recently computed $m_\pi a_{\pi\pi}^{I=2}$ and used the $SU(2)$ extrapolation formula to determine $l_{\pi\pi}^{I=2}$ [94]. Adjusting for conventions and including their largest uncertainty, they determined

$$l_{\pi\pi}^{I=2}(4\pi f_\pi) \simeq -10.9 \pm 1.8\,. \qquad (4.35)$$

Starting with this determination, we can then compare the hairpin contributions in $SU(4|2)$ to those of $SU(6|3)$ and also to the physical contribution at NLO. We collect these results in Table 4.1.

The two-flavor hairpin effects, listed in row (b) of Table 4.1, are not small relative to the (scale independent) χPT NLO contributions (a), and for the lightest two masses shown, are of the same order of magnitude. However, when we consider the three-flavor theory, we see that the additional hairpin effects, (c), are of the same order as the two-flavor hairpin contributions (which also contribute in the three-flavor theory), but opposite in sign. Taking into account all of the hairpin contributions by using the three-flavor theory, one observes that the sum of these unphysical effects, (d), is approximately an order of

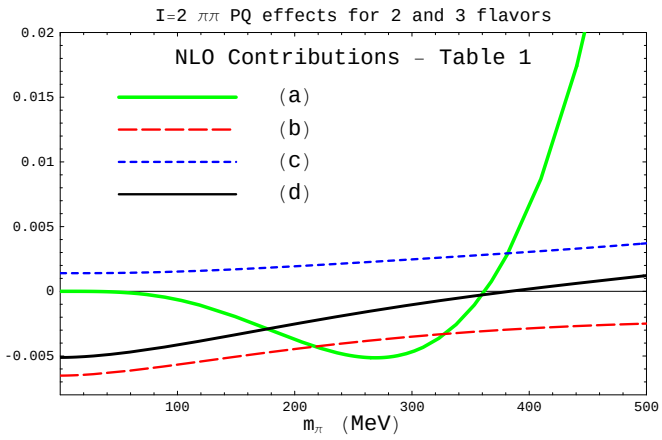

Figure 4.2: We plot the absolute values of the various NLO contributions to $m_\pi a_{\pi\pi}^{I=2}$ listed in Table 4.1. The NLO χPT contribution is given by (a) (green), which demonstrates the large cancellation of the counterterm and the chiral log for light to medium pion masses. The long-dashed curve (red) is the 2-sea flavor hairpin effects, (b), which are the same order of magnitude as (a), for $m_\pi \lesssim 400$ MeV. When the new 3-sea flavor hairpin effects, (c) (blue), are added to the 2-sea flavor effects, one finds that the total 3-sea flavor hairpin effects, (d) (black), are small compared to (a) for $m_\pi \gtrsim 250$ MeV.

magnitude smaller than the physical NLO effects of χPT, but increases in importance as the pion mass is reduced. This justifies our assumption of the determination of $l_{\pi\pi}^{I=2}$ given in Eq. (4.35). This also justifies the $SU(3) \to SU(2)$ matching given in Eq. (4.33), and explains the success found in Ref. [94] of using the $SU(2)$ χPT formula to determine $l_{\pi\pi}^{I=2}$, as the unphysical hairpin corrections to this formula provide a relative shift of about 10% to the NLO contributions for the masses simulated, which is roughly the size of their largest quoted error.

In Fig. 4.2, we plot the absolute values of the various NLO contributions to the $I = 2$ $\pi\pi$ scattering length as a function of the pion mass, which highlight the importance of these hairpin effects. Their relative importance is enhanced for the values listed in Table 4.1 because of the large cancellation of the counterterm and chiral log at NLO, (a). It is clear that these effects will become more important as one moves further into the chiral regime, $(m_\pi \to 0)$.

Table 4.2: Predictions of $m_K a_{KK}^{I=1}$. We use the equality of the $m_K a_{KK}^{I=1}$ and $m_\pi a_{\pi\pi}^{I=2}$ counterterms (expressed in lattice-physical parameters) to predict the values of $m_K a_{KK}^{I=1}$ which would be computed in a MA lattice formulation with domain wall valence quarks on the MILC staggered sea quarks, which we compare both to the tree level prediction as well as the $SU(3)$ χPT prediction, for values of m_K/f_K taken from Refs. [94, 138]. We also provide a prediction of the scattering length at the physical point. The first error is due to the uncertainty in the determination of $L_{KK}^{I=1}$ from Eq. (4.34) and the value of $l_{\pi\pi}^{I=2}$, Eq. (4.35), determined in Ref. [94]. The second error is a power counting estimate of the NNLO contributions to the scattering length.

$m_K : f_K$ (MeV)	577 : 172	593 : 171	639 : 173	690 : 177
$m_K a_{KK}^{I=1}$(LO): $-\frac{m_K^2}{8\pi f_K^2}$	-0.447	-0.479	-0.542	-0.605
$m_K a_{KK}^{I=1}$(NLO: MA)	-0.091	-0.113	-0.162	-0.223
$m_K a_{KK}^{I=1}$(NLO: $SU(3)$)	-0.084	-0.107	-0.157	-0.217
$m_K a_{KK}^{I=1}$(MA)	$-0.540 \pm 0.069 \pm 0.026$	$-0.592 \pm 0.079 \pm 0.031$	$-0.704 \pm 0.102 \pm 0.048$	$-0.828 \pm 0.127 \pm 0.072$
$m_K a_{KK}^{I=1}(SU(3))$	$-0.531 \pm 0.069 \pm 0.026$	$-0.586 \pm 0.079 \pm 0.031$	$-0.699 \pm 0.102 \pm 0.048$	$-0.823 \pm 0.127 \pm 0.072$
physical point	496 : 161			
$m_K a_{KK}^{I=1}(SU(3))$	$-0.424 \pm 0.049 \pm 0.012$			

Given the small contribution of the NLO hairpin effects to $m_\pi a_{\pi\pi}^{I=2}$, we can use the determination of $l_{\pi\pi}^{I=2}(\mu)$ in Eq. (4.35) [94], and the matching of Eq. (4.33) to determine $L_{KK}^{I=1}(\mu)$ and thus predict values of $m_K a_{KK}^{I=1}$, which we provide in Table 4.2. We provide both the comparison of the NLO effects as predicted by both the MA theory as well as $SU(3)$ χPT, which we compare to the tree-level prediction, as well as the total scattering length through NLO. We find that similar to $m_\pi a_{\pi\pi}^{I=2}$, the NLO hairpin effects for $m_K a_{KK}^{I=1}$ are only about 10% of the NLO χPT value, less than the accuracy we claim here. We find that a current MA lattice determination of $m_K a_{KK}^{I=1}$ will not be sensitive to the unphysical hairpin contributions with the expected level of uncertainty, as can be seen by the predicted MA and $SU(3)$ values. However, for both the MA and $SU(3)$ theories, the NLO contributions are 15–30% correction to the LO term showing a convergence expected by power counting.

The first error is due to the uncertainty in the determination of $L_{KK}^{I=1}$ we obtain from the matching in Eq. (4.34) and the extraction of $l_{\pi\pi}^{I=2}$ from Ref. [94], Eq. (4.35). This uncertainty includes estimations of the two-loop contributions to $m_\pi a_{\pi\pi}^{I=2}$ in $SU(2)$ χPT. The second uncertainty listed in Table 4.2 is a power counting estimation of the NNLO contributions to $m_K a_{KK}^{I=1}$. Some of these effects are already included in the first uncertainty

but a conservative estimate of our predicted error is to add these uncertainties in quadrature.

4.3.3 $K\pi$ $I = 3/2$ scattering length, $a_{K\pi}^{I=3/2}$

The $K\pi$ system is also an interesting laboratory for exploring the three-flavor structure of low-energy hadron interactions, and moreover it is experimentally accessible with proposed studies by the DIRAC collaboration [176]. There has recently been a direct MA lattice QCD determination of the $I = 3/2$ $K\pi$ scattering length, which in combination with the theoretical knowledge of the NLO χPT $I = 1/2$ and $I = 3/2$ $K\pi$ scattering lengths [177, 178, 179, 180] has allowed a determination of both isospin scattering lengths [140]. There is additionally a two-loop computation of $K\pi$ scattering in $SU(3)$ χPT which studies the convergence of the theory with standard power counting [181]. Before embarking on a study of the two-loop effects with lattice QCD, one must first understand the lattice corrections at NLO. This is the motivation for this section.

The tree level $I = 3/2$ $K\pi$ scattering length is given by

$$\begin{aligned}(m_\pi + m_K) a_{K\pi}^{I=3/2} &= -\frac{m_\pi m_K}{4\pi f_K f_\pi}\,, \text{ or} \\ \mu_{K\pi} a_{K\pi}^{I=3/2} &= -\frac{\mu_{K\pi}^2}{4\pi f_K f_\pi}\,, \end{aligned} \tag{4.36}$$

where $\mu_{K\pi}$ is the reduced mass of the $K\pi$ system. We chose to express our extrapolation formulae in terms of the product $f_K f_\pi$ since this symmetric treatment of the K and π mesons provides the simplest form of the scattering length. We find, however, that the $I = \frac{3}{2}$ scattering length still depends on the mixed valence-sea meson masses, and therefore on the parameter C_{Mix}. Consequently, accurate chiral extrapolations of this scattering length will require a determination of the value of C_{Mix} appropriate to the particular sea

quark discretization used in the simulation. The form of the MA $I = 3/2$ $K\pi$ scattering length is

$$\mu_{K\pi} a_{K\pi}^{I=3/2} = -\frac{\mu_{K\pi}^2}{4\pi f_K f_\pi}\left[1 - \frac{32 m_K m_\pi}{f_K f_\pi} L_{\pi\pi}^{I=2}(\mu) + \frac{8(m_K - m_\pi)^2}{f_K f_\pi} L_5(\mu)\right] + \mu_{K\pi}\left[a_{vv}^{K\pi,3/2}(\mu) + a_{vs}^{K\pi,3/2}(\mu)\right], \quad (4.37)$$

where $a_{vv}^{K\pi,3/2}(\mu)$ is the valence-valence (including valence-ghost) contribution to the scattering length and $a_{vs}^{K\pi,3/2}(\mu)$ is a non-vanishing contribution from mixed valence-sea mesons to the scattering length. The other important thing to note is that there are two counterterms for this scattering length which can both be determined through its chiral extrapolation formula, but can also independently be determined in other processes; $L_5(\mu)$ can be determined independently by f_K/f_π and $L_{\pi\pi}^{I=3/2}(\mu)$ can be determined either with $I = 2$ $\pi\pi$ or $I = 1$ KK scattering. Now we have explicitly demonstrated that the four observable quantities, $a_{\pi\pi}^{I=2}$, $a_{KK}^{I=1}$, $a_{K\pi}^{I=3/2}$, and f_K/f_π, when expressed in terms of the lattice-physical parameters, only share two linearly independent counterterms through NLO in MA (and PQ) χPT.

Before continuing, we provide the continuum $SU(3)$ χPT form of $a_{K\pi}^{I=3/2}$, which is the same as can be constructed from Ref. [180] with the NLO shift of $f_K \to f_\pi$,

$$\mu_{K\pi}\, a_{K\pi}^{I=3/2} = -\frac{\mu_{K\pi}^2}{4\pi f_K f_\pi}\left\{1 + \frac{1}{(4\pi)^2 f_K f_\pi}\left[\kappa_\pi \ln\frac{m_\pi^2}{\mu^2} + \kappa_K \ln\frac{m_K^2}{\mu^2} + \kappa_\eta \ln\frac{m_\eta^2}{\mu^2} - \frac{86}{9} m_K m_\pi + \kappa_t \arctan\frac{2(m_K - m_\pi)\sqrt{2m_K^2 + m_K m_\pi - m_\pi^2}}{(2m_K - m_\pi)(m_K + 2m_\pi)}\right] - \frac{32 m_K m_\pi}{f_K f_\pi} L_{\pi\pi}^{I=2} + \frac{8(m_K - m_\pi)^2}{f_K f_\pi} L_5\right\}, \quad (4.38)$$

with

$$\kappa_\pi = -\frac{m_\pi^2}{4}\frac{11m_K^2 + 22m_K m_\pi - 5m_\pi^2}{m_K^2 - m_\pi^2}\,, \tag{4.39}$$

$$\kappa_K = \frac{m_K}{18}\frac{134m_K^2 m_\pi - 9m_K^3 + 55m_K m_\pi^2 - 16m_\pi^3}{m_K^2 - m_\pi^2}\,, \tag{4.40}$$

$$\kappa_\eta = \frac{-36m_K^3 - 12m_K^2 m_\pi + m_K m_\pi^2 + 9m_\pi^3}{36(m_K - m_\pi)}\,, \tag{4.41}$$

$$\kappa_t = \frac{16m_K m_\pi}{9}\frac{\sqrt{2m_K^2 + m_K m_\pi - m_\pi^2}}{m_K - m_\pi}\,. \tag{4.42}$$

In Appendix A.6, we provide the full form of the MA $I = 3/2$ $K\pi$ scattering length. Here we wish to examine the valence-sea contribution in more detail. This contribution to the scattering length is given by[20]

$$\mu_{K\pi}\, a_{vs}^{K\pi,3/2}(\mu) = -\frac{\mu_{K\pi}^2}{4\pi f_K f_\pi}\frac{1}{2(4\pi)^2 f_K f_\pi}\sum_{F=j,l,r}\left[C_{Fs}\ln\frac{\tilde{m}_{Fs}^2}{\mu^2} - C_{Fd}\ln\frac{\tilde{m}_{Fd}^2}{\mu^2} + 4m_K m_\pi J(\tilde{m}_{Fd}^2)\right], \tag{4.43}$$

where

$$C_{Fs} = \frac{4m_K^2 m_\pi - \tilde{m}_{Fs}^2(m_K + m_\pi)}{m_K - m_\pi}\,, \tag{4.44}$$

$$C_{Fd} = \frac{4m_K m_\pi^2 - \tilde{m}_{Fd}^2(m_K + m_\pi)}{m_K - m_\pi}\,, \tag{4.45}$$

$$J(M) = 2\frac{\sqrt{M^2 - m_\pi^2}}{m_K - m_\pi}\arctan\left(\frac{(m_K - m_\pi)\sqrt{M^2 - m_\pi^2}}{M^2 + m_K m_\pi - m_\pi^2}\right) - m_K m_\pi\,. \tag{4.46}$$

[20] We note that the summation over sea flavor, F, implicitly includes the appropriate factors for staggered sea quarks, the sum over taste and the factors of $N_s = 1/4$ which arise from the 4^{th}-rooting trick. For other kinds of quark, this is simply a sum over the sea flavors, j, l, and r.

The scale dependence in $a_{vs}^{K\pi,3/2}(\mu)$ can be shown to be

$$a_{vs}^{K\pi,3/2}(\mu) \propto \sum_{F=j,l,r} -\ln(\mu^2)(m_K - m_\pi)^2\,, \tag{4.47}$$

and as claimed, independent of both the lattice spacing, a, and the sea quark masses, and is absorbed by $L_5(\mu)$. We stress again that the $I = 3/2$ $K\pi$ scattering length depends upon mixed valence-sea mesons, which receive lattice spacing dependent mass shifts proportional to the unknown quantity, $C_{\rm Mix}$. This quantity is currently unknown for all variants of MA lattice QCD and must be determined for a correct extrapolation of MA lattice QCD simulations. For this reason, we do not provide a table with post-dictions of $\mu_{K\pi} a_{K\pi}^{I=3/2}$.

4.4 Discussion

Mixed action simulations provide a promising solution to the problem of performing fully dynamical simulations with light quarks which are under theoretical control. This chapter shows that mixed action simulations with Ginsparg-Wilson valence quarks are theoretically clean. We have shown that the counterterms appearing in mesonic scattering lengths are precisely those that occur in QCD, so that one can, in principle measure these counterterms with a single lattice spacing. We also find that the same chiral extrapolation formulae can be used to describe mixed action simulations with GW quarks with mild restrictions on the type of sea quark discretization used—provided, of course, that QCD is recovered in the continuum limit. Thus, our results hold for simulations with domain wall and overlap quarks, Wilson quarks ($\mathcal{O}(a)$ improved and twisted mass quarks at maximal twist) as well as simulations using rooted staggered quarks (assuming that the 4^{th}-rooting procedure is valid and that the replica method correctly captures all of the non-locality introduced by

the rooting procedure - which has been argued to all orders in perturbation theory [182]).

We previously observed in Chapter 3 that the $\pi\pi$ scattering length does not depend on the parameter $C_{\rm Mix}$ of mixed action chiral perturbation theory. In this chapter, we find that this also holds for the KK scattering length. However, the $K\pi$ scattering length does depend on $C_{\rm Mix}$, and, therefore, accurate chiral extrapolations of mixed action data will require a measurement of this quantity. However, we have also computed the ratio f_K/f_π in mixed action chiral perturbation theory, which depends upon on $C_{\rm Mix}$. By varying $C_{\rm Mix}$ over a broad range of values, we find the impact to be modest, on the order of 5%. In addition, taking into account the small hairpin corrections to $m_\pi a_{\pi\pi}^{I=2}$ discussed in Chapter 3 and the equally small predicted corrections to $m_K a_{KK}^{I=1}$, Table 4.2, we expect the impact of $C_{\rm Mix}$ on $a_{K\pi}^{I=3/2}$ to also be small at this order of precision, $\mathcal{O}(\varepsilon_m^4, \varepsilon_m^2\varepsilon_a^2, \varepsilon_a^4)$. In Table 4.2 we provide predictions of $m_K a_{KK}^{I=1}$ for various values of m_K and also provide a prediction at the physical point.

In Section 4.2.2, we have demonstrated why the use of lattice-physical parameters (or on-shell renormalization) significantly simplifies the form of the extrapolation formulae for mesonic systems. We stress that these arguments do not depend upon the momentum of the system, nor upon having only two external mesons, and thus will be applicable not just for scattering lengths, but also for other scattering parameters, such as the effective range, as well as for $N > 2$ mesonic systems. In the appendix we have provided explicit NLO extrapolation formulae for the meson masses and decay constants as well as the three scattering lengths discussed in this chapter, for arbitrary sea quark discretization schemes, expressed in terms of the PQ parameters we introduced in Eq. (4.14). A thorough understanding of the lattice spacing effects at this order will require knowledge of the counterterms in the masses and decay constants.

We would like to conclude with a small point and a few suggestions. If one is interested in removing the unitarity violating effects in MA lattice simulations, for the low-energy dynamics of the system, then theoretical analysis unambiguously advocates the tuning $\tilde{\Delta}_{rs} = \tilde{\Delta}_{ju} = 0$, which is the generalization of $m_{q_{sea}} - m_{q_{val}} = 0$ for PQ theories. This is the most QCD-like scenario for MA theories in which the unitarity violating double pole propagators in Eq. (4.12) are tuned to zero. It has recently been shown that this double-pole structure of the flavor-neutral propagators persists to all orders in PQχPT [183], and thus this will be the appropriate tuning to higher orders as well. From the point of view of doing chiral physics, this is not desirable for the coarse MILC lattices, as the lattice spacing shift to the taste-identity staggered mesons is $a^2\Delta_I \simeq (450 \text{ MeV})^2$, which would make for heavy pions. Therefore we caution users of MA lattice simulations to remember the existence of these unitarity violating effects present in current MA simulations.

The simplified form of MA/PQ extrapolation formulae for the two-meson systems is particularly dependent upon the implications of the chiral symmetry of the valence quarks. However, we conjecture that a similar, but not as strong, simplification will occur for other hadronic observables, in particular for nuclear physics as well as heavy meson observables, if also expressed in terms of lattice-physical parameters, which will lead to improved chiral extrapolations. This is supported by the recent fits of the NPLQCD collaboration [94, 136, 137, 1, 138, 140] and the LHP collaboration [184]. Based upon our theoretical understanding of effective field theories designed to incorporate lattice spacing artifacts, we expect that even for fermion discretization schemes which do not have chiral symmetry, the use of lattice-physical parameters (on-shell renormalization) will in general simplify the chiral extrapolation formulae and improve chiral fits.

Chapter 5

Minimal Extension of the Standard Model Scalar Sector

5.1 Introduction

We now turn our attention away from QCD and toward more speculative physics. For the rest of this thesis, our attention will be occupied by possible extensions of the standard model. We open with a discussion of the simplest extension of the scalar sector. In Chapter 6 we will consider fundamental limitations on effective descriptions of physics at high energies. These constraints are nothing but limitations on the signs of operators in effective Lagrangians. We then move on in Chapter 7 to discuss a specific attempt [10] to change the sign of an operator via a quantum correction; this attempt turns out to be regulator dependent. In Chapters 8 and 9 we consider a new extension of the standard model which solves the hierarchy puzzle.

The scalar sector of the standard model has not been tested directly by experiment, so it is certainly worth examining models with simple extensions of this sector and exploring their phenomenology in some detail. There does not seem to be a compelling motivation for a scalar sector that consists of just a single Higgs doublet. However, if one does not adopt additional symmetry principles [185, 186] then adding more doublets typically gives

unacceptably large tree-level flavor-changing neutral currents. Furthermore scalar fields with nontrivial $SU(2)\times U(1)$ quantum numbers that are different from those of the standard model Higgs doublet must have small vacuum expectation values to preserve the standard model value of the ρ parameter. The phenomenology of the standard model Higgs scalar, models with multiple Higgs doublets, and of supersymmetric extensions of the standard model has been studied extensively, and Ref. [187] contains some excellent reviews.

The simplest extension of the scalar sector of the minimal standard model is to add a single real scalar S that is a gauge singlet. This does not have to be a fundamental degree of freedom; the Higgs doublet and this scalar might be the only light remnants of a more complicated scalar sector that manifests itself at scales that are too high to be directly probed by the next generation of accelerator experiments. In this paper we examine the phenomenology of this extension of the standard model. Extensions of the minimal standard model with one or more singlets S have been studied before in the literature. Many of the models impose a $S \to -S$ symmetry, so that the singlet can be a dark matter candidate. Other works (for example, see Ref. [188]) either do not impose a $S \to -S$ symmetry or break that symmetry, but have some differences with the model we present here (e.g., some possible couplings in the scalar potential are missing, or the lighter scalar is taken to be massless, etc.) In any case, it seems worth reexamining the phenomenology of this model since we are approaching the LHC era. Our work was inspired by Ref. [189], where an additional scalar superfield was added to the minimal supersymmetric standard model to solve the μ problem, and some of our conclusions are similar to theirs.[1]

In the minimal standard model the scalar potential for the Higgs doublet H contains only two parameters which can be eliminated in favor of the Higgs particle mass and the

[1] See also Ref. [190].

vacuum expectation value that breaks $SU(2) \times U(1)$ gauge symmetry. When the singlet scalar S is added the number of parameters of the scalar potential swells to seven. However for most of the phenomenology only a few parameters are relevant, and a very simple picture emerges. The singlet scalar S and the Higgs scalar h mix, and both of the resulting physical particles have couplings to quarks, leptons, and gauge bosons that are proportional to those of the standard model Higgs particle. In addition to decays to the standard model fermions and gauge bosons, the heavier of these two scalar particles may decay to a pair of the lighter ones.

In this brief report we focus on the region of parameter space where the lighter of the two scalar particles is mostly singlet and has a small enough mass so that it can be pair produced in decays of the heavier (mostly) Higgs scalar. This will be the most interesting case for LHC physics. The only new parameters (beyond those in the standard model) that are needed to characterize most of the phenomenology of this model are the $h - S$ mixing angle, the mass of the new light scalar particle, and the branching ratio for the decay of the heavier Higgs scalar to a pair of the lighter ones.

5.2 Scalar Potential

The Lagrange density for the scalar sector of this model is

$$\mathcal{L} = (D_\mu H)^\dagger D^\mu H + \frac{1}{2}\partial_\mu S \partial^\mu S - V(H, S), \tag{5.1}$$

where H denotes the complex Higgs doublet and S the real scalar. Without loss of generality, we shift the field S so it has no vacuum expectation value. Then the potential is given by

$$V(H,S) = \frac{m^2}{2}H^\dagger H + \frac{\lambda}{4}(H^\dagger H)^2 + \frac{\delta_1}{2}H^\dagger H\ S \\ +\frac{\delta_2}{2}H^\dagger H\ S^2 + \left(\frac{\delta_1 m^2}{2\lambda}\right)S + \frac{\kappa_2}{2}S^2 + \frac{\kappa_3}{3}S^3 + \frac{\kappa_4}{4}S^4. \tag{5.2}$$

Note that there is no additional CP violation that comes from the scalar potential.

In unitary gauge the charged component of the Higgs doublet H becomes the longitudinal components of the charged W-bosons and the imaginary part of the neutral component becomes the longitudinal component of the Z-boson. The neutral component is written as

$$H^0 = \frac{v+h}{\sqrt{2}}, \qquad v = \sqrt{\frac{-2m^2}{\lambda}}. \tag{5.3}$$

The mass terms in the scalar potential become

$$V_{\text{mass}} = \frac{1}{2}\left(\mu_h^2 h^2 + \mu_S^2 S^2 + \mu_{hS}^2 hS\right), \tag{5.4}$$

where

$$\mu_h^2 = -m^2 = \lambda v^2/2 \\ \mu_S^2 = \kappa_2 + \delta_2 v^2/2 \\ \mu_{hS}^2 = \delta_1 v. \tag{5.5}$$

The mass eigenstate fields h_+ and h_- are linear combinations of the Higgs scalar field h

and the singlet scalar field S. Explicitly, for the lighter field h_-

$$h_- = \cos\theta\ S - \sin\theta\ h, \tag{5.6}$$

where [188]

$$\tan\theta = \frac{x}{1+\sqrt{1+x^2}}, \quad x = \frac{\mu_{hS}^2}{\mu_h^2 - \mu_S^2}. \tag{5.7}$$

The terms in the scalar potential that break the discrete $S \to -S$ symmetry are proportional to the couplings δ_1 and κ_3 so it is natural for those scalar couplings to be small. The parameter δ_1 controls the mixing of the two scalar states. As we will see, experimental constraints force the mixing angle θ to be small. We assume the heavier state is mostly the Higgs scalar so $\mu_h^2 > \mu_S^2$. The masses of the two scalars are

$$m_\pm^2 = \left(\frac{\mu_h^2 + \mu_S^2}{2}\right) \pm \left(\frac{\mu_h^2 - \mu_S^2}{2}\right)\sqrt{1+x^2}. \tag{5.8}$$

5.3 Phenomenology

The lighter scalar state decays to standard model particles and its couplings to them are proportional to the standard model Higgs couplings with constant of proportionality $\sin\theta$. Consequently, the lighter of the two states has branching ratios equal to those of the standard model Higgs (if it had mass m_-) and its production rates are $\sin^2\theta$ times the production rates for a standard model Higgs (if it had mass m_-). Since $\sin\theta$ can be much smaller than unity, m_- can be much smaller than the mass of the standard model Higgs, which is restricted by the LEP bound to be heavier than 114 GeV.

If $m_+ < 2m_-$ then the heavier state has branching ratios to standard model particles and

production rates approximately equal to those of the standard model Higgs scalar (recall we are working in the limit of small mixing). However if $m_+ > 2m_-$ then the decay channel $h_+ \to h_- h_-$ is available with partial decay width

$$\Gamma(h_+ \to h_- h_-) = \frac{\delta_2^2 v^2}{32\pi m_+}\sqrt{1 - 4m_-^2/m_+^2}. \tag{5.9}$$

For a h_+ that has mass below 140GeV its dominant decay mode to standard model particles is to a bottom-antibottom pair and so in this mass range

$$\frac{\Gamma(h_+ \to h_- h_-)}{\Gamma^{\text{S.M.}}(h)} \simeq \frac{\delta_2^2 v^4}{6m_+^2 m_b^2}\sqrt{1 - 4m_-^2/m_+^2}, \tag{5.10}$$

where $\Gamma^{\text{S.M.}}(h)$ denotes the decay width of the standard model Higgs. Conventional branching ratios of the heavier scalar h_+ are reduced from those of the standard model Higgs by a factor f which is equal to

$$f = \frac{1}{1 + \Gamma(h_+ \to h_- h_-)/\Gamma^{\text{S.M.}}(h)} = 1 - \text{Br}(h_+ \to h_- h_-). \tag{5.11}$$

5.3.1 Very Light h_-

If m_- is much smaller than the weak scale it seems most natural to take $|\delta_2|$ to be of order $2m_-^2/v^2$ or smaller, since if it is much larger than this a strong cancellation between the two terms contributing to μ_S^2 in Eq. (5.5) is necessary. Suppose m_- is less than the b-quark mass, m_b. With $|\delta_2| \sim 2m_-^2/v^2$ we find that in this region of parameter space f is very close to unity since $\Gamma(h_+ \to h_- h_-)/\Gamma^{\text{S.M.}}(h) \sim (m_-/m_b)^2(m_-/m_+)^2 \ll 1$. The heavier scalar state will behave much like the standard model Higgs particle.

The properties of a very light h_- are severely constrained by present experimental data.

Consider, for example, the case where $m_- = 500$ MeV. Then the branching ratio of the h_+ to two h_-s is very small and the h_+ is indistinguishable from the standard model Higgs particle. The dominant decay modes of the h_- are to two pions and to $\mu^+\mu^-$ with partial decay rates[2],

$$\Gamma(h_- \to \pi^+\pi^-) = 2\Gamma(h_- \to \pi^0\pi^0) = \frac{\sin^2\theta\ m_-^3}{324v^2\pi} \times \left[1 + \frac{11}{2}\left(\frac{m_\pi^2}{m_-^2}\right)\right]^2 \sqrt{1 - \frac{4m_\pi^2}{m_-^2}}, \tag{5.12}$$

and

$$\Gamma(h_- \to \mu^+\mu^-) = \frac{\sin^2\theta\ m_- m_\mu^2}{8v^2\pi}\left[1 - \frac{4m_\mu^2}{m_-^2}\right]^{3/2}. \tag{5.13}$$

These imply that $\mathrm{Br}(h_- \to \mu^+\mu^-) \simeq 34\%$ and that the lifetime of the h_- is $\tau_{h_-} \simeq (9/\sin^2\theta) \times 10^{-17}$ sec. A strong constraint on the mixing angle θ comes from the decay $B \to h_- X$ which has branching ratio $\mathrm{Br}(B \to h_- X) \simeq 8\ \sin^2\theta$. The experimental limit $\mathrm{Br}(B \to \mu^+\mu^- X) < 3.2\ \times 10^{-4}$ [192] implies that $\sin^2\theta < 1 \times 10^{-4}$. Hence the lifetime of the h_- is at least 8×10^{-13}sec (i.e., about the B meson lifetime). It may be possible to derive stronger constraints on the mixing angle from exclusive decays of the B meson.

The h_- can be produced directly in Z decays. Single h_- production is suppressed by the the small mixing angle, $\mathrm{Br}(Z \to h_- \bar{f} f)/\mathrm{Br}(Z \to \bar{f} f) \simeq 10^{-2}\sin^2\theta < 1 \times 10^{-6}$, where f denotes any of the light standard model fermions. The h_- can also be pair-produced through a virtual h_+, with a rate that is not suppressed by the small mixing angle θ, via the process $Z \to h_+^* \bar{f} f \to h_- h_- \bar{f} f$. We find that this rate is negligible[3] when $|\delta_2| \sim 2m_-^2/v^2$.

[2]The rate to two pions is calculated at leading order in chiral perturbation theory [191]. With $m_- = 500$ MeV one can expect sizeable corrections from, for example, $\pi\pi$ final state interactions. These are expected to increase the decay rate to two pions.

[3]For $\kappa_2 = 0$, $m_+ = 120$ GeV and $m_- = 5$GeV, we find that $\mathrm{Br}(Z \to h_+^* \bar{f} f \to h_- h_- \bar{f} f)/\mathrm{Br}(Z \to \bar{f} f) = 5.4 \times 10^{-13}$. The rate is even smaller for smaller values of m_-.

5.3.2 $5\ \text{GeV} < m_- < 50\ \text{GeV}$

This mass range is interesting because the decays of the heavier scalar, which is mostly the standard model Higgs, can be quite different from what the minimal standard model predicts. In this mass range the h_- is light enough that the decay $h_+ \to h_- h_-$ is kinematically allowed. In addition the h_- is heavy enough so that values of δ_2 that give this decay a significant branching ratio do not require a delicate cancellation between the two terms contributing to μ_S^2 in Eq. (5.5). At the lower end of this mass range we would not expect the dominant decay of the h_+ to be to two h_-s; however, with no awkward cancellation between the two terms contributing to μ_S^2, the h_+ could easily decay about the same amount of time to two h_-s as it does to two photons. At the upper end of the mass range it is quite reasonable to have the h_+ decaying mostly to two h_-s.

In Fig. 5.1 we plot the suppression factor $f = 1 - \text{Br}(h_+ \to h_- h_-) = \text{Br}(h_+ \to \gamma\gamma)/\text{Br}^{\text{S.M.}}(h \to \gamma\gamma)$, where $\text{Br}^{\text{S.M.}}(h \to \gamma\gamma)$ is the standard model branching fraction, assuming that the parameter $\kappa_2 = -\delta_2 v^2/4, 0, +\delta_2 v^2/4, +\delta_2 v^2$ and that the mixing angle θ is very small. Notice that as one approaches the upper range of the mass range we are considering, decays of the h_+ can be dominated by the final state $h_- h_-$, and consequently the branching ratio to the the two-photon mode is suppressed compared to what it is in the standard model. The dependence of f on the mass of the h_- arises because the same coupling in the Lagrangian that gives rise to this branching ratio also contributes to the h_- mass. If κ_2 is larger than $\delta_2 v^2$, then f will be close to unity throughout the whole range we consider.

Since the h_+ may decay dominantly to a pair of the lighter h_- scalars it is useful to understand the ensuing h_- decays. We plot the branching ratios of the h_- in Fig. 5.2. In the upper end of the mass range we are considering, the h_- decays mostly to a bottom-

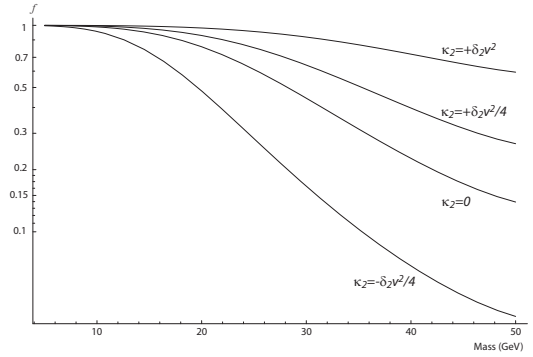

Figure 5.1: The suppression factor f discussed in the text, plotted as a function of the h_- mass

antibottom pair but it also has substantial branching fractions to $c\bar{c}$ and to $\tau^+\tau^-$. Considerable attention has been given to a different class of models where the the heavier Higgs scalar decays mostly to a singlet scalar that consequently decays to neutrinos [193].

In Ref. [194] it was noted that new physics at the TeV scale can easily give rise to a large reduction (or enhancement) in the dominant gluon fusion Higgs scalar production rate, and hence the final two photon signal. However, it is very unlikely that such physics could alter the associated production rate of the Higgs since it arises from the tree coupling to the massive weak bosons. The situation is different here. All the standard model decays of the heavier Higgs-like scalar h_+ are reduced by the same factor f independent of its production mechanism.

The production of h_- scalars from gluon fusion is suppressed from the production rate for a standard model Higgs of the same mass by $\sin^2\theta$. Since the h_- was not observed at LEP there is a mass-dependent limit on $\sin^2\theta$ from LEP data [195] (very roughly, $\sin^2\theta < 2\times10^{-2}$ over the mass range we are considering). However, the h_- production rate via gluon fusion at the Tevatron and LHC increases rapidly as its mass decreases. For example, using leading order CTEQ5 parton distributions [196] an h_- of mass 10 GeV has a production rate roughly 100 times greater than one with a mass of 120 GeV at the LHC and $1,000$

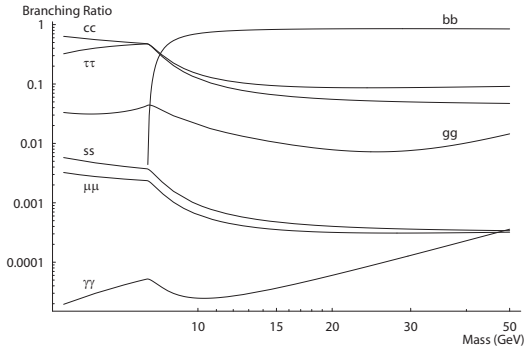

Figure 5.2: The branching ratios of the light h_- scalar particle, plotted as a function of its mass

times greater at the Tevatron. Even with a small value for $\sin^2\theta$ the h_- may be directly observable at the LHC.

5.4 Concluding Remarks

The literature on extensions of the minimal standard model with a more complicated scalar sector is vast. Here, we have considered the simplest alternative possibility, in which a single gauge-singlet scalar is added. It mixes with, and couples to, the standard model Higgs. We concentrate on the region of allowed singlet scalar masses where it is light enough to be pair produced in Higgs decay and, hence, suppress the Higgs "golden mode" branching ratio to two photons. We found that this suppression is unlikely to be significant if the new scalar is very light but can easily be large if the (mostly) singlet scalar is heavier than about 10 GeV. Under this scenario, there is a scalar that has a mass below the LEP Higgs mass lower bound with decay branching ratios that are identical to those of a standard model Higgs of the same mass. However its production rate is suppressed by a small mixing angle. Potential signatures of such light scalars include the observation of Higgs decay products with invariant mass well below 114 GeV or unusual final states in Higgs decay such as two b-jets and a $\tau^+\tau^-$ (or $\mu^+\mu^-$) pair.

Chapter 6

The Story of $\mathcal{O}$: Positivity constraints in effective field theories

6.1 Introduction

A variety of classical and quantum arguments have been formulated to require the positivity of the coefficients of higher-dimensional (i.e., irrelevant) operators in effective field theories, including General Relativity (see, for instance [197, 198, 9, 199]). These arguments are based on the axioms of S-matrix theory: unitarity, analyticity, and causality. In this chapter, we will make some remarks which help to clarify which operators one expects to obey positivity constraints, as well as the connection between the diverse positivity arguments in the literature. In particular, we will argue that positivity is expected to follow from causality for operators of the form

$$\mathcal{O} \propto \mathcal{O}_1^{\mu_1 \ldots \mu_j} \mathcal{P}^{(j)}_{\mu_1 \ldots \mu_j ; \nu_1 \ldots \nu_j} \mathcal{O}_1^{\nu_1 \ldots \nu_j} \ , \tag{6.1}$$

where $\mathcal{O}_1$ contains sufficient derivatives and $\mathcal{P}^{(j)}_{\mu_1 \ldots \mu_j ; \nu_1 \ldots \mu_j}$ is the zero-momentum propagator for a massive, spin-j mediator. We do not expect positivity constraints from causality alone

for operators of the form

$$\mathcal{O} \propto \mathcal{O}_1^{\mu_1 \ldots \mu_j} \mathcal{P}^{(j)}_{\mu_1 \ldots \mu_j ; \nu_1 \ldots \nu_j} \mathcal{O}_2^{\nu_1 \ldots \nu_j} \ . \tag{6.2}$$

Furthermore, we shall argue that theories with such $\mathcal{O}$s that violate positivity do not admit stable, perturbative UV completions, and that the instabilities near the cutoff scale of non-positive effective theories are associated to the superluminal modes that may appear in the IR. We shall comment on the implications of this for the ghost condensate mechanism that has been proposed as a model of gravity in a Higgs phase [200], for the chiral Lagrangian, and for theories in which Lorentz invariance is spontaneously broken by a VEV for a vector quantity. This discussion is motivated principally by [9], whose notation we will adopt.

6.2 Superluminality and Analyticity

Consider the Lagrangian

$$\mathcal{L} = \frac{1}{2} \left(\partial_\mu \pi \right)^2 - \frac{1}{2} m^2 \pi^2 + \frac{c_3}{2\Lambda^4} \left(\partial_\mu \pi \right)^4 + \ldots \ , \tag{6.3}$$

which could describe an effective theory, at energy scales well below Λ, for a scalar field π with a very small mass m.[1] In [9], the authors offer two distinct causality arguments to constrain c_3. The first is classical and applies for $m = 0$: Consider a background π_0 such

[1] For $m \neq 0$ Eq. (6.3) has no shift symmetry in π and we would expect other self-interactions such as π^4, $\pi \left(\partial_\mu \pi \right)^2$, etc. However, we will be concerned here mostly with the limit $m \to 0$.

that $\partial_\mu \pi_0 = C_\mu$, for constant C. For $\left|C^2\right| \ll \Lambda^4$, we obtain the linear dispersion relation

$$k^2 + \frac{4c_3}{\Lambda^4}(C \cdot k)^2 = 0 \ , \tag{6.4}$$

where k is the 4-momentum of a plane wave of the perturbation $\varphi \equiv \pi - \pi_0$, which is the non-relativistic Goldstone of the spontaneous breaking of the shift symmetry $\pi \to \pi + c$ by the background. Absence of superluminal excitations then requires $c_3 \geq 0$. For $c_3 < 0$, the superluminal excitations are not tachyons and the background π_0 is stable, even though the Hamiltonian is not minimized by it, because shift-symmetry implies the conservation of

$$Q = \int d^3x \, \dot{\pi} \left[1 + \frac{2c_3}{\Lambda^4}\left(\dot{\pi}^2 - |\boldsymbol{\nabla}\pi|^2\right)\right] \tag{6.5}$$

and small perturbations φ that conserve Q cannot lower the energy [201, 202, 203]. If c_3 were negative, it would be possible to use these superluminal excitations to construct closed timelike curves in certain non-trivial backgrounds [9].

Let us now consider the case $m \neq 0$ in Eq. (6.3). The shift symmetry is then explicitly broken at a scale m, which should also be the scale of the mass of the pseudo-Goldstone φ. Subluminality of φ at long wavelengths is assured as long as $m^2 > 0$. We expect that absence of superluminal φ near the cutoff scale will impose, at best, only a limit of the form

$$c_3 \gtrsim -\frac{m^2}{\Lambda^2} \ . \tag{6.6}$$

The second argument in [9] is based on the analyticity of the S-matrix for Eq. (6.3). Let $\mathcal{M}(s,t)$ be the amplitude for $\pi\pi \to \pi\pi$ scattering and consider the analytic continuation of $\mathcal{A}(s) \equiv \mathcal{M}(s, t = 0)$ onto the complex plane. For an intermediate scale M such that

$m \ll M \ll \Lambda$, analyticity requires that $\mathcal{A}''(M^2)$ be strictly positive. Since $\mathcal{A}''(M^2)$ is equal to $2c_3/\Lambda^4$ plus loop corrections suppressed by M^4/Λ^8, we expect a limit of the form

$$c_3 > 0 \tag{6.7}$$

regardless of the value of the small mass m.[2] It therefore seems that the two positivity arguments in [9] are not equivalent and that analyticity of the S-matrix imposes a more stringent constraint on c_3.

There is another important difference between the positivity argument based on Eq. (6.4) and the argument from analyticity of the S-matrix. The former identifies a violation of causality which is present already in the IR. The latter requires closing the contour on the complex plane out at $|s| \to \infty$ and therefore should be interpreted as an obstruction to finding a causal UV-completion of the effective theory. This is the spirit in which the argument has been proposed in [204] as providing a falsifiable prediction of string theory.

6.3 The Ghost Condensate

The positivity constraints of [9] present an obstruction to the ghost condensate of [200]. For $X \equiv (\partial_\mu \pi)^2$, the ghost condensate has an action of the form

$$\mathcal{L} = P(X) \ , \tag{6.8}$$

where P is a polynomial with $P'(X_*) = 0$ and $P''(X_*) \neq 0$ at $X_* \neq 0$. For such an action there will generally be some background $X_0 = (\partial_\mu \pi_0)^2 = C^2$ for which the Goldstone φ is

[2] In fact, the S-matrix analyticity argument in [9] requires the introduction of a regulator mass m, which may be taken to zero at the end.

superluminal. This can be seen from the formula for the speed v of linear waves in φ. If $X_0 > 0$ then, in the frame where $C^\mu = (C, 0, 0, 0)$, we have

$$v^2 = \frac{1}{1 + 2\,|X_0|\,P''(X_0)/P'(X_0)} \tag{6.9}$$

for $P'(X_0) \neq 0$.[3] For X_0 in one half-neighborhood of X_*, the quantity $|X_0|\,P''(X_0)/P'(X_0)$ is very large and negative. In that case $v^2 < 0$ in Eq. (6.9), signaling an instability. But there will generally be a region where $|X_0|\,P''(X_0)/P'(X_0)$ is small and negative, leading to $v^2 > 1$ and indicating the presence of stable superluminal perturbations which could be used to build closed timelike curves.

Note also that in the limit $M_{\rm Pl} \to \infty$. where the ghost condensate decouples from gravity, the overall coefficient of the action in Eq. (6.8) is irrelevant. If we normalize it to have a normal leading kinetic term $X/2$ then analyticity of the S-matrix for $\pi\pi \to \pi\pi$ forbids negative coefficients for higher powers of X, thus preventing the polynomial $P(X)$ from having a point $P'(X_*) = 0$ for $X_* \neq 0$.[4]

6.4 The Story of $\mathcal{O}$

The theory in Eq. (6.3) with only a c_3 self-interaction is equivalent to

$$\mathcal{L} = \frac{1}{2}\,(\partial_\mu \pi)^2 - \frac{1}{2} m^2 \pi^2 - \frac{c_3}{2}\Lambda^2 \Phi^2 - \epsilon \frac{c_3}{\Lambda}\Phi\,(\partial_\mu \pi)^2 \ , \tag{6.10}$$

[3] If $X_0 < 0$, then the speed of perturbations moving along the direction of C^μ (in the frame where $C^0 = 0$) is given by $v^2 = 1 - 2\,|X_0|\,P''(X_0)/P'(X_0)$. This reproduces Eq. (6.9) for $|X_0|\,P''(X_0)/P'(X_0) \ll 1$.

[4] This could signal an obstruction to finding a high-energy completion for the ghost condensate (see [205, 206]). We shall discuss this point further in the next chapter.

where $\epsilon = \pm 1$, since integrating out the auxiliary field Φ corresponds exactly to substituting its equation of motion $\Phi = -\epsilon \left(\partial_\mu \pi\right)^2 / \Lambda^3$. We could therefore think of Eq. (6.3) as describing the low-energy behavior of

$$\mathcal{L}' = \left(\frac{1}{2} - \epsilon \frac{c_3}{\Lambda} \Phi\right) \left(\partial_\mu \pi\right)^2 - \frac{1}{2} m^2 \pi^2 + \frac{1}{2} \left(\partial_\mu \Phi\right)^2 - \frac{c_3}{2} \Lambda^2 \Phi^2 \ . \tag{6.11}$$

Regardless of whether m vanishes or not, the wrong sign of c_3 in Eq. (6.11) leads to an instability at energy scales near the cutoff for Eq. (6.3). If, for the wrong sign of the Φ^2 term, we attempt to make Eq. (6.10) stable by adding higher-order potential terms for Φ, then the corresponding low-energy effective action will still have $c_3 > 0$ if Φ sits at a stable point of its potential.[5] Transition from $c_3 > 0$ to $c_3 < 0$ in Eq. (6.3) corresponds to the destabilization of the fixed point at which the heavy field Φ in Eq. (6.11) sits.

The theory described by Eq. (6.11) is not a true high-energy completion of Eq. (6.3) because it is not renormalizable. However, it is easy to check that for $c_3 > 0$ the forward scattering amplitudes for $\pi\pi \to \pi\pi$, $\pi\Phi \to \pi\Phi$, and $\Phi\Phi \to \Phi\Phi$ all have the right sign of $\mathcal{A}''(s)$, as required by [9], and could therefore admit a perturbative UV-completion with an analytic S-matrix. The sign constrained by the analyticity argument of [9] has become the sign of the mass-squared for the auxiliary field Φ (i.e., the analyticity constraint has become a simple stability constraint). Eq. (6.11) could then be an approximation, at intermediate energies, to a (perhaps fine-tuned) analytic UV-completion.[6]

[5] It will also have operators $(\partial_\mu \pi)^{2n}$ for $n > 2$, whose coefficients are also positive when Φ sits at a stable point.

[6] We could imagine fine-tuning $|c_3| \ll 1$ in Eq. (6.11) so that radiative corrections leading to other couplings are under control. Alternatively, we could control radiative corrections by considering small m, so that the π field has an approximate shift symmetry. For $m = 0$, the action for $U(1)$ linear sigma model $\mathcal{L} = \frac{1}{2} \left|\partial_\mu \phi\right|^2 - \lambda \left(|\phi|^2 - v^2\right)^2$, for a complex scalar field $\phi = (v + h) \exp(i\pi/v)$, takes the form of Eq. (6.11) for small values of h. The authors of [9] point out that this linear sigma model leads to positive c_3 in the effective action for π when h is integrated out.

Consider now more generally

$$\mathcal{L}' = a\Phi \cdot \mathcal{O}_1 - \frac{b}{2}\Lambda^2\Phi^2 \ , \tag{6.12}$$

where $\mathcal{O}_1$ is some arbitrary operator and the coefficient a has the appropriate mass dimension. Then $\mathcal{L}'$ is equivalent to

$$\frac{a^2}{2b\Lambda^2}\mathcal{O}_1^2 \ . \tag{6.13}$$

The condition that Φ be non-tachyonic if it is made dynamical then imposes a constraint on the sign of $\mathcal{O} = \mathcal{O}_1^2$. This method trivially succeeds in identifying many other positivity constraints worked out in the literature, such as the positivity of c_1 and c_2 for the $U(1)$ gauge field action discussed in [9]

$$\mathcal{L} = -\frac{1}{4}F_{\mu\nu}F^{\mu\nu} + \frac{c_1}{\Lambda^4}\left(F_{\mu\nu}F^{\mu\nu}\right)^2 + \frac{c_2}{\Lambda^4}\left(F_{\mu\nu}\tilde{F}^{\mu\nu}\right)^2 + \cdots \tag{6.14}$$

or the positivity of the higher-dimensional operators in General Relativity (e.g., R^2) discussed in [197, 198, 199].

That we expect positivity constraints on operators of the form $\mathcal{O} = \mathcal{O}_1^2$ where $\mathcal{O}_1$ has enough derivatives is clear from the analyticity argument in [9], which constrains the signs of the coefficients of s^{2n} in the power expansion of the forward scattering amplitude $\mathcal{A}(s)$, for $n \geq 1$. We do not expect our auxiliary field method to yield a constraint on an operator without derivatives, such as $-\lambda\pi^4$. In that case

$$\begin{aligned} \mathcal{L}' &= \lambda\left(2\Lambda\Phi\pi^2 + \Lambda^2\Phi^2\right) \\ &= \lambda\Lambda^2\left(\Phi + \frac{\pi^2}{\Lambda}\right)^2 - \lambda\pi^4 \ , \end{aligned} \tag{6.15}$$

which is always an unstable potential, regardless of the sign of λ. Furthermore, we should not constrain the sign of an ordinary kinetic term $(\partial_\mu \pi)^2$. In that case we could write

$$\mathcal{L}' = \Lambda A^\mu \left(\partial_\mu \pi\right) + \frac{1}{2}\Lambda^2 A^2, \tag{6.16}$$

but the coupling of the auxiliary field can be removed upon integrating by parts, since $\partial_\mu A^\mu = 0$ for a massive vector field.

The method we have used to identify operators with positivity constraints amounts to a very simple-minded inverse Operator Product Expansion. We take an operator $\mathcal{O}$ and split it up into two parts joined by a massive, zero-momentum mediator. We expect a positivity constraint if the theory that results after the mediator is made dynamical is stable if and only if the coefficient of $\mathcal{O}$ was positive. We do not expect a constraint from causality if the theory can be made stable regardless of the sign of $\mathcal{O}$.

We therefore never expect positivity constraints from causality alone for operators that can be written in the form $\mathcal{O} = \mathcal{O}_1 \cdot \mathcal{O}_2$. In that case it is always possible to write

$$\mathcal{L}' = a_1 \Phi \cdot \mathcal{O}_1 + a_2 \Phi \cdot \mathcal{O}_2 - \frac{b}{2}\Lambda^2 \Phi^2 \ , \tag{6.17}$$

and the sign of $\mathcal{O}$ in the equivalent action will depend on the sign of $a_1 \cdot a_2$, which we can set freely. For example, consider the operator

$$\mathcal{O} \propto \left(\partial_\mu \pi_1\right)^2 \left(\partial_\nu \pi_2\right)^2 \ . \tag{6.18}$$

The arguments of [9] do not constrain its coefficient because it does not contribute to forward $\pi_1 \pi_2 \to \pi_1 \pi_2$ scattering.

On the other hand, the operator

$$\mathcal{O}' \propto (\partial_\mu \pi_1)(\partial_\nu \pi_2)(\partial^\nu \pi_1)(\partial^\mu \pi_2) = (\partial_\mu \pi_1 \partial^\mu \pi_2)^2 \tag{6.19}$$

does have a positivity constraint from both classical causality and analyticity of $\pi_1\pi_2 \to \pi_1\pi_2$ scattering. Naively this would seem to conflict with the possibility of obtaining the operator from

$$\mathcal{L}' = \frac{a_1}{\Lambda} h_{\mu\nu} \left(\partial^\mu \pi_1 \partial^\nu \pi_1\right) + \frac{a_2}{\Lambda} h_{\mu\nu} \left(\partial^\mu \pi_2 \partial^\nu \pi_2\right) + \frac{1}{2} m^2 h^2 \tag{6.20}$$

for a spin-2 auxiliary field $h_{\mu\nu}$. Eq. (6.20) does not, however, actually yield an equivalent action. For example, for the classical solutions $\partial^\mu \pi_{1,2} = C^\mu_{1,2}$, where $C^\mu_{1,2}$ are constant, the coupling terms in Eq. (6.20) contribute nothing to the total action, since they can be removed by integrating by parts and using $\partial_\mu h^{\mu\nu} = 0$.

6.5 The Chiral Lagrangian

Let us now consider how our method applies to the coefficients of the next-to-leading order operators of the $SU(2)$ chiral Lagrangian

$$\begin{aligned} \mathcal{L} &= \frac{1}{4} v^2 \operatorname{tr}\left(\partial^\mu \Sigma^\dagger \partial_\mu \Sigma\right) + \frac{1}{4} m^2 v^2 \operatorname{tr}\left(\Sigma^\dagger + \Sigma\right) \\ &\quad + \frac{1}{4}\ell_1 \left[\operatorname{tr}\left(\partial^\mu \Sigma^\dagger \partial_\mu \Sigma\right)\right]^2 + \frac{1}{4}\ell_2 \left[\operatorname{tr}\left(\partial^\mu \Sigma^\dagger \partial^\nu \Sigma\right)\right]\left[\operatorname{tr}\left(\partial_\mu \Sigma^\dagger \partial_\nu \Sigma\right)\right] + \ldots \end{aligned} \tag{6.21}$$

where $\Sigma(x) \equiv \exp\left(i\pi^i(x)\sigma^i/v\right)$, with π^i being the pion fields and σ^i the Pauli matrices. We shall see that this example illustrates a subtlety which may appear when considering operators of the form $\mathcal{O} = \mathcal{O}_1^{\mu_1 \ldots \mu_j} \mathcal{O}_{1\ \mu_1 \ldots \mu_j}$ for $j > 1$.

The Lagrangian in Eq. (6.21) can be rewritten as

$$\begin{aligned}\mathcal{L} &= \frac{1}{4}v^2\,\mathrm{tr}\left(\partial^\mu\Sigma^\dagger\partial_\mu\Sigma\right)+\frac{1}{4}m^2v^2\,\mathrm{tr}\left(\Sigma^\dagger+\Sigma\right)\\ &\quad+\frac{1}{4}\left[\ell_2 P^{(2)}_{\mu\nu;\rho\sigma}+\left(\frac{\ell_2}{D-2}+\ell_1\right)P^{(0)}_{\mu\nu;\rho\sigma}\right]\left[\mathrm{tr}\left(\partial^\mu\Sigma^\dagger\partial^\nu\Sigma\right)\right]\left[\mathrm{tr}\left(\partial^\rho\Sigma^\dagger\partial^\sigma\Sigma\right)\right]+\cdots\end{aligned} \tag{6.22}$$

where

$$P^{(2)}_{\mu\nu;\rho\sigma}\equiv\frac{1}{2}\left(g_{\mu\rho}g_{\nu\sigma}+g_{\mu\sigma}g_{\nu\rho}-\frac{2}{D-2}g_{\mu\nu}g_{\rho\sigma}\right) \tag{6.23}$$

gives the index structure, in D space-time dimensions, of the propagator for a massive spin-2 particle with zero momentum, while

$$P^{(0)}_{\mu\nu;\rho\sigma}\equiv g_{\mu\nu}g_{\rho\sigma}\ . \tag{6.24}$$

We can therefore write an action with spin-2 and spin-0 auxiliary fields which reproduces Eq. (6.21). Making those fields non-tachyonic requires

$$\begin{cases}\ell_2>0\\ \ell_1+\frac{\ell_2}{D-2}>0\end{cases}\ . \tag{6.25}$$

For $D\geq 3$, this implies that

$$\begin{cases}\ell_2>0\\ \ell_1+\ell_2>0\end{cases}\ , \tag{6.26}$$

which agrees with the constraints obtained in [204] from avoiding superluminal perturbations around the classical background $\Sigma=\exp\left(ic\cdot x\sigma^3\right)$ in the limit that $m\to 0$.

The authors of [9] point out that quantum corrections make $\ell_{1,2}$ logarithmically scale-dependent. The constraints of Eq. (6.26) should therefore be interpreted as the classical

requirement of causality at a particular energy scale. Quantum corrections naturally push $\ell_{1,2}$ in the positive direction. Positivity of $\ell_{1,2}$ should obtain all the way up to the cutoff scale. For weakly-coupled chiral Lagrangians, the analyticity constraints on the observed $\ell_{1,2}$ have been studied in [207, 208, 209, 204].

6.6 Superluminality and Instabilities

The auxiliary field method that we have described could also shed light on the connection between the obstruction to UV-completion and the appearance of stable superluminal modes in the IR. From the equation of motion for Φ in Eq. (6.11) we have that, for perturbations about a background Φ_0 and π_0,

$$\partial^2(\delta\Phi) + c_3\Lambda^2\,\delta\Phi = -\frac{2c_3\epsilon}{\Lambda}\left[(\partial_\mu\pi_0)\,\partial^\mu(\delta\pi)\right] \ . \tag{6.27}$$

If $\partial_\mu\pi_0 \neq 0$, then perturbations $\delta\pi$ lead to non-zero $\delta\Phi$, which is tachyonic for $c_3 < 0$. We *conjecture* that superluminal perturbations in the IR are generally associated with instabilities near the cutoff scale.[7]

Our approach may also rule out superluminal Goldstones in theories in which Lorentz invariance is spontaneously broken by a timelike vector VEV, $\langle S^\mu\rangle \neq 0$. It should be pointed out, though, that the scattering of these Goldstones, being Lorentz non-invariant, is not adequately characterized by the kinematic variables s and t. The connection between our auxiliary field method and causality as encoded in the analytic structure of the S-matrix is no longer transparent.

[7] This could be related to the instabilities near the cutoff scale that have been identified in ghost condensate models [202]. As we have discussed, for certain backgrounds the ghost condensate also exhibits stable superluminal excitations in the deep IR.

At the two-derivative level, the general effective action for such Goldstones can be written as

$$\mathcal{L} = c_1 \partial_\alpha S^\beta \partial^\alpha S_\beta + (c_2 + c_3) \partial_\mu S^\mu \partial_\nu S^\nu + c_4 S^\mu \partial_\mu S^\alpha S^\nu \partial_\nu S_\alpha \ . \tag{6.28}$$

If we normalize to $S^2 = 1$ and work in the frame in which only S^0 is non-vanishing, we may write

$$S^\mu(x) \equiv \frac{1}{\sqrt{1 - \boldsymbol{\phi}^2}} \left(1, \boldsymbol{\phi}\right) \ , \tag{6.29}$$

where $\boldsymbol{\phi}$ is as 3-vector whose components correspond to the Goldstones [210].[8] Classically, the linear Goldstone action is therefore

$$\mathcal{L} = \frac{1}{2} \sum_{i=1,2,3} \left[\left(\partial_\mu \phi^i\right)^2 - \alpha \left(\partial_i \phi^i\right)^2 + \beta \left(\partial_0 \phi^i\right)^2 \right] \ , \tag{6.30}$$

where $\alpha \equiv (c_2 + c_3)/c_1$ and $\beta \equiv c_4/c_1$. Absence of superluminal Goldstones requires $\beta > 0$ and $\alpha < \beta$. The action in Eq. (6.28) is equivalent to

$$\mathcal{L}' = c_1 \left[\partial_\alpha S^\beta \partial^\alpha S_\beta + 2\alpha \Phi \left(\partial_\mu S^\mu\right) + 2\beta A_\mu \left(S^\nu \partial_\nu S^\mu\right) - \alpha \Phi^2 - \beta A^2 \right] + \frac{1}{2} \left(\partial_\mu \Phi\right)^2 - \frac{1}{4} F_{\mu\nu}^2 \tag{6.31}$$

for zero momentum of Φ_1 and A_μ. Avoiding ghosts implies $c_1 < 0$. Stability of Eq. (6.31) then requires that there be no superluminal Goldstones in Eq. (6.28).[9] This observation might help to resolve the question of whether superluminal excitations should be forbidden or not in theories with spontaneous Lorentz violation [211, 212]. This issue is significant because the experimental constraint on spontaneous Lorentz violation coupled only to gravity is much tighter if superluminality of the Goldstones is forbidden [213, 214].

[8] Notice that the S^μs are dimensionless while the c_is have mass dimension two.

[9] In fact, it also requires that the longitudinal mode, with $v_{\rm lgt}^2 = (1+\alpha)/(1+\beta)$, propagate more slowly than the two transverse modes, with $v_{\rm trv}^2 = 1/(1+\beta)$.

Analogously to what occurred in Eq. (6.27) for the scalar field, we see from the equation of motion for the action in Eq. (6.31) that stable superluminal Goldstones in Eq. (6.28) are connected to excitations of tachyonic Φ or A_μ. We therefore conjecture that superluminal Goldstones are associated with instabilities that appear near the scale at which the spontaneously-broken Lorentz symmetry is restored.

6.7 Conclusions

We have described a very simple method for identifying a family of higher-dimensional operators in effective theories whose coefficient must be positive by causality: We introduce auxiliary fields such that the original effective theory is reproduced when the auxiliary fields have zero momentum. For operators of the form $\mathcal{O} = \mathcal{O}_1 \cdot \mathcal{O}_1$, where $\mathcal{O}_1$ contains enough derivatives, the positivity constraint on $\mathcal{O}$ from S-matrix analyticity is recast as a stability constraint on the sign of the mass-squared for the corresponding auxiliary field.

This procedure also identifies a family of operators for which causality alone should not impose positivity: those for which the theory with the auxiliary field can be stable and analytic regardless of the sign of $\mathcal{O}$. It is, of course, possible that there are other kinds of operators which must be positive by causality (or by another reason) but which our prescription does not detect. For instance, some other positivity constraints which do not follow from our conjecture are obtained in [215] from avoidance of "Planck remnants" (i.e., charged black holes that cannot decay quantum-mechanically). For the operators which our conjecture does constrain, our results are consistent with [215].

We have also conjectured that what we have seen when applying our auxiliary field procedure is true in general: that stable superluminal modes in the IR of non-positive effective theories are connected to an instability that appears near the cutoff scale. Finally, we have

commented on what positivity constraints and causality imply for the ghost condensate, the chiral Lagrangian, and theories with spontaneous Lorentz violation.

Chapter 7

Regulator Dependence of the Proposed UV Completion of the Ghost Condensate

7.1 Introduction

The ghost condensate proposal of [200] has received considerable attention recently [10, 216, 217, 218, 219, 220, 221, 202, 222, 203, 223]. The condensate is a mechanism for modifying gravity in the infrared. The starting point of the model is a scalar field, ϕ, with a shift symmetry

$$\phi \to \phi + \alpha \tag{7.1}$$

such that the effective action for the scalar is of the form $\mathcal{L} = P(X)$, where $X = \partial_\mu \phi \partial^\mu \phi$ (we ignore terms such as $(\partial^2 \phi)^2$ as they will not be important in our discussion). Moreover, we assume that ϕ is a ghost, so that $P(X)$ is of the form shown in Figure 7.1. The origin, $\phi = 0$, is an unstable field configuration in this scenario; note that this corresponds to choosing the opposite sign for the usual kinetic term for ϕ. The ghost then condenses so that $(\partial\phi)^2$ has a value near the minimum of P. It is also possible that there is no ghost at the origin but a non-trivial minimum elsewhere, as shown in Figure 7.2; in such a theory

there would still be a ghost condensate near the minimum of P. This class of theories is of considerable phenomenological interest because a ghost condensate has equation of state $w = -1$ and could therefore be relevant for explaining the observed small but non-zero cosmological constant [200].

It is also of interest, however, to understand how the effective action $\mathcal{L} = P(X)$ could arise as a low-energy effective theory of some more familiar UV quantum field theory [202]. Since the scalar field must have a shift symmetry, it is natural to seek a completion in which ϕ is the Goldstone boson of a spontaneously broken $U(1)$ symmetry. It was shown in [10] that it is impossible, classically, to generate a ghostly low energy effective action for such a Goldstone boson from a high-energy theory with standard kinetic terms. However, the authors went on to find a theory in which a quantum correction could change the sign of the kinetic term of the Goldstone boson. In that proposal, all fields start out with standard kinetic terms. However, interactions between ϕ and certain heavy fermions correct the kinetic term of ϕ. It was found that under certain assumptions, these corrections could produce an effective Lagrangian for ϕ of the form shown in Figure 7.1 at scales much smaller than the fermion mass m. We do not expect to find an effective Lagrangian of the form shown in Figure 7.2 because the higher order terms in the expansion of $P(X)$ are suppressed by powers of the cutoff.

The model described in [10] has some shortcomings. The high-energy theory has a Landau pole. Moreover, in dimensional regularization it was found that to change the sign of the bosonic kinetic term, the mass of the fermions has to be close to the Landau pole. This circumstance may cause some concern that the calculation could be regulator dependent. To alleviate these concerns, the authors demonstrated that their conclusion holds in a large class of momentum-dependent regulators, provided that the fermion masses were taken to

be of order of the regulator. These regulators, however, violate unitarity, so again it is not clear to what extent the sign of the kinetic term is a well-defined quantity.

In this chapter, we re-examine the theory presented in [10] using a lattice regulator. This regulator is non-perturbatively valid and preserves unitarity. We will see that there is never a ghost when the theory is regulated in this way. As a consequence, it seems that the conclusions of [10] are regulator dependent.

7.2 Computation

We begin by describing the theory we will be working with in more detail. The candidate ghost field, ϕ, must have a shift symmetry so it is natural to suppose that it is a Goldstone boson associated with the breaking of some $U(1)$ symmetry. Hence, following [10], we choose as the bosonic part of the Lagrangian the usual spontaneous symmetry breaking Lagrangian for a complex scalar field Φ,

$$\mathcal{L}_b = \partial_\mu \Phi^* \partial^\mu \Phi - \frac{\lambda}{4}\left(|\Phi|^2 - v^2\right)^2 . \tag{7.2}$$

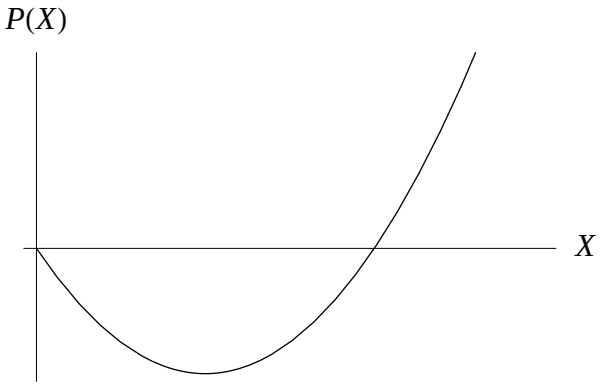

Figure 7.1: One possible form for $P(X)$

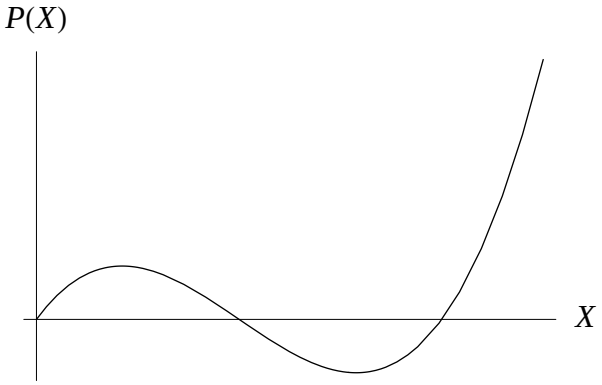

Figure 7.2: Another possible form for $P(X)$, with no ghost at the origin

The Goldstone boson, ϕ, associated with the spontaneous symmetry breaking is the candidate ghost field. We couple Φ to two families of fermions ψ_i, $i = 1, 2$ of charges $+1$ and -1 respectively. We will assume that there are N identical fermions in each family, and that each fermion has the same mass m. The fermions are coupled to Φ by a Yukawa term with coupling g. Hence, the total Lagrangian density is

$$\mathcal{L} = \mathcal{L}_b + \sum_{j=1}^{N} \left[\sum_{i=1,2} \left(i\bar{\psi}_i^{(j)} \gamma^\mu \partial_\mu \psi_i^{(j)} - m\bar{\psi}_i^{(j)} \psi_i^{(j)} \right) - g\Phi \bar{\psi}_2^{(j)} \psi_1^{(j)} - g\Phi^* \bar{\psi}_1^{(j)} \psi_2^{(j)} \right]. \quad (7.3)$$

The low energy effective action for Φ is obtained by integrating the fermions out. The effective action can be written

$$\mathcal{L}_{eff} = \Phi^* G(-\partial^2)\Phi - V(|\Phi|) \quad (7.4)$$

where

$$G(p^2) = p^2 + g^2 N f(p^2). \quad (7.5)$$

The function $f(p^2)$ describes the effects of the quantum corrections to the bosonic kinetic term. If $G(p^2) < 0$ for some range of p^2, then the theory can have a ghost. This can only

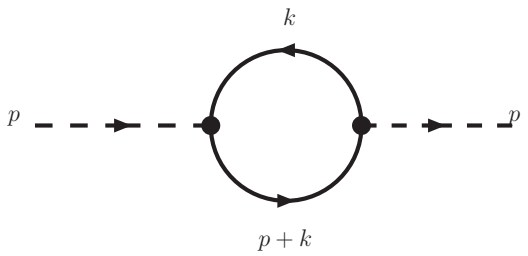

Figure 7.3: The relevant Feynman graph. Dashed lines represent the boson while full lines are the fermions.

happen if $g^2 N f(p^2)$ is negative and larger than the tree-level term p^2. Since this signals a breakdown in perturbation theory, we work in the large N limit with $g^2 N$ fixed to maintain control over the calculation.

Let us now move on to compute $f(p^2)$. To do so, we must evaluate the Feynman graph shown in Figure 7.3. After Wick rotating both momenta into Euclidean space, we find

$$f(p^2) = -4 \int \frac{d^4k}{(2\pi)^4} \frac{m^2 - k \cdot (p+k)}{(k^2+m^2)((p+k)^2+m^2)}. \tag{7.6}$$

This expression is divergent and requires regulation. We choose a lattice regulator with lattice spacing a. Since we are working in the large N limit, the phenomenon of fermion doubling [224] will not pose a problem. Therefore, we will use naive lattice fermions. The (Euclidean) fermion propagator is given by [224]

$$G(p) = a \frac{-i \sum_\mu \gamma_\mu \sin(p_\mu a) + ma}{\sum_\mu \sin^2 p_\mu a + m^2 a^2} \tag{7.7}$$

where γ_μ are Euclidean gamma matrices. On this lattice, momentum components lie in the first Brillouin zone, so $-\pi < p_\mu a < \pi$. The regulated Feynman graph (Fig. 7.3) is

$$f(p^2) = -4 \int_{\mathcal{B}} \frac{d^4k}{(2\pi)^4} a^2 \frac{m^2 a^2 - \sum_\mu \sin a k_\mu \cdot \sin a(p_\mu + k_\mu)}{\left[\sum_\nu \sin^2 a k_\nu + m^2 a^2\right] \left[\sum_\rho \sin^2 a(p_\rho + k_\rho) + m^2 a^2\right]} \tag{7.8}$$

where the integral is over the Brillouin zone $\mathcal{B}$. Note that as $a \to 0$, the regulated expression Eq. (7.8) reduces to the continuum expression Eq. (7.6).

In [10], there was a ghost at the origin. Since our goal is to check for potential regulator dependence of this statement, it suffices to extract the order p^2 part of $f(p^2)$. Thus, we expand Eq. (7.8) in p_μ and extract the second order term. We find

$$f(p^2) \simeq -4a^2 \sum_\mu p_\mu p_\mu a^2 \int_{\mathcal{B}} \frac{d^4k}{(2\pi)^4} \frac{a^2}{(m^2a^2 + \sum_\nu \sin^2 k_\nu a)^2} \left[-\frac{m^2a^2 - \sum_\nu \sin^2 k_\nu a}{m^2a^2 + \sum_\nu \sin^2 k_\nu a} \cos 2k_\mu a \right.$$
$$\left. + \frac{1}{2} \sin^2 k_\mu a + \frac{1}{2} \frac{\sin^2 2k_\mu a}{m^2a^2 + \sum_\nu \sin^2 k_\nu a} + \frac{m^2a^2 - \sum_\nu \sin^2 k_\nu a}{(m^2a^2 + \sum_\nu \sin^2 k_\nu a)^2} \sin^2 2k_\mu a \right]. \quad (7.9)$$

Now, in [10], the sign of the kinetic term was altered if the fermion mass was taken to be at least of order of the cutoff. For fermion masses large compared to the cutoff, analytic results were obtained demonstrating the presence of a ghost. In our case, we can obtain an analytic result when $ma \gg 1$. In this limit, the coefficient of p^2 induced by the quantum correction is given by

$$f(p^2) = -4a^2 \left(\frac{1}{m^2a^2} \right)^2 \int_{\mathcal{B}} \frac{d^4k}{(2\pi)^4} \sum_\mu \left[\frac{1}{2} p_\mu p_\mu a^2 \sin^2 k_\mu a - p_\mu p_\mu a^2 \cos 2k_\mu a \right] \quad (7.10)$$
$$= -4a^2 \left(\frac{1}{m^2a^2} \right)^2 \frac{p^2}{4a^2}. \quad (7.11)$$

Rotating back into Euclidean space, we find

$$G(p^2) \simeq p^2 + g^2 N \left(\frac{1}{ma} \right)^4 p^2. \quad (7.12)$$

Clearly, this quantity never becomes negative, so the sign of the kinetic term does not change in this theory, at least when $ma \gg 1$.

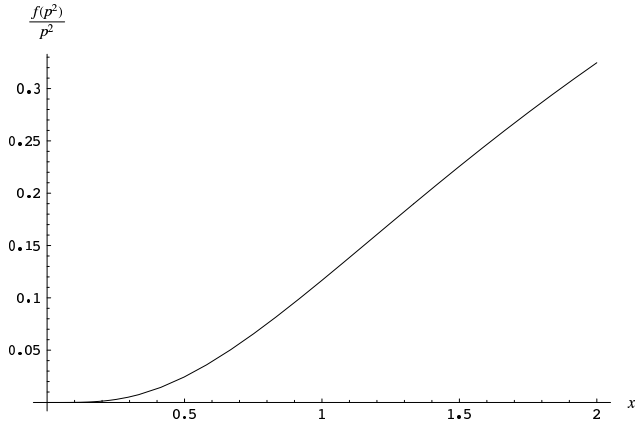

Figure 7.4: The quantum correction, $f(p^2)$, as a function of $x = 1/ma$. We have shown $f(p^2)/p^2$ for clarity.

To check for a sign change away from this limit, we have numerically integrated Eq. (7.9) to find the coefficient of p^2 induced by quantum corrections, as a function of $x = 1/(ma)$. The result is shown in Figure 7.4 for $0 \leq x \leq 2$. Evidently, $f(p^2)/p^2$ is never negative, so there can be no change in the sign. For large x, the fermion mass is much smaller than the cutoff so we need not worry about regulator dependence; therefore, we know from the results of [10] that there is no ghost in the region $x > 2$. This completes our demonstration that the sign of the kinetic term is always positive if the theory is regulated on a spacetime lattice.

7.3 Conclusions

We have examined the proposed high energy completion of the ghost condensate [10]. Using a lattice regulator, which is valid without invoking perturbation theory, and which is unitary, we have shown that this theory does not have a ghostly low energy effective action. The effect noted in [10], which involved changing the sign of the kinetic term for a scalar ϕ, appears to be a regulator dependent phenomenon. Thus, the search for a UV completion for the ghost condensate must continue.

Chapter 8

The Lee-Wick Standard Model

8.1 Introduction

The extreme fine-tuning needed to keep the Higgs mass small compared to the Planck scale (i.e., the hierarchy puzzle) has motivated many extensions of the minimal standard model. All of these contain new physics, beyond that in the minimal standard model, which might be observed at the Large Hadron Collider (LHC). The most widely explored of these extensions is low energy supersymmetry. In this chapter we introduce another extension of the standard model that solves the hierarchy puzzle.

Our approach builds on the work of Lee and Wick [11, 12] who studied the possibility that the regulator propagator in Pauli-Villars corresponds to a physical degree of freedom. Quantum electrodynamics with a photon propagator that includes the regulator term is a higher derivative version of QED. The higher derivative propagator contains two poles, one corresponding to the massless photon, and the other corresponding to a massive Lee-Wick-photon (LW-photon). A problem with this approach is that the residue of the massive LW-photon pole has the wrong sign. Lee and Wick argued that one can make physical sense of such a theory. There is no problem with unitarity since the massive LW-photon is not in the spectrum; it decays through its couplings to ordinary fermions. However, the wrong

sign residue moves the poles in the photon two point function that are associated with this massive resonance from the second sheet to the physical sheet, introducing time dependence that grows exponentially. Lee and Wick and Cutkosky et al. [225] propose a modification of the usual integration contour in Feynman diagrams that removes this growth and preserves unitarity of the S matrix[1]. This was further discussed in [227, 228].

The theory of QED that Lee and Wick studied is finite. In this chapter we propose to extend their idea to the standard model, removing the quadratic divergence associated with the Higgs mass, and thus solving the hierarchy problem. In the LW-standard model, every field in the minimal standard model has a higher derivative kinetic term that introduces a corresponding massive LW-resonance. These masses are additional free parameters in the theory and must be high enough to evade current experimental constraints. For the non-Abelian gauge bosons the higher derivative kinetic term has, because of gauge invariance, new higher derivative interactions. Hence the resulting theory is not finite; however, we argue that it does not give rise to a quadratic divergence in the Higgs mass, and so solves the hierarchy puzzle. A power counting argument and some explicit one-loop calculations are given to demonstrate this. For explicit calculations, and to make the physics clearer, it is useful to remove the higher derivative terms in the Lagrangian density by introducing auxiliary LW-fields that, when integrated out, reproduce the higher derivative terms in the action.

The LW-standard model[2] has a new parameter for each standard model field, which corresponds physically to the tree-level mass of its LW-partner resonance. Explicit calculations can be performed in this theory at any order in perturbation theory, and the experimental consequences for physics at the LHC, and elsewhere, can be studied. The nonperturbative

[1] The consistency of this approach is controversial [226].

[2] "LW extension of the standard model" would be more precise.

formulation of Lee-Wick theories has been studied in [229, 230]. Lee-Wick theories are unusual; however, even if one does not take the particular model we present as the correct theory of nature at the TeV scale our work does suggest that a further examination of higher derivative theories is warranted. Some previous work on field theories with non-local actions that contain terms with an infinite number of derivatives can be found in Ref. [231].

8.2 A Toy Model

To illustrate the physics of Lee-Wick theory [11, 12, 230] in a simple setting, we consider in this section a theory of one self-interacting scalar field, $\hat{\phi}$, with a higher derivative term. The Lagrangian density is

$$\mathcal{L}_{\rm hd} = \frac{1}{2}\partial_\mu\hat{\phi}\partial^\mu\hat{\phi} - \frac{1}{2M^2}(\partial^2\hat{\phi})^2 - \frac{1}{2}m^2\hat{\phi}^2 - \frac{1}{3!}g\hat{\phi}^3, \tag{8.1}$$

so the propagator of $\hat{\phi}$ in momentum space is given by

$$\hat{D}(p) = \frac{i}{p^2 - p^4/M^2 - m^2}. \tag{8.2}$$

For $M \gg m$, this propagator has poles at $p^2 \simeq m^2$ and also at $p^2 \simeq M^2$. Thus, the propagator describes more than one degree of freedom.

We can make these new degrees of freedom manifest in the Lagrangian density in a simple way. First, let us introduce an auxiliary scalar field $\tilde{\phi}$, so that we can write the theory as

$$\mathcal{L} = \frac{1}{2}\partial_\mu\hat{\phi}\partial^\mu\hat{\phi} - \frac{1}{2}m^2\hat{\phi}^2 - \tilde{\phi}\partial^2\hat{\phi} + \frac{1}{2}M^2\tilde{\phi}^2 - \frac{1}{3!}g\hat{\phi}^3. \tag{8.3}$$

Since $\mathcal{L}$ is quadratic in $\tilde{\phi}$, the equations of motion of $\tilde{\phi}$ are exact at the quantum level.

Removing $\tilde{\phi}$ from $\mathcal{L}$ with their equations of motion reproduces $\mathcal{L}_{\rm hd}$ in Eq. (8.1).

Next, we define $\phi = \hat{\phi}+\tilde{\phi}$. In terms of this variable, the Lagrangian in Eq. (8.3) becomes, after integrating by parts,

$$\mathcal{L} = \frac{1}{2}\partial_\mu\phi\partial^\mu\phi - \frac{1}{2}\partial_\mu\tilde{\phi}\partial^\mu\tilde{\phi} + \frac{1}{2}M^2\tilde{\phi}^2 - \frac{1}{2}m^2(\phi-\tilde{\phi})^2 - \frac{1}{3!}g(\phi-\tilde{\phi})^3. \tag{8.4}$$

In this form, it is clear that there are two kinds of scalar field: a normal scalar field ϕ and a new field $\tilde{\phi}$, which we will refer to as an LW-field. The sign of the quadratic Lagrangian of the LW-field is opposite to the usual sign so one may worry about stability of the theory, even at the classical level. We will return to this point. If we neglect the mass m for simplicity, the propagator of $\tilde{\phi}$ is given by

$$\tilde{D}(p) = \frac{-i}{p^2 - M^2}. \tag{8.5}$$

The LW-field is associated with a non-positive definite norm on the Hilbert space, as indicated by the unusual sign of its propagator. Consequently, if this state were to be stable, unitarity of the S matrix would be violated. However, as emphasized by Lee and Wick, unitarity is preserved provided that $\tilde{\phi}$ decays. This occurs in the theory described by Eq. (8.4) because $\tilde{\phi}$ is heavy and can decay to two ϕ-particles.

In the presence of the mass m, there is mixing between the scalar field ϕ and the LW-scalar $\tilde{\phi}$. We can diagonalize this mixing without spoiling the diagonal form of the derivative terms by performing a symplectic rotation on the fields:

$$\begin{pmatrix}\phi\\ \tilde{\phi}\end{pmatrix} = \begin{pmatrix}\cosh\theta & \sinh\theta\\ \sinh\theta & \cosh\theta\end{pmatrix}\begin{pmatrix}\phi'\\ \tilde{\phi}'\end{pmatrix}. \tag{8.6}$$

This transformation diagonalizes the Lagrangian if

$$\tanh 2\theta = \frac{-2m^2/M^2}{1-2m^2/M^2}. \tag{8.7}$$

A solution for the angle θ exists provided $M > 2m$. The Lagrangian (8.4) describing the system becomes

$$\mathcal{L} = \frac{1}{2}\partial_\mu\phi'\partial^\mu\phi' - \frac{1}{2}m'^2\phi'^2 - \frac{1}{2}\partial_\mu\tilde{\phi}'\partial^\mu\tilde{\phi}' + \frac{1}{2}M'^2\tilde{\phi}'^2 - \frac{1}{3!}(\cosh\theta - \sinh\theta)^3 g(\phi' - \tilde{\phi}')^3, \tag{8.8}$$

where m' and M' are the masses of the diagonalized fields. Notice the form of the interaction; we can define $g' = (\cosh\theta - \sinh\theta)^3 g$ and then drop the primes to obtain a convenient Lagrangian for computation.[3]

Introducing the LW-fields makes the physics of the theory clear. There are two fields; the heavy LW-scalar decays to the lighter scalar. At loop level, the presence of the heavier scalar improves the convergence of loop graphs at high energy consistent with our expectations from the higher derivative form of the theory. We can use the familiar technology of perturbative quantum field theory (appropriately modified [225]) to compute quantum corrections to the physics.

It is worth pausing for a moment to consider loop corrections to the two point function of the LW-field. Using the one-loop self energy, the full propagator for the LW-scalar is given, near $p^2 = M^2$, by

$$\begin{aligned}\tilde{D}(p) &= \frac{-i}{p^2-M^2} + \frac{-i}{p^2-M^2}(-i\Sigma(p^2))\frac{-i}{p^2-M^2} + \cdots \\ &= \frac{-i}{p^2-M^2+\Sigma(p^2)}.\end{aligned} \tag{8.9}$$

[3]In the following, we will always assume that $M \gg m$ so that $g' \simeq g$.

Note that, unlike for ordinary scalars, there is a plus sign in front of the self energy $\Sigma(p^2)$ in the denominator. This sign is significant; for example, if one defines the width in the usual way (i.e., near the pole the propagator has denominator $p^2 - M^2 + iM\Gamma$) then, from a one loop computation of the self energy Σ, the width of the LW-field is

$$\Gamma = -\frac{g^2}{32\pi M}\sqrt{1 - \frac{4m^2}{M^2}}. \tag{8.10}$$

This width differs in sign from widths of the usual particles we encounter. With this result in hand, we can demonstrate how unitarity of the theory is maintained in an explicit example. Consider $\phi\phi$ scattering in this theory. From unitarity, the imaginary part of the forward scattering amplitude, $\mathcal{M}$, must be a positive quantity. Near $p^2 = M^2$, the scattering is dominated by the $\tilde{\phi}$ pole and therefore the imaginary part of the amplitude is given by

$$\mathrm{Im}\mathcal{M} = -g^2\frac{M\Gamma}{(p^2 - M^2)^2 + M^2\Gamma^2}. \tag{8.11}$$

The unusual sign of the propagator is compensated by the unusual sign of the decay width.

As another consequence of this sign, the poles associated with these LW-particles occur on the physical sheet of the analytic continuation of the S matrix, in violation of the usual rules of S matrix theory [4]. These signs are also associated with exponential growth of disturbances, which is related to the stability concerns alluded to earlier. Lee and Wick, and Cutkowsky et al. argued that one can nevertheless make sense of these theories by modifying the usual contour prescription for momentum integrals. The Feynman $i\epsilon$ prescription can be thought of as a deformation of the contour such that the poles on the real axis are appropriately above or below the contour. The Lee-Wick prescription is to deform the

[4]Notice that since the usual S matrix analyticity conditions are explicitly violated in this theory, the constraints discussed in Chapter 6 need not apply.

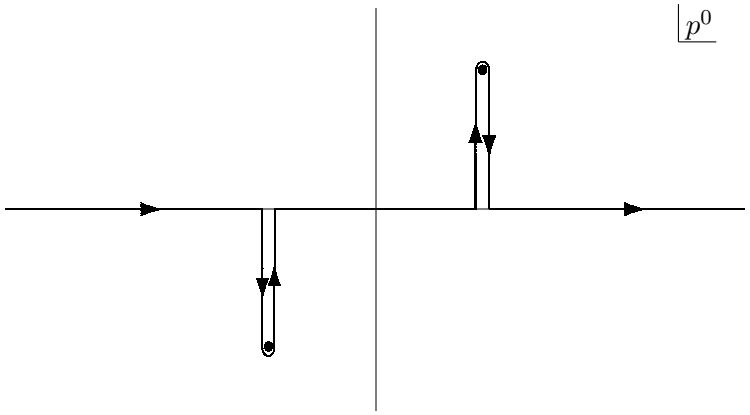

Figure 8.1: The Lee-Wick prescription for the contour of integration in the complex energy plane. The dots represent poles occurring in the integrand.

contour so that these poles are still above or below the contour as before in the presence of the finite width, as shown in Figure 8.1. Hence, the negative width in Eq. (8.10) leads to exponential decay.

The Lee-Wick prescription is equivalent to imposing the boundary condition that there are no outgoing exponentially growing modes. It is well known that such future boundary conditions cause violations of causality. In the Lee-Wick theory the acausal effects occur only on microscopic scales, and show up as peculiar behavior of resonances in scattering experiments. It is believed that this theory does not produce violations of causality on a macroscopic scale [228].

8.3 The Hierarchy Problem and Lee-Wick Theory

In this section, we consider a scalar in the fundamental representation interacting with gauge bosons. We find the Lagrange density for the LW version of such a theory and show by power counting appropriate to the higher derivative version of the theory that the scalar mass is free of quadratic divergences. We then show by an explicit one-loop calculation that the ordinary scalar and the massive LW-fields do not receive a quadratically divergent

contribution to their pole masses.

8.3.1 Gauge Fields

The higher derivative Lagrangian in the gauge sector is

$$\mathcal{L}_{\rm hd} = -\frac{1}{2}\,\mathrm{tr}\,\hat{F}_{\mu\nu}\hat{F}^{\mu\nu} + \frac{1}{M_A^2}\,\mathrm{tr}\left(\hat{D}^\mu \hat{F}_{\mu\nu}\right)\left(\hat{D}^\lambda \hat{F}_\lambda{}^\nu\right), \tag{8.12}$$

where $\hat{F}_{\mu\nu} = \partial_\mu \hat{A}_\nu - \partial_\nu \hat{A}_\mu - ig[\hat{A}_\mu, \hat{A}_\nu]$, and $\hat{A}_\mu = \hat{A}_\mu^A T^A$ with T^A the generators of the gauge group G in the fundamental representation. We can now eliminate the higher derivative term by introducing auxiliary massive gauge bosons $\tilde{A}$. Each gauge boson is described by a Lagrangian

$$\mathcal{L} = -\frac{1}{2}\,\mathrm{tr}\,\hat{F}_{\mu\nu}\hat{F}^{\mu\nu} - M_A^2\,\mathrm{tr}\,\tilde{A}_\mu\tilde{A}^\mu + 2\,\mathrm{tr}\,\hat{F}_{\mu\nu}\hat{D}^\mu\tilde{A}^\nu, \tag{8.13}$$

where $\hat{D}_\mu \tilde{A}_\nu = \partial_\mu \tilde{A}_\nu - ig[\hat{A}_\mu, \tilde{A}_\nu]$. To diagonalize the kinetic terms, we introduce shifted fields defined by

$$\hat{A}_\mu = A_\mu + \tilde{A}_\mu. \tag{8.14}$$

The Lagrangian becomes

$$\begin{aligned}\mathcal{L} = &-\frac{1}{2}\,\mathrm{tr}\,F_{\mu\nu}F^{\mu\nu} + \frac{1}{2}\,\mathrm{tr}\left(D_\mu\tilde{A}_\nu - D_\nu\tilde{A}_\mu\right)\left(D^\mu\tilde{A}^\nu - D^\nu\tilde{A}^\mu\right) - ig\,\mathrm{tr}\left(\left[\tilde{A}_\mu, \tilde{A}_\nu\right]F^{\mu\nu}\right)\\ &- \frac{3}{2}g^2\,\mathrm{tr}\left(\left[\tilde{A}_\mu, \tilde{A}_\nu\right]\left[\tilde{A}^\mu, \tilde{A}^\nu\right]\right) - 4ig\,\mathrm{tr}\left(\left[\tilde{A}_\mu, \tilde{A}_\nu\right]D^\mu\tilde{A}^\nu\right) - M_A^2\,\mathrm{tr}\left(\tilde{A}_\mu\tilde{A}^\mu\right).\end{aligned} \tag{8.15}$$

Note that for a $U(1)$ gauge boson all the commutators vanish, there are no traces and an extra overall factor of $1/2$.

To perform perturbative calculations, we must introduce a gauge fixing term. We could introduce such a term in the higher derivative Lagrangian, Eq. (8.12), in terms of the

Lagrangian involving A and $\tilde{A}$, Eq. (8.15), or even in the Lagrangian with mixed kinetic terms for $\hat{A}$ and $\tilde{A}$, Eq. (8.13). As is usual in gauge theories, all of these choices will yield the same results for physical quantities, but they may differ for unphysical quantities. Different gauge choices can differ on how divergent unphysical quantities are. Therefore, we will only compute physical pole masses below. In these computations, we introduce a covariant gauge fixing term for the gauge bosons, A_μ^A, in the two-field description of the theory given in Eq. (8.15). In this choice of gauge, the propagator for the gauge bosons is given by

$$D_{\mu\nu}^{AB}(p) = \delta^{AB}\frac{i}{p^2}\left(\eta_{\mu\nu} - (1-\xi)\frac{p_\mu p_\nu}{p^2}\right), \tag{8.16}$$

while the propagator for the LW-gauge field is

$$\tilde{D}_{\mu\nu}^{AB}(p) = \delta^{AB}\frac{-i}{p^2 - M_A^2}\left(\eta_{\mu\nu} - \frac{p_\mu p_\nu}{M_A^2}\right). \tag{8.17}$$

8.3.2 Scalar Matter

Let us move on to consider scalar matter transforming in the fundamental representation of the gauge group. In ordinary field theory, such a scalar field has a quadratic divergence in its pole mass. The higher derivative Lagrangian is given in terms of the scalar field $\hat{\phi}$ by

$$\mathcal{L}_{\rm hd} = \left(\hat{D}_\mu\hat{\phi}\right)^\dagger\left(\hat{D}^\mu\hat{\phi}\right) - \frac{1}{M_\phi^2}\left(\hat{D}_\mu\hat{D}^\mu\hat{\phi}\right)^\dagger\left(\hat{D}_\nu\hat{D}^\nu\hat{\phi}\right) - V(\hat{\phi}). \tag{8.18}$$

We eliminate the higher derivative term by introducing an LW-scalar multiplet $\tilde{\phi}$. Then the Lagrangian is given in terms of the two fields $\hat{\phi}$ and $\tilde{\phi}$ by

$$\mathcal{L} = \left(\hat{D}_\mu\hat{\phi}\right)^\dagger\left(\hat{D}^\mu\hat{\phi}\right) + M_\phi^2\tilde{\phi}^\dagger\tilde{\phi} + \left(\hat{D}_\mu\hat{\phi}\right)^\dagger\left(\hat{D}^\mu\tilde{\phi}\right) + \left(\hat{D}^\mu\tilde{\phi}\right)^\dagger\left(\hat{D}^\mu\hat{\phi}\right) - V(\hat{\phi}), \tag{8.19}$$

where the covariant derivative is

$$\hat{D}_\mu = \partial_\mu + ig\hat{A}^A_\mu T^A. \tag{8.20}$$

For simplicity we take the ordinary scalar to have no potential at tree level, $V(\hat{\phi}) = 0$. It is not hard to include a potential for $\hat{\phi}$ in the analysis, and to show that the potential does not change our results.

We diagonalized the pure gauge sector by shifting the gauge fields; in terms of the shifted gauge fields the hatted covariant derivative is

$$\hat{D}_\mu = D_\mu + ig\tilde{A}^A_\mu T^A, \tag{8.21}$$

where $D_\mu = \partial_\mu + igA^A_\mu T^A$ is the usual covariant derivative. To diagonalize the scalar kinetic terms, we again shift the field

$$\hat{\phi} = \phi - \tilde{\phi}. \tag{8.22}$$

The scalar Lagrangian becomes

$$\begin{aligned}\mathcal{L} = {} & (D_\mu\phi)^\dagger D^\mu\phi - (D_\mu\tilde{\phi})^\dagger D^\mu\tilde{\phi} + M^2_\phi\tilde{\phi}^\dagger\tilde{\phi} + ig(D^\mu\phi)^\dagger\tilde{A}^A_\mu T^A\phi + g^2\phi^\dagger\tilde{A}^A_\mu T^A\tilde{A}^{B\mu}T^B\phi \\ & -ig\phi^\dagger\tilde{A}^A_\mu T^A D^\mu\phi - ig(D^\mu\tilde{\phi})^\dagger\tilde{A}^A_\mu T^A\tilde{\phi} + ig\tilde{\phi}^\dagger\tilde{A}^A_\mu T^A D^\mu\tilde{\phi} - g^2\tilde{\phi}^\dagger\tilde{A}^A_\mu T^A\tilde{A}^{B\mu}T^B\tilde{\phi}.\end{aligned} \tag{8.23}$$

8.3.3 Power Counting

Having defined the higher derivative and LW forms of the theory, we present a power counting argument for the higher derivative version of the theory which indicates that the only physical divergences in the theory are logarithmic. Since the power counting argument

depends on the behaviour of Feynman graphs at high energies, we only need to consider the terms in the Lagrangian which are most important at high energies.

For the perturbative power counting argument in the higher derivative theory, it is necessary to fix the gauge. We choose to add a covariant gauge fixing term $-(\partial_\mu \hat{A}^{A\mu})^2/2\xi$ to the Lagrange density and introduce Faddeev-Popov ghosts that couple to the gauge bosons in the usual way. Then the propagator for the gauge field is

$$\hat{D}^{AB}_{\mu\nu}(p) = \delta^{AB} \frac{-i}{p^2 - p^4/M_A^2} \left(\eta_{\mu\nu} - (1-\xi)\frac{p_\mu p_\nu}{p^2} - \xi \frac{p_\mu p_\nu}{M_A^2} \right). \tag{8.24}$$

We work in $\xi = 0$ gauge. Note that $\xi = 0$ corresponds to Landau gauge and that the gauge boson propagator scales as p^{-4} at high energy. The propagator for the scalar in the fundamental representation is

$$\hat{D}^{ab}(p) = \delta^{ab} \frac{i}{p^2 - p^4/M_\phi^2}. \tag{8.25}$$

At large momenta the scalar propagator scales as p^{-4} while the Faddeev-Popov ghost propagator scales as p^{-2}, as usual. There are three kinds of vertices: those where only gauge bosons interact, vertices where gauge bosons interact with two scalars, and vertices where two ghosts interact with one gauge boson. A vertex where n vectors interact (with no scalars) scales as p^{6-n} while a vertex with two scalars and n vectors scales as p^{4-n}. The vertex between two ghosts and one gauge field scales as one power of p, as usual.

Consider an arbitrary Feynman graph with L loops, I' internal vector lines, I internal scalar lines, I_g internal ghost lines, and with V'_n or V_n vertices with n vectors and zero or two scalar particles, respectively. We also suppose there are V_g ghost vertices. Then the

superficial degree of divergence, d, is

$$d = 4L - 4I' - 4I - 2I_g + \sum_n V'_n(6-n) + \sum_n V_n(4-n) + V_g. \tag{8.26}$$

We can simplify this expression using some identities. First, the number of loops is related to the total number of propagators and vertices by

$$L = I + I' + I_g - \sum_n (V'_n + V_n) - V_g + 1, \tag{8.27}$$

while the total number of lines entering or leaving the vertices is related to the number of propagators and external lines by

$$\sum_n \left(nV'_n + (n+2)V_n\right) + 3V_g = 2(I + I' + I_g) + E + E' + E_g, \tag{8.28}$$

where E is the number of external scalars, E' is the number of external vectors, and E_g is the number of external ghosts. Finally, because the Lagrangian is quadratic in the number of scalars and ghosts, the number of scalar lines and ghost lines is separately conserved. Thus,

$$2\sum_n V_n = 2I + E, \quad 2V_g = 2I_g + E_g. \tag{8.29}$$

With these identities in hand, we may express the superficial degree of divergence as

$$d = 6 - 2L - E - E' - 2E_g. \tag{8.30}$$

Gauge invariance removes the potential quadratic divergence in the gauge boson two-point function. Scalar mass renormalizations have $E = 2$, so that $d = 4 - 2L$. Consequently,

the only possible quadratic divergence in the scalar mass is at one loop. However, gauge invariance also removes the divergence in the scalar mass renormalization, because two of the derivatives must act on the external legs. To see this, note that the interaction involves

$$\phi^\dagger D^4 \phi \sim \phi^\dagger (\partial^2 + \partial \cdot A + A \cdot \partial + A^2)^2 \phi. \tag{8.31}$$

Since we are working in Lorentz gauge, $\partial \cdot A = 0$. We may ignore the A^2 term compared to the $A \cdot \partial$ term, as it is less divergent. Thus the most divergent terms in the interaction are $\phi^\dagger A \cdot \partial \partial^2 \phi$ or $\phi^\dagger \partial^2 A \cdot \partial \phi$, where the ϕ acted on by the derivatives is an internal line. But by integration by parts and use of the gauge condition, we see that, at one loop, we can always take one of the derivatives to act on the external scalar. Thus the theory at hand is at most logarithmically divergent.[5]

8.3.4 One-Loop Pole Mass

The power counting argument above was presented in the higher derivative version of the theory. As a check of the formalism we show, in the LW version of the theory, that the shift in the pole masses of the ordinary scalar, the LW-scalar and the LW-gauge boson do not receive quadratically divergent contributions at one loop. It is important to compute a physical quantity since it is for these that the higher derivative theory and the theory with LW-fields give equivalent results[6]. We perform the computations in Feynman gauge, using the propagators in Eqs. (8.16) and (8.17), and regulate our diagrams where necessary using dimensional regularization with dimension n.

[5] It may seem that adding operators with more than four derivatives could yield a finite theory, but that is not the case. These theories are still logarithmically divergent.

[6] We have fixed different gauges in our discussion of the power counting argument in the higher derivative theory and our explicit computations in the LW version of the theory. Consequently, we can only expect agreement between these theories for physical quantities.

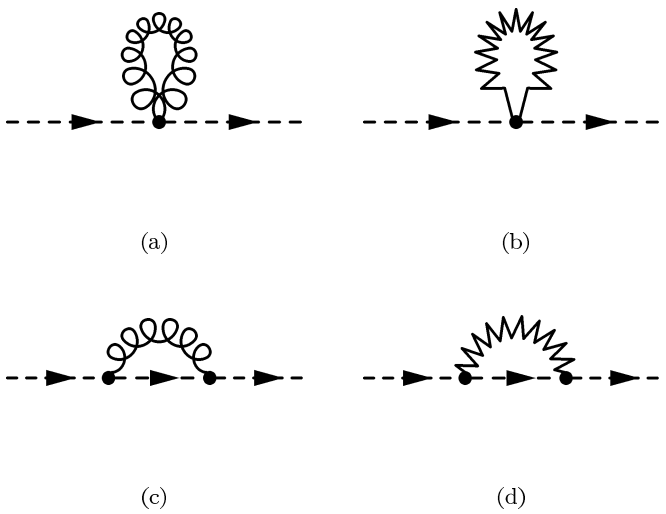

Figure 8.2: One-loop mass renormalization of the normal scalar field. The curly line is a gauge field while the zigzag line is the LW-gauge field. The dashed line represents the scalar field.

8.3.4.1 The normal scalar

At one loop, there are four graphs contributing to the scalar mass, as shown in Figure 8.2.

We find

$$-i\Sigma_a(0) = g^2 C_2(N) \int \frac{d^n k}{(2\pi)^n} \frac{n}{k^2} \tag{8.32a}$$

$$-i\Sigma_b(0) = -g^2 C_2(N) \int \frac{d^n k}{(2\pi)^n} \left(\frac{n-1}{k^2 - M_A^2} - \frac{1}{M_A^2} \right) \tag{8.32b}$$

$$-i\Sigma_c(0) = -g^2 C_2(N) \int \frac{d^n k}{(2\pi)^n} \frac{1}{k^2} \tag{8.32c}$$

$$-i\Sigma_d(0) = -g^2 C_2(N) \int \frac{d^n k}{(2\pi)^n} \frac{1}{M_A^2}. \tag{8.32d}$$

We see that the quartic and quadratic divergences in this expressions cancel in the sum, so that the mass is only logarithmically divergent.

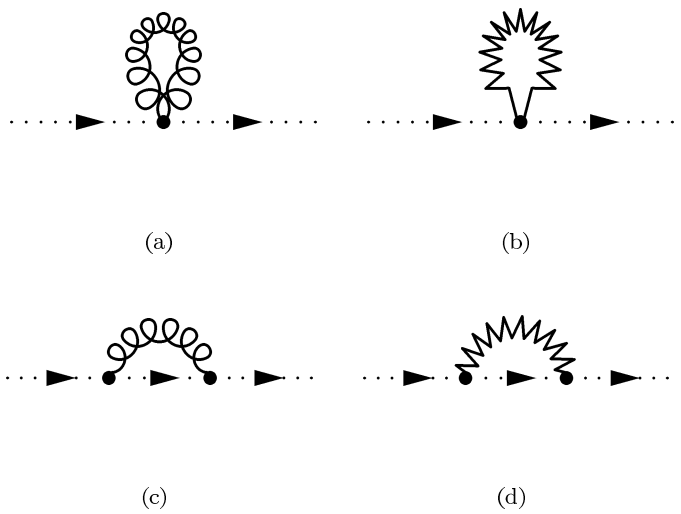

Figure 8.3: One-loop mass renormalization of the LW-scalar field. The dotted line represents the LW-scalar field while the other propagators are as in Figure 8.2.

8.3.4.2 The LW-scalar

At one loop the shift in the pole mass is determined by the self energy $\Sigma(p^2)$ evaluated at $p^2 = M_\phi^2$. The Feynman graphs are shown in Figure 8.3. We find

$$-i\Sigma_a(M_\phi^2) = -g^2 C_2(N) \int \frac{d^n k}{(2\pi)^n} \frac{n}{k^2} \tag{8.33a}$$

$$-i\Sigma_b(M_\phi^2) = g^2 C_2(N) \int \frac{d^n k}{(2\pi)^n} \left(\frac{n-1}{k^2 - M_A^2} - \frac{1}{M_A^2} \right) \tag{8.33b}$$

$$-i\Sigma_c(M_\phi^2) = g^2 C_2(N) \int \frac{d^n k}{(2\pi)^n} \left(\frac{1}{k^2 - 2p\cdot k} + \frac{4M_\phi^2 - 4p\cdot k}{k^2(k^2 - 2p\cdot k)} \right) \tag{8.33c}$$

$$-i\Sigma_d(M_\phi^2) = g^2 C_2(N) \int \frac{d^n k}{(2\pi)^n} \left(\frac{1}{M_A^2} - \frac{4M_\phi^2 - 2p\cdot k}{(k^2 - M_A^2)(k^2 - 2p\cdot k)} \right). \tag{8.33d}$$

Once again, the quartic and quadratic divergence cancel in the sum of the graphs, so that there is only a logarithmic divergence in the mass of the LW-scalar.

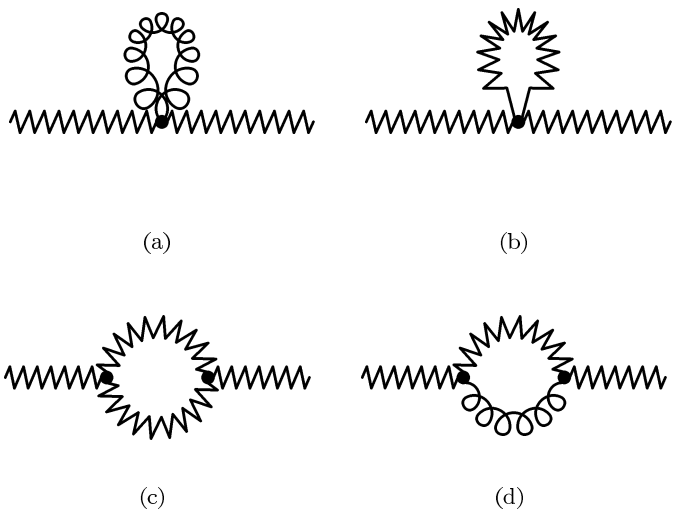

Figure 8.4: One-loop mass renormalization of the LW-vector field. The propagators are as in Figure 8.2.

8.3.4.3 The LW-vector

For the LW-vectors the self energy tensor has the form

$$\Sigma^{AB}_{\mu\nu}(p^2) = \delta^{AB}\left[\Sigma(p^2)\eta_{\mu\nu} + \Sigma'(p^2)p_\mu p_\nu\right]. \tag{8.34}$$

The shift in the pole mass is determined by $\Sigma(M_A^2)$. The relevant graphs are shown in Figure 8.4. They are very divergent. There are individual terms in Figure 8.4(c) that diverge as the sixth power of a momentum cutoff. However these cancel. There is also a quartic divergence in diagrams (b), (c), and (d) that cancels between them. To check that the quadratic divergence cancels we regulate the diagrams with dimensional regularization. In n dimensions, a quadratic divergence manifests itself as a pole at $n = 2$. Hence, we set $n = 2 - \epsilon$, expand about $\epsilon = 0$ and extract the $1/\epsilon$ part of $\Sigma(M_A^2)$. We find that

$$-i\Sigma_a(M_A^2) = \frac{ig^2}{4\pi}C_2(G)\left(-\frac{2}{\epsilon}\right) \tag{8.35a}$$

$$-i\Sigma_b(M_A^2) = \frac{ig^2}{4\pi}C_2(G)\left(\frac{3}{\epsilon}\right) \tag{8.35b}$$

$$-i\Sigma_c(M_A^2) = \frac{ig^2}{4\pi}C_2(G)\left(-\frac{6}{\epsilon}\right) \tag{8.35c}$$

$$-i\Sigma_d(M_A^2) = \frac{ig^2}{4\pi}C_2(G)\left(\frac{5}{\epsilon}\right). \tag{8.35d}$$

As expected, the $1/\epsilon$ pole cancels in the sum. Finally, we note that there are quadratic divergences in $\Sigma_{\mu\nu}^{AB}(p^2)$. Only the gauge invariant physical quantity $\Sigma(M_A^2)$ must be free of quadratic divergences.

8.4 Lee-Wick Standard Model Lagrangian

Now that we have understood why the radiative correction to the Higgs mass cancels in these higher derivative theories, we move on to discuss the Lagrangian which describes the standard model extended to include a Lee-Wick partner for each particle. The gauge sector is as before.

8.4.1 The Higgs Sector

A higher derivative Lee-Wick Higgs sector was considered previously in [229]. We take the higher derivative Lagrangian for the Higgs doublet $\hat{H}$ to be

$$\mathcal{L}_{\rm hd} = \left(\hat{D}_\mu\hat{H}\right)^\dagger\left(\hat{D}^\mu\hat{H}\right) - \frac{1}{M_H^2}\left(\hat{D}_\mu\hat{D}^\mu\hat{H}\right)^\dagger\left(\hat{D}_\nu\hat{D}^\nu\hat{H}\right) - V(\hat{H}), \tag{8.36}$$

where the covariant derivative is given by

$$\hat{D}_\mu = \partial_\mu + ig\hat{A}_\mu^A T^A + ig_2\hat{W}_\mu^a T^a + ig_1\hat{B}_\mu Y, \tag{8.37}$$

while the potential is

$$V(\hat{H}) = \frac{\lambda}{4}\left(\hat{H}^\dagger \hat{H} - \frac{v^2}{2}\right)^2. \tag{8.38}$$

We can then eliminate the higher derivative term by introducing an LW-Higgs doublet $\tilde{H}$. As before, we then diagonalize the Lagrangian by introducing the shifted field $\hat{H} = H - \tilde{H}$. To diagonalize the gauge field Lagrangian, we introduced Lee-Wick gauge bosons $\tilde{A}$, $\tilde{B}$, and $\tilde{W}$ as well as the usual gauge fields A, B and W. In terms of these fields the covariant derivative is

$$\hat{D}_\mu = D_\mu + ig\tilde{A}^A_\mu T^A + ig_2\tilde{W}^a_\mu T^a + ig_1\tilde{B}_\mu Y, \tag{8.39}$$

where

$$D_\mu = \partial_\mu + igA^A_\mu T^A + ig_2 W^a_\mu T^a + ig_1 B_\mu Y \tag{8.40}$$

is the usual standard model covariant derivative. We introduce the notation

$$\tilde{\mathbf{A}}_\mu = g\tilde{A}^A_\mu T^A + g_2\tilde{W}^a_\mu T^a + g_1\tilde{B}_\mu Y \tag{8.41}$$

for the LW-gauge bosons. The Lee-Wick form of the Higgs Lagrangian is then

$$\begin{aligned}\mathcal{L} = {} & (D_\mu H)^\dagger D^\mu H - \left(D_\mu \tilde{H}\right)^\dagger D^\mu \tilde{H} + M_H^2 \tilde{H}^\dagger \tilde{H} - V(H, \tilde{H}) + i\left(D_\mu H\right)^\dagger \tilde{\mathbf{A}}^\mu H \\ & - iH^\dagger \tilde{\mathbf{A}}_\mu D^\mu H + H^\dagger \tilde{\mathbf{A}}_\mu \tilde{\mathbf{A}}^\mu H - i\left(D_\mu \tilde{H}\right)^\dagger \tilde{\mathbf{A}}^\mu \tilde{H} + i\tilde{H}^\dagger \tilde{\mathbf{A}}_\mu D^\mu \tilde{H} - \tilde{H}^\dagger \tilde{\mathbf{A}}_\mu \tilde{\mathbf{A}}^\mu \tilde{H}, \end{aligned} \tag{8.42}$$

where V is given by the expression

$$\begin{aligned} V(H,\tilde{H}) &= V(H-\tilde{H}) \\ &= \frac{\lambda}{4}\left(H^\dagger H-\frac{v^2}{2}\right)^2+\frac{\lambda}{2}\left(H^\dagger H-\frac{v^2}{2}\right)\tilde{H}^\dagger\tilde{H}-\frac{\lambda}{2}\left(H^\dagger H-\frac{v^2}{2}\right)\left(\tilde{H}^\dagger H+H^\dagger\tilde{H}\right) \\ &\quad +\frac{\lambda}{4}\left[\left(H^\dagger\tilde{H}\right)^2+\left(\tilde{H}^\dagger H\right)^2+\left(\tilde{H}^\dagger\tilde{H}\right)^2+2\left(H^\dagger\tilde{H}\right)\left(\tilde{H}^\dagger H\right)-2\left(H^\dagger\tilde{H}\right)\left(\tilde{H}^\dagger\tilde{H}\right)\right. \\ &\quad \left.-2\left(\tilde{H}^\dagger H\right)\left(\tilde{H}^\dagger\tilde{H}\right)\right]. \end{aligned} \tag{8.43}$$

In unitary gauge, we write

$$H=\begin{pmatrix}0\\ \\ \frac{v+h}{\sqrt{2}}\end{pmatrix},\qquad \tilde{H}=\begin{pmatrix}\tilde{h}^+\\ \\ \frac{\tilde{h}+i\tilde{P}}{\sqrt{2}}\end{pmatrix}. \tag{8.44}$$

With this choice, the mass Lagrangian for the Higgs scalar, its partner, the charged LW-Higgs and pseudoscalar LW-Higgs fields is

$$\mathcal{L}_{\text{mass}}=-\frac{\lambda}{4}v^2(h-\tilde{h})^2+\frac{M_H^2}{2}\left(\tilde{h}\tilde{h}+\tilde{P}\tilde{P}+2\tilde{h}^+\tilde{h}^-\right). \tag{8.45}$$

There is mixing between the usual Higgs scalar and its partner; this mixing can be treated perturbatively. It is possible to diagonalize the mass matrices of these particles via a symplectic rotation, which preserves the diagonal form of the kinetic terms.

The Higgs vacuum expectation value induces masses for the gauge bosons. First, we focus on the mass Lagrangian for the LW-gauge bosons. In terms of the $SU(2)$ and $U(1)$ LW-gauge fields, the Lagrangian is

$$\mathcal{L}_{mass}=\frac{g_2^2v^2}{8}\left(\tilde{W}_\mu^a\tilde{W}^{a\mu}\right)-\frac{g_1g_2v^2}{4}\tilde{W}_\mu^3\tilde{B}^\mu+\frac{g_1^2v^2}{8}\tilde{B}_\mu\tilde{B}^\mu-\frac{M_1^2}{2}\tilde{B}_\mu\tilde{B}^\mu-\frac{M_2^2}{2}\tilde{W}_\mu^a\tilde{W}^{a\mu}. \tag{8.46}$$

There is mixing between the $\tilde{W}^3$ and $\tilde{B}$ LW-gauge fields. We can diagonalize this Lagrangian by writing

$$\begin{pmatrix} \tilde{W}^3 \\ \tilde{B} \end{pmatrix} = \begin{pmatrix} \cos\phi & \sin\phi \\ -\sin\phi & \cos\phi \end{pmatrix} \begin{pmatrix} \tilde{U} \\ \tilde{V} \end{pmatrix}, \tag{8.47}$$

where the mixing angle is given by

$$\tan 2\phi = \frac{g_1 g_2 v^2}{2} \left(M_1^2 - M_2^2 + (g_2^2 - g_1^2)\frac{v^2}{4} \right)^{-1}. \tag{8.48}$$

We expect that $M_{1,2}$ lie in the TeV range, so that ϕ is a small angle.

There is also mixing between the gauge fields and the LW-gauge fields. We will treat this mixing perturbatively. The Lagrangian describing this mixing is

$$\mathcal{L}_{\text{mix}} = M_W^2 \left(W_\mu^+ \tilde{W}^{-\mu} + \tilde{W}_\mu^+ W^{-\mu} \right) + M_Z^2 Z_\mu \left(\cos\theta_W \tilde{W}^{3\mu} - \sin\theta_W \tilde{B}^\mu \right), \tag{8.49}$$

where θ_W is the Weinberg angle and M_W, M_Z are the usual tree-level standard model masses for the W and Z gauge bosons. One consequence of the mixing is that there is a tree-level correction to the electroweak ρ parameter

$$\Delta\rho = \rho - 1 = -\frac{\sin^2\theta_W M_Z^2}{M_1^2}. \tag{8.50}$$

The current experimental constraint on this parameter is $|\Delta\rho| \lesssim 10^{-3}$ [192], which leads to $M_1 \gtrsim 1\text{TeV}$.

8.4.2 Fermion Kinetic Terms

For simplicity, we discuss explicitly the case of a single left-handed quark doublet Q_L. It is straightforward to generalize this work to the other representations, and to include generation indices.

The higher derivative theory is

$$\mathcal{L}_{\rm hd} = \overline{\hat{Q}}_L i\hat{\not{D}}\hat{Q}_L + \frac{1}{M_Q^2}\overline{\hat{Q}}_L i\hat{\not{D}}\hat{\not{D}}\hat{\not{D}}\hat{Q}_L. \tag{8.51}$$

Naive power counting of the possible divergences in this higher derivative theory shows that there are potential quadratic divergences in one-loop graphs containing two external gauge bosons and a fermionic loop. However, gauge invariance forces these graphs to be proportional to two powers of the external momentum so that the graphs are only logarithmically divergent. In this case, this cancellation is most easily understood in the LW description of the theory, which we now construct.

We eliminate the higher derivative term by introducing LW-quark doublets $\tilde{Q}_L$, $\tilde{Q}'_R$ which form a real representation of the gauge groups. The Lagrangian in this formulation becomes

$$\mathcal{L} = \overline{\hat{Q}}_L i\hat{\not{D}}\hat{Q}_L + M_Q\left(\overline{\tilde{Q}}_L\tilde{Q}'_R + \overline{\tilde{Q}'}_R\tilde{Q}_L\right) + \overline{\tilde{Q}}_L i\hat{\not{D}}\hat{Q}_L + \overline{\hat{Q}}_L i\hat{\not{D}}\tilde{Q}_L - \overline{\tilde{Q}'}_R i\hat{\not{D}}\tilde{Q}'_R. \tag{8.52}$$

Eliminating the LW-fermions with their equations of motion

$$\tilde{Q}'_R = -\frac{i\hat{\not{D}}}{M_Q}\hat{Q}_L, \quad \tilde{Q}_L = \frac{\hat{\not{D}}\hat{\not{D}}}{M_Q^2}\hat{Q}_L, \tag{8.53}$$

reproduces the higher derivative Lagrangian, Eq. (8.51).

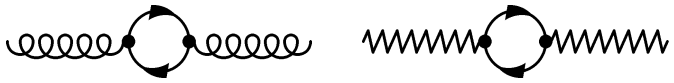

(a) (b)

Figure 8.5: One-loop graphs involving fermions which are potentially quadratically divergent. The solid lines represent fermion propagators while the curly and zigzag lines represent gauge bosons and LW-gauge bosons, respectively.

To diagonalize the kinetic terms, we introduce the shift $\hat{Q}_L = Q_L - \tilde{Q}_L$, and the Lagrangian becomes

$$\mathcal{L} = \overline{Q}_L i\not{D} Q_L - \overline{\tilde{Q}}_L i\not{D} \tilde{Q}_L - \overline{\tilde{Q}'}_R i\not{D} \tilde{Q}'_R + M_Q \left(\overline{\tilde{Q}}_L \tilde{Q}'_R + \overline{\tilde{Q}'}_R \tilde{Q}_L \right)$$
$$-\overline{Q_L} \gamma_\mu \tilde{\mathbf{A}}^\mu Q_L + \overline{\tilde{Q}_L} \gamma_\mu \tilde{\mathbf{A}}^\mu \tilde{Q}_L + \overline{\tilde{Q}'_R} \gamma_\mu \tilde{\mathbf{A}}^\mu \tilde{Q}'_R. \tag{8.54}$$

Note that $\tilde{Q}_L$ and $\tilde{Q}'_R$ combine into a single Dirac spinor of mass M_Q.

Now let us return to the issue of potential quadratic divergences in the theory. Inspection of the Lagrangian, Eq. (8.54), shows that the only one loop graphs involving fermionic loops are the graphs of Figure 8.5. Figure 8.5a is a one-loop correction to the gauge boson propagator, and consequently is proportional to p^2, where p is the momentum flowing into the graph. Thus, the graph is logarithmically divergent, as is well known. Figure 8.5b is a one-loop correction to the LW-gauge boson propagator. One might think that this graph could introduce a quadratic divergence of the LW-gauge boson mass. However, the vertices between the fermions and the gauge bosons are equal to the vertices between the fermions and the LW-gauge bosons, as can be seen in Eq. (8.54). Thus, Figure 8.5b is logarithmically divergent. Higher loop graphs in the theory are at most logarithmically divergent by power counting.

8.4.3 Fermion Yukawa Interactions

To simplify the discussion in this section, we will neglect neutrino masses. In the higher derivative formulation, the fermion Yukawas are

$$\mathcal{L}_Y = g_u^{ij}\overline{\hat{u}^i}_R\hat{H}\epsilon\hat{Q}_L^j - g_d^{ij}\overline{\hat{d}^i}_R\hat{H}^\dagger\hat{Q}_L^j - g_e^{ij}\overline{\hat{e}^i}_R\hat{H}^\dagger\hat{L}_L^j + \text{h.c.}, \tag{8.55}$$

where repeated flavor indices are summed. In the formulation of the theory in which there are no higher derivatives, and in which the kinetic terms are diagonal, this becomes

$$\begin{aligned}\mathcal{L}_Y = {} & g_u^{ij}(\overline{u^i}_R - \overline{\tilde{u}^i}_R)(H - \tilde{H})\epsilon(Q_L^j - \tilde{Q}_L^j) - g_d^{ij}(\overline{d^i}_R - \overline{\tilde{d}^i}_R)(H^\dagger - \tilde{H}^\dagger)(Q_L^j - \tilde{Q}_L^j) \\ & - g_e^{ij}(\overline{e^i}_R - \overline{\tilde{e}^i}_R)(H^\dagger - \tilde{H}^\dagger)(L_L^j - \tilde{L}_L^j) + \text{h.c.}.\end{aligned} \tag{8.56}$$

The presence of the LW-fields in this equation improves the degree of convergence at one loop. For example, consider a one-loop correction to the Higgs two-point function coming from the first term of Eq. (8.56). Various degrees of freedom can propagate in the loop: the u_R and Q_L quarks, and also the $\tilde{u}_R$ and $\tilde{Q}_L$ LW-quarks. The presence of the LW-quarks cancels the quadratic divergence in the loop with only the quarks. The sum of these four graphs reproduces the result one would find by computing the corresponding correction in the higher derivative formulation of the theory, Eq. (8.55).

To simplify the flavor structure of the theory, we adopt the principle of minimal flavor violation [186]. This forces all LW-fermions in the same representation of the gauge group have the same mass. Now the Yukawas can be diagonalized in the standard fashion. For notational brevity, we choose to use the same symbol for the weak and mass eigenstates.

In terms of the mass eigenstate fields[7],

$$\mathcal{L}_Y = \frac{\sqrt{2}}{v}\sum_i \Big[m_u^i(\overline{u^i}_R - \overline{\tilde{u}^i}_R)(H-\tilde{H})\epsilon(Q_L^i - \tilde{Q}_L^i) - m_d^i(\overline{d^i}_R - \overline{\tilde{d}^i}_R)(H^\dagger - \tilde{H}^\dagger)(Q_L^i - \tilde{Q}_L^i)$$
$$-m_e^i(\overline{e^i}_R - \overline{\tilde{e}^i}_R)(H^\dagger - \tilde{H}^\dagger)(L_L^i - \tilde{L}_L^i) + \text{h.c.}\Big], \tag{8.57}$$

where

$$Q_L = \begin{pmatrix} u_L \\ V d_L \end{pmatrix}, \quad \tilde{Q}_L = \begin{pmatrix} \tilde{u}_L \\ V\tilde{d}_L \end{pmatrix}, \quad \tilde{Q}'_R = \begin{pmatrix} \tilde{u}'_R \\ V\tilde{d}'_R \end{pmatrix}. \tag{8.58}$$

Here V is the usual CKM matrix. The LW-fermions decay via the Yukawa interactions; for example, $\tilde{\nu}_e \to e^-\tilde{h}^+ \to e^- t\bar{b}$. LW-gauge bosons can decay to pairs of ordinary fermions. All the heavy LW-particles decay in this theory, so the only sources of missing energy in collider experiments are the usual standard model neutrinos.

8.5 Conclusions

In this chapter we have developed an extension of the minimal standard model that is free of quadratic divergences. It is based on the work of Lee and Wick who constructed a finite version of QED by associating the regulator propagator in Pauli-Villars with a physical degree of freedom. Our model is a higher derivative theory and as such contains propagators with wrong sign residues about the new poles. Lee and Wick, and Cutkosky et al. provide a prescription for handling this issue. The LW-particles associated with these new poles are not in the spectrum, but instead decay to ordinary degrees of freedom. Their resummed propagators do not satisfy the usual analyticity properties since the poles are on the physical sheet. Lee and Wick (see also Cutkosky et al.) propose deforming integration contours in

[7] They are mass eigenstate fields when mixing between the normal and LW-fields is neglected. This mixing can be treated as a perturbation.

Feynman diagrams so that there is no catastrophic exponential growth as time increases. This amounts to a future boundary condition and so LW-theories violate the usual causal conditions. While the Lee-Wick interpretation is peculiar it seems to be consistent, at least in perturbation theory, and predictions for physical observables can be made order by order in perturbation theory.

Since the extension of the standard model presented here is free of quadratic divergences it solves the hierarchy problem. Our theory contains one new parameter, the mass of the LW-partner, for each field. We reduced the number of parameters by imposing minimal flavor violation to simplify the flavor structure of the theory. To make the physical interpretation clearer and the calculations easier we introduced auxiliary LW-fields. The Lagrangian written in terms of these fields does not contain any higher derivative terms. When the LW-fields are integrated out, the higher derivative theory is recovered.

This chapter focused on the the structure of the Lagrange density for the Lee-Wick extension of the standard model. We constructed the Lagrange density, examined the divergence structure and showed how to introduce auxiliary fields to clarify the physical interpretation. For the future, a more extensive discussion of the phenomenology of the theory, including its implications for LHC physics, is appropriate.

Chapter 9

Neutrino Masses in the Lee-Wick Standard Model

In Chapter 8, we suggested, using ideas proposed by Lee and Wick [11, 12] to extend the standard model so that it does not contain quadratic divergences in the Higgs mass. Higher derivative kinetic terms for each of the standard model fields were added which improve the convergence of Feynman diagrams and give rise to a theory in which there are no quadratically divergent radiative corrections to the Higgs mass. The higher derivative terms induce new poles in the propagators of standard model fields which are interpreted as massive resonances. These resonances have wrong-sign kinetic terms which naively give rise to unacceptable instabilities. Lee and Wick propose altering the energy integrations in the definition of Feynman amplitudes so that the exponential growth does not occur. It appears that this can be done order by order in perturbation theory[1] in a way which preserves unitarity. However, there is acausal behavior due to this deformation of the contour of integration. Physically this acausality is associated with the future boundary condition needed to forbid the exponentially growing modes. As long as the masses and widths of the LW-resonances are large enough, this acausality does not manifest itself on macroscopic scales and is not in conflict with experiment. The proposal to use Lee-Wick

[1] This is somewhat controversial. See [225, 226, 227].

theory for the Higgs sector of the standard model was first presented in [229].

The massive resonances associated with the higher derivative terms in Lee-Wick theories have unusual properties. For example, they correspond to poles on the physical sheet in scattering amplitudes. At the LHC, we may well discover new resonances, and it would be interesting to determine whether they are of normal or Lee-Wick type. This issue has recently been discussed in [13].

In the minimal standard model the fermions get their masses through Yukawa couplings to the Higgs doublet. Gauge invariance forbids traditional mass terms. These Yukawa couplings do not give mass to the left-handed neutrinos. To describe neutrino masses, one can extend the particle content to include right-handed neutrinos. Right-handed neutrinos have no standard model gauge quantum numbers and so Majorana mass terms for them are allowed. If the right-handed neutrino Majorana masses are very large we can understand the smallness of the observed neutrino masses, since the light neutrino masses scale as $m_\nu \sim v^2/m_R$, where v is the vacuum expectation value for the Higgs doublet and m_R is the mass scale associated with the right-handed neutrino Majorana masses. This attractive picture for the generation of neutrino masses is known as the see-saw mechanism [232].

Since the generation structure and the quarks are not the focus of this chapter, let us simplify the notation by just considering a single standard model generation of leptons containing the left-handed doublet denoted by L and the right-handed singlet e_R. Adding the right-handed neutrino ν_R, the lepton sector of the standard model has Lagrange density,

$$\mathcal{L} = \bar{L} i \not{D} L + \bar{e}_R i \not{D} e_R + \bar{\nu}_R i \not{\partial} \nu_R - (m_R \bar{\nu}_R^c \nu_R + g_e \bar{e}_R L H^\dagger + g_Y \bar{\nu}_R H^T \epsilon L + \text{h.c.}). \qquad (9.1)$$

It was pointed out in [233] that the Feynman diagram in Fig. 9.1 gives a contribution to

Figure 9.1: One-loop correction to the Higgs doublet mass. The dashed line represents the Higgs scalar, the solid arrowed line is the left-handed lepton, while the plain solid line is the right-handed neutrino.

the mass term for the Higgs doublet that is quadratically divergent. If one uses dimensional regularization, which throws away quadratic divergences, there is still a finite correction

$$\delta m_H^2 \simeq -\frac{g_Y^2}{8\pi^2} m_R^2 \log(m_R^2/\mu^2) \tag{9.2}$$

which is large compared to the physical mass squared of the Higgs boson if $m_R \gtrsim 10^7$ GeV [233]. This is a manifestation of the hierarchy problem. In this chapter we show that if one used the LW-standard model this does not occur. Even though the right-handed neutrinos are very heavy the higher derivative kinetic terms for the standard model fields are powerful enough to prevent the Higgs mass squared from getting a radiative correction that is proportional to m_R^2.

For simplicity, we gauge only $SU(2)_W$ so there is one set of gauge bosons, $\hat{A}_\mu^A$. The LW-standard model can be formulated either as a higher derivative theory, or as a theory without higher derivatives but with auxiliary LW-fields. For the purposes of the present discussion, it is convenient to work with the higher derivative version of the theory. To emphasize that this is the LW-extended model, the fields with higher derivative kinetic terms are denoted by the presence of a hat. In this simplified version of the LW standard

model the Lagrangian density is,

$$\begin{aligned}\mathcal{L} = &-\frac{1}{2}\mathrm{tr}\hat{F}_{\mu\nu}\hat{F}^{\mu\nu} + \frac{1}{M_A^2}\mathrm{tr}\left(\hat{D}^\mu\hat{F}_{\mu\nu}\right)\left(\hat{D}^\lambda\hat{F}_\lambda{}^\nu\right) + \left(\hat{D}_\mu\hat{H}\right)^\dagger\left(\hat{D}^\mu\hat{H}\right) \\ &-\frac{1}{M_H^2}\left(\hat{D}_\mu\hat{D}^\mu\hat{H}\right)^\dagger\left(\hat{D}_\nu\hat{D}^\nu\hat{H}\right) - V(\hat{H}) + \overline{\hat{L}}i\hat{\not{D}}\hat{L} + \frac{1}{M_L^2}\overline{\hat{L}}i\hat{\not{D}}\hat{\not{D}}\hat{\not{D}}\hat{L} + \overline{\hat{e}}_R i\hat{\not{\partial}}\hat{e}_R \\ &+\frac{1}{M_E^2}\overline{\hat{e}}_R i\hat{\not{\partial}}\hat{\not{\partial}}\hat{\not{\partial}}\hat{e}_R + \bar{\nu}_R i\not{\partial}\nu_R - (m_R\bar{\nu}_R^c\nu_R + g_e\overline{\hat{e}}_R\hat{L}\hat{H}^\dagger + g_Y\bar{\nu}_R\hat{H}^T\epsilon\hat{L} + \text{h.c.}). \quad (9.3)\end{aligned}$$

Note that we have not added any higher derivative terms for the right-handed neutrino. Calculating the diagram in Fig. 9.1 in the LW-standard model, and using a momentum cutoff Λ to regularize the ultraviolet divergence, we find (neglecting the Lee-Wick mass parameter M_L in comparison with m_R and Λ) that

$$\delta m_{\hat{H}}^2 = -\frac{g_Y^2}{8\pi^2}M_L^2\log\left(\frac{m_R^2+\Lambda^2}{m_R^2}\right). \quad (9.4)$$

This leads to acceptably small corrections to the Higgs mass if $g_Y M_L \lesssim 10$ TeV.[2] Thus, we have shown that, at one loop order, the Higgs mass is not destabilized by the presence of the right-handed neutrino. To go further, we will establish a power counting argument which shows that the divergence in the Higgs mass squared is at most logarithmic to all orders of perturbation theory. This is sufficient to show that there are no large finite corrections to the Higgs mass since we take m_R of order the cutoff in our power counting.

To construct a perturbative power counting argument that shows to all orders in perturbation theory there is no quadratic divergence in the Higgs doublet mass term, we must fix a gauge in the higher derivative theory. We choose to add a covariant gauge fixing term $-(\partial_\mu\hat{A}^{A\mu})^2/2\xi$ to the Lagrange density and introduce Faddeev-Popov ghosts that couple to

[2] If we include a higher derivative term for the right-handed neutrino in Eq. (9.3), the correction to the Higgs mass is still proportional to $g_Y M_L$, leading to the same conclusion.

the gauge bosons in the usual way. Then the propagator for the gauge field is

$$\hat{D}^{AB}_{\mu\nu}(p) = \delta^{AB}\frac{-i}{p^2 - p^4/M_A^2}\left(\eta_{\mu\nu} - (1-\xi)\frac{p_\mu p_\nu}{p^2} - \xi\frac{p_\mu p_\nu}{M_A^2}\right). \tag{9.5}$$

We work in Landau gauge, $\xi = 0$, where the gauge boson propagator scales as p^{-4} at high energy. The propagator for the Higgs scales at large momenta as p^{-4} while the LW-standard model leptons, $\hat{L}$ and $\hat{e}_R$, have that scale as p^{-3} at large momenta. Finally the right-handed neutrino propagator and the Faddeev-Popov ghost propagator scales as p^{-1} and p^{-2}, as usual. There are five kinds of vertices: those where only gauge bosons interact, vertices where gauge bosons interact with two scalars, and vertices where two ghosts interact with one gauge boson. A vertex where n vectors interact (with no scalars) scales as p^{6-n}, a vertex with two scalars and n vectors scales as p^{4-n}, while a vertex with two fermions and n vectors scales as p^{3-n}. The vertex between two ghosts and one gauge field scales as one power of p, as usual, and the vertex from the Yukawa interaction of the Higgs doublet with the fermions has no factors of momentum.

Consider an arbitrary Feynman graph with E external Higgs lines, L loops, I' internal vector lines, I internal scalar lines, I_R internal right-handed neutrino lines, I_L standard model lepton lines, and I_g internal ghost lines and with V'_n vector self-interaction vertices, V_n and $\bar{V}_n$ vertices with n vectors and two scalar Higgs particles or left-handed leptons, respectively. We also suppose there are V_g ghost vertices and V_Y Yukawa vertices with two fermions and a Higgs doublet. Then the superficial degree of divergence, d, is

$$d = 4L - 4I' - 4I - I_R - 3I_L - 2I_g + \sum_n V'_n(6-n) + \sum_n V_n(4-n)\sum_n \bar{V}_n(3-n) + V_g. \tag{9.6}$$

We can simplify this expression using some identities. First, the number of loops is related

to the total number of propagators and vertices by

$$L = I + I' + I_R + I_L + I_g - \sum_n (V'_n + V_n + \bar{V}_n) - V_Y - V_g + 1, \tag{9.7}$$

while the total number of lines entering or leaving the vertices is related to the number of propagators and external lines by

$$\sum_n \left(nV'_n + (n+2)V_n + (n+2)\bar{V}_n \right) + 3V_g + 3V_Y = 2(I + I' + I_R + I_L + I_g) + E, \tag{9.8}$$

where E is the number of external scalars. Finally, we have the additional relations,

$$2\sum_n V_n + V_Y = 2I + E, \quad 2V_g = 2I_g, \quad V_Y = 2I_R, \quad \sum_n \bar{V}_n + V_Y = I_R + I_L. \tag{9.9}$$

With these identities in hand, we may express the superficial degree of divergence as

$$d = 6 - 2L - V_Y - E. \tag{9.10}$$

Scalar mass renormalizations have $E = 2$. The only possible quadratic divergence in the scalar mass is at one loop with $V_Y = 0$. As was discussed in Chapter 8, gauge invariance removes this potential quadratic divergence. Diagrams involving the leptons have at least $V_Y = 2$ and so are at most logarithmically divergent. Diagrams with other external lines (which can be subdiagrams in the calculation of the Higgs mass term) can be analyzed similarly and do not change our conclusions.

We have shown that in at least one case it is possible to couple LW standard model fields to degrees of freedom that are much heavier and still preserve the stability of the

Higgs mass. Furthermore this case is well motivated by the observed neutrino masses. However, this result is not true in general. Suppose, for example, there was a very heavy complex (normal) scalar S. An interaction term of the type $\mathcal{L}_{\text{int}} = g\hat{H}^\dagger \hat{H} S^\dagger S$ would lead to a large contribution to the Higgs boson mass. However, consider coupling the Higgs to a gauge singlet scalar $\hat{S}$ which has a higher derivative term in its Lagrange density:

$$\mathcal{L} = \left(\partial_\mu \hat{S}\right)^\dagger \partial^\mu \hat{S} - M^2 \hat{S}^\dagger \hat{S} - \frac{1}{m^2} \hat{S}^\dagger \partial^4 \hat{S} + g\hat{H}^\dagger \hat{H} \hat{S}^\dagger \hat{S}. \tag{9.11}$$

Then the $\hat{S}$ propagator is given by

$$\hat{D} = \frac{m^2}{p^4 - p^2 m^2 + M^2 m^2}. \tag{9.12}$$

If we take the mass parameter M to be large, as in the case of the scalar S, and choose the mass parameter m to be of order of the weak scale, then the radiative corrections to the Higgs mass are still small despite the presence of the large scale M. The scalar $\hat{S}$ has unusual properties: for example, from the location of the poles in its propagator, one can see that it has a tree-level width which is large compared to its mass. We have not studied the consistency of this approach in detail.

In summary, we have shown in this chapter that it is possible to couple the Lee-Wick standard model to physics at a much higher scale without destabilizing the Higgs mass. One of the best motivated examples of high-scale physics is provided by experimental information on neutrino masses, and we find that the Lee-Wick standard model can easily be extended to incorporate a heavy right-handed neutrino without reintroducing fine tuning of the Higgs mass. In addition, we have briefly described a scenario in which more general physics can be coupled to the Lee-Wick standard model while maintaining a naturally light Higgs.

Appendix A

Explicit Extrapolation Formulae

We gather together the chiral extrapolation formulae discussed in Chapters 3 and 4 in this appendix. We also present results for various other physical quantities of interest. Some of these quantities have been derived elsewhere, but in this appendix we consistently present results expressed in terms of the lattice-physical parameters whose virtues are discussed in the text.

A.1 m_π and f_π for 2-Sea Flavors

In this section, we provide the explicit formulae for the pion mass and decay constant in a two-sea flavor MA theory. These were first computed in Refs. [101, 103]. Here we provide the answers expressed in terms of the PQ parameters we introduced in Eq. (4.14).

$$m_\pi^2 = 2B_0\hat{m}\Bigg\{1 + \frac{m_\pi^2}{(4\pi f)^2}\ln\left(\frac{m_\pi^2}{\mu^2}\right) - \frac{m_\pi^2}{f^2}\ell^{(m)}(\mu) - \frac{\tilde{\Delta}_{ju}^2}{(4\pi f)^2}\left[1 + \ln\left(\frac{m_\pi^2}{\mu^2}\right)\right] - \frac{\Delta_{ju}^2}{f^2}\ell_{PQ}^{(m)}(\mu) + \frac{a^2}{f^2}\ell_{a^2}^{(m)}(\mu)\Bigg\}. \tag{A.1}$$

$$f_\pi = f\left\{1 - \frac{2\tilde{m}_{ju}^2}{(4\pi f)^2}\ln\left(\frac{\tilde{m}_{ju}^2}{\mu^2}\right) + \frac{m_\pi^2}{f^2}\ell^{(f)}(\mu) + \frac{\Delta_{ju}^2}{f^2}\ell_{PQ}^{(f)}(\mu) + \frac{a^2}{f^2}\ell_{a^2}^{(f)}(\mu)\right\}. \tag{A.2}$$

A.2 Meson Masses

In this section we collect the pion and kaon mass and decay constant for a three-sea flavor MA theory. These were first computed in Refs. [101, 103]. Here we provide the answers expressed in terms of the PQ parameters we introduced in Eq. (4.14).

$$\begin{aligned} m_\pi^2 = 2B_0\hat{m}\Bigg\{ & 1 + \ln\left(\frac{m_\pi^2}{\mu^2}\right)\left[\frac{m_\pi^2}{(4\pi f)^2} - \frac{\tilde{\Delta}_{ju}^2(3\tilde{m}_X^2 - m_\pi^2)}{3(4\pi f)^2(\tilde{m}_X^2 - m_\pi^2)} + \frac{\tilde{\Delta}_{ju}^4\tilde{m}_X^2}{3(4\pi f)^2(\tilde{m}_X^2 - m_\pi^2)^2}\right] \\ & - \ln\left(\frac{\tilde{m}_X^2}{\mu^2}\right)\left[\frac{\tilde{m}_X^2}{3(4\pi f)^2} - \frac{2\tilde{\Delta}_{ju}^2\tilde{m}_X^2}{3(4\pi f)^2(\tilde{m}_X^2 - m_\pi^2)} + \frac{\tilde{\Delta}_{ju}^4\tilde{m}_X^2}{3(4\pi f)^2(\tilde{m}_X^2 - m_\pi^2)^2}\right] \\ & - \frac{16m_\pi^2}{f^2}\Big[L_4(\mu) + L_5(\mu) - 2L_6(\mu) - 2L_8(\mu)\Big] - \frac{32m_K^2}{f^2}\Big[L_4(\mu) - 2L_6(\mu)\Big] + \frac{a^2}{f^2}L_{ma^2}(\mu) \\ & - \left(\frac{32\Delta_{ju}^2}{f^2} + \frac{16\Delta_{rs}^2}{f^2}\right)\Big[L_4(\mu) - 2L_6(\mu)\Big] - \frac{\tilde{\Delta}_{ju}^2}{(4\pi f)^2} + \frac{\tilde{\Delta}_{ju}^4}{3(4\pi f)^2(\tilde{m}_X^2 - m_\pi^2)}\Bigg\}. \end{aligned} \tag{A.3}$$

$$\begin{aligned} m_K^2 = {} & B_0(\hat{m} + m_s) - \frac{16m_K^4}{f^2}\Big[2L_4(\mu) + L_5(\mu) - 4L_6(\mu) - 2L_8(\mu)\Big] \\ & - \frac{16m_K^2m_\pi^2}{f^2}\Big[L_4(\mu) - 2L_6(\mu)\Big] - \frac{16m_K^2}{f^2}\Big(2\tilde{\Delta}_{ju}^2 + \tilde{\Delta}_{rs}^2\Big)\Big[L_4(\mu) - 2L_6(\mu)\Big] + \frac{a^2m_K^2}{f^2}L_{ma^2} \\ & + \ln\left(\frac{\tilde{m}_X^2}{\mu^2}\right)\left[\frac{2m_K^2\tilde{m}_X^2}{3(4\pi f)^2} - \frac{\tilde{\Delta}_{ju}^2\tilde{m}_X^2(8m_K^2 + 3\tilde{m}_X^2 + m_\pi^2)}{18(4\pi f)^2(\tilde{m}_X^2 - m_\pi^2)} + \frac{\tilde{\Delta}_{ju}^4\tilde{m}_X^2}{18(4\pi f)^2(\tilde{m}_X^2 - m_\pi^2)}\right. \\ & \qquad \left. - \frac{2\tilde{\Delta}_{rs}^2\tilde{m}_X^2m_K^2}{3(4\pi f)^2(\tilde{m}_X^2 + m_\pi^2 - 2m_K^2)} + \frac{\tilde{\Delta}_{ju}^2\tilde{\Delta}_{rs}^2\tilde{m}_X^2(\tilde{m}_X^2 + 4m_K^2 + m_\pi^2)}{9(4\pi f)^2(\tilde{m}_X^2 - m_\pi^2)(\tilde{m}_X^2 + m_\pi^2 - 2m_K^2)}\right] \\ & + \ln\left(\frac{m_\pi^2}{\mu^2}\right)\frac{\tilde{\Delta}_{ju}^2\, m_\pi^2}{(4\pi f)^2}\left[\frac{3\tilde{m}_X^2 + 8m_K^2 + m_\pi^2}{18(\tilde{m}_X^2 - m_\pi^2)} - \frac{\tilde{\Delta}_{ju}^2}{18(\tilde{m}_X^2 - m_\pi^2)} + \frac{\tilde{\Delta}_{rs}^2(2m_K^2 + m_\pi^2)}{9(m_K^2 - m_\pi^2)(\tilde{m}_X^2 - m_\pi^2)}\right] \\ & + \ln\left(\frac{m_{ss}^2}{\mu^2}\right)\frac{\tilde{\Delta}_{rs}^2\, m_K^2}{(4\pi f)^2}\left[\frac{2(2m_K^2 - m_\pi^2)}{3(\tilde{m}_X^2 + m_\pi^2 - 2m_K^2)} - \frac{\tilde{\Delta}_{ju}^2(2m_K^2 - m_\pi^2)}{3(m_K^2 - m_\pi^2)(\tilde{m}_X^2 + m_\pi^2 - 2m_K^2)}\right]. \end{aligned} \tag{A.4}$$

Note that the lattice spacing dependent counterterms for the meson masses have the same coefficient; this is because the discretization scheme is flavor-blind.

A.3 Decay Constants and f_K/f_π

The pion decay constant is given by

$$f_\pi = f\Bigg\{1 - \frac{2\tilde{m}_{ju}^2}{(4\pi f)^2}\,\ln\left(\frac{\tilde{m}_{ju}^2}{\mu^2}\right) - \frac{\tilde{m}_{ru}^2}{(4\pi f)^2}\,\ln\left(\frac{\tilde{m}_{ru}^2}{\mu^2}\right) + \frac{8m_\pi^2}{f^2}\Big(L_5(\mu) + L_4(\mu)\Big) + \frac{16m_K^2}{f^2}\,L_4(\mu) + \frac{8(2\Delta_{ju}^2 + \Delta_{rs}^2)}{f^2}\,L_4(\mu) + \frac{a^2}{f^2}\,L_{fa^2}(\mu)\Bigg\}, \tag{A.5}$$

while the kaon decay constant is

$$\begin{aligned} f_K = f\Bigg\{&1 - \frac{\tilde{m}_{sj}^2}{(4\pi f)^2}\,\ln\left(\frac{\tilde{m}_{sj}^2}{\mu^2}\right) - \frac{\tilde{m}_{ru}^2}{2(4\pi f)^2}\,\ln\left(\frac{\tilde{m}_{ru}^2}{\mu^2}\right) - \frac{\tilde{m}_{ju}^2}{(4\pi f)^2}\,\ln\left(\frac{\tilde{m}_{ju}^2}{\mu^2}\right) \\ &- \frac{\tilde{m}_{rs}^2}{2(4\pi f)^2}\,\ln\left(\frac{\tilde{m}_{rs}^2}{\mu^2}\right) + \frac{8m_\pi^2}{f^2}\,L_4(\mu) + \frac{8m_K^2}{f^2}\Big[L_5(\mu) + 2L_4(\mu)\Big] + \frac{8(2\Delta_{ju}^2 + \Delta_{rs}^2)}{f^2}\,L_4(\mu) \\ &+ \frac{a^2}{f^2}\,L_{fa^2}(\mu) - \frac{\tilde{\Delta}_{ju}^2}{4(4\pi f)^2} + \frac{\tilde{\Delta}_{ju}^4}{12(4\pi f)^2(\tilde{m}_X^2 - m_\pi^2)} + \frac{\tilde{\Delta}_{rs}^2(m_K^2 - m_\pi^2)}{3(4\pi f)^2(\tilde{m}_X^2 - m_{ss}^2)} \\ &- \frac{\tilde{\Delta}_{ju}^2\tilde{\Delta}_{rs}^2}{6(4\pi f)^2(\tilde{m}_X^2 - m_{ss}^2)} + \frac{1}{12(4\pi f)^2}\ln\left(\frac{m_\pi^2}{\mu^2}\right)\Bigg[3m_\pi^2 - \frac{3\tilde{\Delta}_{ju}^2(\tilde{m}_X^2 + m_\pi^2)}{\tilde{m}_X^2 - m_\pi^2} + \frac{\tilde{\Delta}_{ju}^4\tilde{m}_X^2}{(\tilde{m}_X^2 - m_\pi^2)^2} \\ &- \frac{4\tilde{\Delta}_{ju}^2\tilde{\Delta}_{rs}^2 m_\pi^2}{(\tilde{m}_X^2 - m_\pi^2)(m_{ss}^2 - m_\pi^2)}\Bigg] - \frac{\tilde{m}_X^2}{12(4\pi f)^2}\ln\left(\frac{\tilde{m}_X^2}{\mu^2}\right)\Bigg[9 - \frac{6\tilde{\Delta}_{ju}^2}{\tilde{m}_X^2 - m_\pi^2} + \frac{\tilde{\Delta}_{ju}^4}{(\tilde{m}_X^2 - m_\pi^2)^2} \\ &+ \frac{\tilde{\Delta}_{rs}^2\Big(4(m_K^2 - m_\pi^2) + 6(m_{ss}^2 - \tilde{m}_X^2)\Big)}{(\tilde{m}_X^2 - m_{ss}^2)^2} - \frac{2\tilde{\Delta}_{ju}^2\tilde{\Delta}_{rs}^2(2m_{ss}^2 - m_\pi^2 - \tilde{m}_X^2)}{(\tilde{m}_X^2 - m_{ss}^2)^2(\tilde{m}_X^2 - m_\pi^2)}\Bigg] \\ &+ \frac{1}{6(4\pi f)^2}\ln\left(\frac{m_{ss}^2}{\mu^2}\right)\Bigg[3m_{ss}^2 + \frac{\tilde{\Delta}_{rs}^2\Big(3m_{ss}^4 + 2(m_K^2 - m_\pi^2)\tilde{m}_X^2 - 3m_{ss}^2\tilde{m}_X^2\Big)}{(\tilde{m}_X^2 - m_{ss}^2)^2} \\ &- \frac{\tilde{\Delta}_{ju}^2\tilde{\Delta}_{rs}^2(2m_{ss}^4 - \tilde{m}_X^2(m_{ss}^2 + m_\pi^2)}{(\tilde{m}_X^2 - m_{ss}^2)^2(m_{ss}^2 - m_\pi^2)}\Bigg]\Bigg\}. \end{aligned} \tag{A.6}$$

The two important things to note are that the additive lattice spacing modifications to the decay constants are the same and also that at this order, they can be absorbed into a redefinition of the Lagrangian parameter, f. We can then use these formulae to estimate the size of the corrections to the recent determination of $L_5(\mu)$ by NPLQCD [138]. Thus, we form the ratio

$$\Delta\left(\frac{f_K}{f_\pi}\right) = \frac{\left.\frac{f_K}{f_\pi}\right|_{MA} - \left.\frac{f_K}{f_\pi}\right|_{QCD}}{\left.\frac{f_K}{f_\pi}\right|_{QCD}}, \tag{A.7}$$

where, using Eqs. (A.5) and (A.6), and the tuning used in Ref. [138] which was to set the valence-valence meson masses equal to the taste-ξ_5 sea-sea mesons, we have

$$\begin{aligned}
&\left.\frac{f_K}{f_\pi}\right|_{MA} - \left.\frac{f_K}{f_\pi}\right|_{QCD} = \frac{m_\pi^2 + a^2\Delta_{\rm Mix}}{(4\pi f_\pi)^2}\,\ln\frac{m_\pi^2 + a^2\Delta_{\rm Mix}}{\mu^2} - \frac{m_\pi^2}{(4\pi f_\pi)^2}\,\ln\frac{m_\pi^2}{\mu^2} + \frac{m_K^2}{2(4\pi f_\pi)^2}\,\ln\frac{m_K^2}{\mu^2} \\
&- \frac{m_K^2 + a^2\Delta_{\rm Mix}}{2(4\pi f_\pi)^2}\,\ln\frac{m_K^2 + a^2\Delta_{\rm Mix}}{\mu^2} - \frac{3}{4(4\pi)^2}\left[\frac{m_\eta^2 + a^2\Delta_I}{f_\pi^2}\,\ln\left(\frac{m_\eta^2 + a^2\Delta_I}{\mu^2}\right) - \frac{m_\eta^2}{f_\pi^2}\,\ln\left(\frac{m_\eta^2}{\mu^2}\right)\right] \\
&- \frac{1}{2(4\pi)^2}\left[\frac{m_{ss}^2 + a^2\Delta_{\rm Mix}}{f_\pi^2}\,\ln\left(\frac{m_{ss}^2 + a^2\Delta_{\rm Mix}}{\mu^2}\right) - \frac{m_{ss}^2}{f_\pi^2}\,\ln\left(\frac{m_{ss}^2}{\mu^2}\right)\right] \\
&- \left(\frac{a^2\Delta_I}{f_\pi^2}\right)\frac{1}{12(4\pi)^2}\left\{3 + \frac{4(m_K^2 - m_\pi^2)}{m_{ss}^2 - m_\eta^2 - a^2\Delta_I} + \frac{3(m_\eta^2 + a^2\Delta_I + m_\pi^2)}{m_\eta^2 + a^2\Delta_I - m_\pi^2}\,\ln\left(\frac{m_\pi^2}{\mu^2}\right)\right. \\
&- \frac{2\Big(3m_{ss}^4 - (m_\eta^2 + a^2\Delta_I)(3m_{ss}^2 - 2m_K^2 + 2m_\pi^2)\Big)}{(m_{ss}^2 - m_\eta^2 - a^2\Delta_I)^2}\,\ln\left(\frac{m_{ss}^2}{\mu^2}\right) \\
&\left.+ 2(m_\eta^2 + a^2\Delta_I)\,\ln\left(\frac{m_\eta^2 + a^2\Delta_I}{\mu^2}\right)\left[\frac{3m_{ss}^2 - 3(m_\eta^2 + a^2\Delta_I) + 2m_K^2 - 2m_\pi^2}{(m_{ss}^2 - m_\eta^2 - a^2\Delta_I)^2} - \frac{3}{m_\eta^2 + a^2\Delta_I - m_\pi^2}\right]\right\} \\
&+ \left(\frac{a^2\Delta_I}{f_\pi^2}\right)^2\frac{1}{12(4\pi)^2}\left\{\frac{f_\pi^2}{m_\eta^2 + a^2\Delta_I - m_\pi^2} - \frac{2f_\pi^2}{m_\eta^2 + a^2\Delta_I - m_{ss}^2} + \ln\left(\frac{m_\pi^2}{\mu^2}\right)\left[\frac{f_\pi^2(m_\eta^2 + a^2\Delta_I)}{(m_\eta^2 + a^2\Delta_I - m_\pi^2)^2}\right.\right. \\
&\left.- \frac{4f_\pi^2 m_\pi^2}{(m_\eta^2 + a^2\Delta_I - m_\pi^2)(m_{ss}^2 - m_\pi^2)}\right] - \ln\left(\frac{m_{ss}^2}{\mu^2}\right)\frac{2f_\pi^2\Big(2m_{ss}^4 - (m_\eta^2 + a^2\Delta_I)(m_{ss}^2 + m_\pi^2)\Big)}{(m_{ss}^2 - m_\pi^2)(m_\eta^2 + a^2\Delta_I - m_{ss}^2)^2} \\
&\left.\left.- \frac{m_\eta^2 + a^2\Delta_I}{f_\pi^2}\,\ln\left(\frac{m_\eta^2 + a^2\Delta_I}{\mu^2}\right)\left[\frac{f_\pi^4}{(m_\eta^2 + a^2\Delta_I - m_\pi^2)^2} + \frac{2f_\pi^4(m_\eta^2 + a^2\Delta_I + m_\pi^2 - 2m_{ss}^2)}{(m_\eta^2 + a^2\Delta_I - m_\pi^2)(m_\eta^2 + a^2\Delta_I - m_{ss}^2)^2}\right]\right\}.
\end{aligned} \tag{A.8}$$

A.4 $\pi^+\pi^+$ Scattering

We present here the formulae for the $I = 2$ $\pi\pi$ scattering length determined in both MAχPT and PQχPT discussed in Chapter 3, for both two and three flavors of sea quark.

Two-Sea-Quark Flavors, $m_\pi a_{\pi\pi}^{I=2}$

$$m_\pi a_{\pi\pi}^{I=2} = \frac{-m_\pi^2}{8\pi f_\pi^2}\left\{1 + \frac{m_\pi^2}{(4\pi f_\pi)^2}\left[3\ln\left(\frac{m_\pi^2}{\mu^2}\right) - 1 - l_{\pi\pi}^{I=2}(\mu)\right] - \frac{m_\pi^2}{(4\pi f_\pi)^2}\,\frac{\tilde{\Delta}_{ju}^4}{6m_\pi^4}\right\}. \tag{A.9}$$

Three-Sea-Quark Flavors, $m_\pi a_{\pi\pi}^{I=2}$

$$m_\pi a_{\pi\pi}^{I=2} = \frac{-m_\pi^2}{8\pi f_\pi^2}\Bigg\{1 + \frac{m_\pi^2}{(4\pi f_\pi)^2}\left[3\ln\left(\frac{m_\pi^2}{\mu^2}\right) - 1 + \frac{1}{9}\ln\left(\frac{\tilde{m}_X^2}{\mu^2}\right) + \frac{1}{9} - 32(4\pi)^2\, L_{\pi\pi}^{I=2}(\mu)\right] + \frac{m_\pi^2}{(4\pi f_\pi)^2}\left[-\frac{\tilde{\Delta}_{ju}^4}{6m_\pi^4} + \sum_{n=1}^{4}\left(\frac{\tilde{\Delta}_{ju}^2}{m_\pi^2}\right)^n \mathcal{F}_n(m_\pi^2/\tilde{m}_X^2)\right]\Bigg\}, \quad \text{(A.10)}$$

where the functions $\mathcal{F}_n(y)$ are given by

$$\mathcal{F}_1(y) = -\frac{2y}{9(1-y)^2}\Big[5(1-y) + (3+2y)\ln(y)\Big], \quad \text{(A.11a)}$$

$$\mathcal{F}_2(y) = \frac{2y}{3(1-y)^3}\Big[(1-y)(1+3y) + y(3+y)\ln(y)\Big], \quad \text{(A.11b)}$$

$$\mathcal{F}_3(y) = \frac{y}{9(1-y)^4}\Big[(1-y)(1-7y-12y^2) - 2y^2(7+2y)\ln(y)\Big], \quad \text{(A.11c)}$$

$$\mathcal{F}_4(y) = -\frac{y^2}{54(1-y)^5}\Big[(1-y)(1-8y-17y^2) - 6y^2(3+y)\ln(y)\Big]. \quad \text{(A.11d)}$$

A.5 K^+K^+ Scattering

The $I = 1$ KK and $I = 3/2$ $K\pi$ scattering lengths involve lengthy expressions. Therefore, we introduce the following notation to make the answers more presentable.

$$m_K = k m_\pi \quad , \quad \tilde{\Delta}_{ju} = \delta_{ju} m_\pi \quad , \quad \tilde{\Delta}_{rs} = \delta_{rs} m_\pi\,. \quad \text{(A.12)}$$

The $I = 1$ KK scattering length is given by Eq. (4.30), which we repeat here for convenience

$$m_K a_{KK}^{I=1} = -\frac{m_K^2}{8\pi f_K^2}\Bigg\{1 + \frac{m_K^2}{(4\pi f_K)^2}\left[C_\pi \ln\left(\frac{m_\pi^2}{\mu^2}\right) + C_K \ln\left(\frac{m_K^2}{\mu^2}\right) + C_X \ln\left(\frac{\tilde{m}_X^2}{\mu^2}\right) + C_{ss}\ln\left(\frac{m_{ss}^2}{\mu^2}\right) + C_0 - 32(4\pi)^2\, L_{KK}^{I=1}\right]\Bigg\}, \quad \text{(A.13)}$$

where

$$C_K = 2\,, \tag{A.14}$$

$$\begin{aligned} C_\pi =& \frac{2-2k^2-\delta_{rs}^2}{(k^2-1)^3(4k^2-4+\delta_{ju}^2+2\delta_{rs}^2)^3}\big\{16(k^2-1)^4+16(k^2-1)^3\delta_{rs}^2+4(k^2-1)^2\delta_{rs}^4 \\ &+\delta_{ju}^2\big[4(k^2-1)^3(5+4k^2)+2(k^2-1)^2(5+8k^2)\delta_{rs}^2+4k^2(k^2-1)\delta_{rs}^4\big] \\ &-\delta_{ju}^4\big[4(k^2-1)^2+4(k^4-1)\delta_{rs}^2+2k^2\delta_{rs}^4\big]-\delta_{ju}^6\big[(k^2-1)^2+k^2\delta_{rs}^2\big]\big\}\,, \end{aligned} \tag{A.15}$$

$$\begin{aligned} C_X =& -\frac{8(2-2k^2+\delta_{ju}^2-\delta_{rs}^2)^2}{9(2-2k^2+\delta_{ju}^2+2\delta_{rs}^2)^3(4k^2-4+\delta_{ju}^2+2\delta_{rs}^2)^3}\Big[8(k^2-1)^3(20k^2-11) \\ &+4(k^2-1)^2(152k^2-53)\delta_{rs}^2+12(38k^4-61k^2+23)\delta_{rs}^4+80(k^2-1)\delta_{rs}^6-8\delta_{rs}^8 \\ &+\delta_{ju}^2\Big(14(k^2-1)^2(1+8k^2)-24(5k^4-4-k^2)\delta_{rs}^2-(312k^2-132)\delta_{rs}^4-112\delta_{rs}^6\Big) \\ &-\delta_{ju}^4\Big(33(2k^4-k^2-1)+(210k^2-138)\delta_{rs}^2+102\delta_{rs}^4\Big)-\delta_{ju}^6\Big(17k^2-26+22\delta_{rs}^2\Big)+\delta_{ju}^8\Big]\,, \end{aligned} \tag{A.16}$$

$$\begin{aligned} C_{ss} =& \frac{\delta_{rs}^2}{(k^2-1)^3(2-2k^2+\delta_{ju}^2+2\delta_{rs}^2)^3}\Big[8(k^2-1)^4(7k^2-3)-4(k^2-1)^3(4k^2-1)\delta_{rs}^2 \\ &+4(k^2-1)^2(2k^2-1)\delta_{rs}^4-\delta_{ju}^2\Big(4(k^2-1)^3(17k^2-7)+2(k^2-1)^2(4k^2-3)\delta_{rs}^2-4k^2(k^2-1)\delta_{rs}^4\Big) \\ &+\delta_{ju}^4\Big(2(k^2-1)^2(13k^2-5)+2(5k^4-7k^2+2)\delta_{rs}^2-2k^2\delta_{rs}^4\Big)-\delta_{ju}^6\Big(3k^4-4k^2+1+k^2\delta_{rs}^2\Big)\Big]\,, \end{aligned} \tag{A.17}$$

$$C_0 = \frac{2}{9(k^2-1)^2(4k^2-4+\delta_{ju}^2+2\delta_{rs}^2)^2(2-2k^2+\delta_{ju}^2+2\delta_{rs}^2)^2}\Big[-448(k^2-1)^6+1120(k^2-1)^5\delta_{rs}^2$$
$$+912(k^2-1)^4\delta_{rs}^4-152(k^2-1)^3\delta_{rs}^6-136(k^2-1)^2\delta_{rs}^8+\delta_{ju}^8\Big(8(k^2-1)^2+18(k^2-1)\delta_{rs}^2+9\delta_{rs}^4\Big)$$
$$-\delta_{ju}^2\Big(112(k^2-1)^5-48(k^2-1)^4\delta_{rs}^2+876(k^2-1)^3\delta_{rs}^4+608(k^2-1)^2\delta_{rs}^6+72(k^2-1)\delta_{rs}^8\Big)$$
$$+\delta_{ju}^4\Big(480(k^2-1)^4-96(k^2-1)^3\delta_{rs}^2-330(k^2-1)^2\delta_{rs}^4+36(k^2-1)\delta_{rs}^6+36\delta_{rs}^8\Big)$$
$$-\delta_{ju}^6\Big(172(k^2-1)^3+140(k^2-1)^2\delta_{rs}^2-72(k^2-1)\delta_{rs}^4-36\delta_{rs}^6\Big)\Big]. \tag{A.18}$$

A.6 $K^+\pi^+$ Scattering

The $K\pi$ scattering length at $I=3/2$ is given by:

$$\mu_{K\pi}a_{K\pi}^{I=3/2} = -\frac{\mu_{K\pi}^2}{4\pi f_K f_\pi}\left[1-\frac{32m_K m_\pi}{f_K f_\pi}L_{\pi\pi}^{I=2}+\frac{8(m_K-m_\pi)^2}{f_K f_\pi}L_5\right]+\mu_{K\pi}\left[a_{vv}^{K\pi,3/2}+a_{vs}^{K\pi,3/2}\right], \tag{A.19}$$

where $a_{vs}^{K\pi,3/2}(\mu)$ is given in Eq. (4.43).

$$\mu_{K\pi}\,a_{vs}^{K\pi,3/2}(\mu) = -\frac{\mu_{K\pi}^2}{4\pi f_K f_\pi}\frac{1}{2(4\pi)^2 f_K f_\pi}\sum_{F=j,l,r}\left[C_{Fs}\ln\frac{\tilde{m}_{Fs}^2}{\mu^2}-C_{Fd}\ln\frac{\tilde{m}_{Fd}^2}{\mu^2}+4m_K m_\pi J(\tilde{m}_{Fd}^2)\right], \tag{A.20}$$

where the coefficients $C_{Fd,s}$, and the function $J(m)$ are defined in Eqs. (4.44)–(4.46). We reiterate that the $\ln(\mu^2)$ dependence in $a_{vs}^{K\pi,3/2}(\mu)$ only depends upon the valence-valence meson masses, Eq. (4.47), as we argued in Section 4.2.2. The valence-valence (and valence-ghost) contribution to the scattering length is given by

$$\mu_{K\pi}a_{vv}^{K\pi,3/2}(\mu) = \frac{\mu_{K\pi}^2}{4\pi f_K f_\pi}\frac{m_\pi^2}{2(4\pi)^2 f_K f_\pi}\Big[A_\pi\,\ln\left(\frac{m_\pi^2}{\mu^2}\right)+A_K\,\ln\left(\frac{m_K^2}{\mu^2}\right)$$
$$+A_X\,\ln\left(\frac{\tilde{m}_X^2}{\mu^2}\right)+A_{ss}\,\ln\left(\frac{m_{ss}^2}{\mu^2}\right)+A_{tan}+A_0\Big]. \tag{A.21}$$

We use the notation defined in Eq. (A.12) to simplify the form of these coefficients. We find

$$
\begin{aligned}
A_\pi = \frac{1}{(k^2-1)^3(4k^2-4+\delta_{ju}^2+2\delta_{rs}^2)^4}\Big[&8(k^2-1)^2(14k-k^2-1)(2k^2-2+\delta_{rs}^2)^4\\
&+8\delta_{ju}^2(k^2-1)(2k^2-2+\delta_{rs}^2)^3\Big(2k^6+k^4(\delta_{rs}^2-1)+28k^3+k^2(\delta_{rs}^2-2)-k(28-\delta_{rs}^2)+1\Big)\\
&+2\delta_{ju}^4(2k^2-2+\delta_{rs}^2)^2\Big(12k^8+48k^7+3k^6(-5+2\delta_{rs}^2)+32k^5\delta_{rs}^2-9k^4\\
&\quad-2k^3(72+21\delta_{rs}^2-2\delta_{rs}^4)+k^2(15-6\delta_{rs}^2)+2k(48+5\delta_{rs}^2-\delta_{rs}^4)-3\Big)\\
&+2\delta_{ju}^6\Big(4(k^2-1)^3(3k^4+12k^3+2k^2+5k-1)+2\delta_{rs}^2(k^2-1)^2(6k^4+32k^3+5k^2-2k-1)\\
&\quad+k\delta_{rs}^4(3k^5+28k^4-39k^2-3k+11)+2k\delta_{rs}^6(2k^2-1)\Big)\\
&+\delta_{ju}^8\Big(2k^8-k^6(3-\delta_{rs}^2)+2k^5(5+2\delta_{rs}^2)-k^4-k^3(20+5\delta_{rs}^2-2\delta_{rs}^4)\\
&\quad+k^2(3-\delta_{rs}^2)+k(10+\delta_{rs}^2-\delta_{rs}^4)-1\Big)\Big],
\end{aligned}
\tag{A.22}
$$

$$
A_K = \frac{-2k}{9(k-1)^2(k+1)}\Big[40k^3-26k^2-4k-10-(1+k)(2\delta_{ju}^2+\delta_{rs}^2)\Big],
\tag{A.23}
$$

$$
\begin{aligned}
A_{ss} = -\frac{1}{(k^2-1)^3(2-2k^2+\delta_{ju}^2+2\delta_{rs}^2)^2}\Big[&2(k-1)^2(k+1)^3\Big(4k^7-4k^6+2k^5(-5+\delta_{rs}^2)\\
&\quad+2k^4(3+5\delta_{rs}^2)+2k^3(4-\delta_{rs}^2)-8k^2(\delta_{rs}^2+\delta_{rs}^4)-k(2+2\delta_{rs}^2+5\delta_{rs}^4)-2-\delta_{rs}^4\Big)\\
&-2\delta_{ju}^2(k^2-1)\Big(4k^8+2k^6(-7+\delta_{rs}^2)+4k^5(-1+3\delta_{rs}^2)+k^4(14+8\delta_{rs}^2-\delta_{rs}^4)\\
&\quad-2k^3(-4+5\delta_{rs}^2+\delta_{rs}^4)-k^2(2+10\delta_{rs}^2+5\delta_{rs}^4)-k(4+2\delta_{rs}^2+3\delta_{rs}^4)-2\Big)\\
&+\delta_{ju}^4\Big(2k^8-k^6(7-\delta_{rs}^2)-k^5(2-6\delta_{rs}^2)+k^4(7+4\delta_{rs}^2)-k^3(-4+5\delta_{rs}^2-2\delta_{rs}^4)\\
&\quad-k^2(1+5\delta_{rs}^2)-k(2+\delta_{rs}^2+\delta_{rs}^4)-1\Big)\Big],
\end{aligned}
\tag{A.24}
$$

$$
\begin{aligned}
A_X = \; & \frac{4(2-2k^2+\delta_{ju}^2-\delta_{rs}^2)^2}{9(k-1)^2(2-2k^2+\delta_{ju}^2+2\delta_{rs}^2)^2(4k^2-4+\delta_{ju}^2+2\delta_{rs}^2)^4}\Big\{ -\delta_{ju}^{10}k - 2k\delta_{ju}^8\Big[5k^2+7k-12+5\delta_{rs}^2\Big] \\
& + 2\delta_{ju}^6\Big[9k^6-126k^5+113k^4+k^3(139-100\delta_{rs}^2)+k^2(-167+64\delta_{rs}^2)+k(41+36\delta_{rs}^2-20\delta_{rs}^4)-9\Big] \\
& + 2\delta_{ju}^4\Big[108k^8-488k^7+3k^6(73+18\delta_{rs}^2)+k^5(570-828\delta_{rs}^2)+3k^4(-47+274\delta_{rs}^2)+81-54\delta_{rs}^2 \\
& - 6k^3(36-97\delta_{rs}^2+62\delta_{rs}^4)+3k^2(-89-214\delta_{rs}^2+112\delta_{rs}^4)+k(134+66\delta_{rs}^2+36\delta_{rs}^4-40\delta_{rs}^6)\Big] \\
& + 8\delta_{ju}^2\Big[108k^{10}-56k^9+2k^8(-251+54\delta_{rs}^2)-4k^7(-87+86\delta_{rs}^2)+3k^6(232-23\delta_{rs}^2+9\delta_{rs}^4) \\
& - 6k^5(82-104\delta_{rs}^2+57\delta_{rs}^4)+3k^4(-124+13\delta_{rs}^2+89\delta_{rs}^4)+k^3(164-360\delta_{rs}^2+273\delta_{rs}^4-112\delta_{rs}^6) \\
& + k^2(124-159\delta_{rs}^2-141\delta_{rs}^4+88\delta_{rs}^6)+k(36+80\delta_{rs}^2-57\delta_{rs}^4+24\delta_{rs}^6-10\delta_{rs}^8)-27(2-3\delta_{rs}^2+\delta_{rs}^4)\Big] \\
& + 8(2k^2-2+\delta_{rs}^2)^2\Big[36k^8-24k^7+k^6(-85+18\delta_{rs}^2)+k^5(40-28\delta_{rs}^2)+k^4(71-46\delta_{rs}^2)+9 \\
& - 2k^3(4-33\delta_{rs}^2+8\delta_{rs}^4)+k^2(-31+10\delta_{rs}^2-4\delta_{rs}^4)-2k(4+\delta_{rs}^2-10\delta_{rs}^4+2\delta_{rs}^6)-18\delta_{rs}^2\Big]\Big\}, \quad \text{(A.25)}
\end{aligned}
$$

$$
\begin{aligned}
A_0 = \; & \frac{-2}{9(k^2-1)^2(2-2k^2+\delta_{ju}^2+2\delta_{rs}^2)(4k^2-4+\delta_{ju}^2+2\delta_{rs}^2)^3}\Big\{4096k(k^2-1)^6 \\
& + 64\delta_{rs}^2(k^2-1)^5(9k^2+56k+9)+96\delta_{rs}^4(k^2-1)^4(9k^2-8k+9) \\
& + 16(k^2-1)^3(27k^2-88k+27)\delta_{rs}^6+8(k^2-1)^2(9k^2-40k+9)\delta_{rs}^8 \\
& + \delta_{ju}^2\Big[32(k^2-1)^5(9k^2+14k+9)+96\delta_{rs}^2(k^2-1)^4(3k^2-35k+3) \\
& - 24\delta_{rs}^4(k^2-1)^3(9k^2+166k+9)-8\delta_{rs}^6(k^2-1)^2(36k^2+155k+36)-72\delta_{rs}^8(k^4+k^3-k-1)\Big] \\
& + \delta_{ju}^4\Big[48k(k^2-1)^4(6k^2+5)+12\delta_{rs}^2(k^2-1)^3(12k^3-27k^2-136k-27) \\
& - 6\delta_{rs}^4(k^2-1)^2(36k^3+63k^2+230k+63)-36\delta_{rs}^6(5k^5+3k^4+2k^3-7k-3)-36\delta_{rs}^8k^3\Big] \\
& - \delta_{ju}^6\Big[2(k^2-1)^3(36k^3+27k^2+394k+27)+2\delta_{rs}^2(k^2-1)^2(108k^3+63k^2+323k+63) \\
& + 18\delta_{rs}^4(+9k^5+3k^4-4k^3-5k-3)+36\delta_{rs}^6k^3\Big] \\
& - \delta_{ju}^8\Big[(k^2-1)^2(36k^3+9k^2-22k+9)+9(4k^5+k^4-5k^3+k-1)\delta_{rs}^2+9k^3\delta_{rs}^4\Big]\Big\}, \qquad \text{(A.26)}
\end{aligned}
$$

$$A_{tan} = \frac{4k}{(k-1)(2-2k^2+\delta_{ju}^2+2\delta_{rs}^2)^2\sqrt{(k-1)^3(k+1)}} \arctan\left(\frac{\sqrt{(k-1)^3(k+1)}}{k^2+k-1}\right)$$
$$\times \Big[8(k-1)^4(k+1)^3 + 4\delta_{rs}^2(k^2-1)^2 + 4\delta_{rs}^4(k^3-2k^2-k+2)$$
$$- \delta_{ju}^2\Big(8(k-1)^3(k+1)^2 + 4\delta_{rs}^2(k^2-1) - 2\delta_{rs}^4\Big) + \delta_{ju}^4\Big(2(k-1)^2(k+1) + \delta_{rs}^2\Big)\Big]$$

$$- \frac{8k(2-2k^2+\delta_{ju}^2-\delta_{rs}^2)^2\sqrt{(8k^2-12k+4-\delta_{ju}^2-2\delta_{rs}^2)(4k^2-4+\delta_{ju}^2+2\delta_{rs}^2)}}{9(k-1)^2(2-2k^2+\delta_{ju}^2+2\delta_{rs}^2)^2}$$
$$\times \arctan\left(\frac{\sqrt{(8k^2-12k+4-\delta_{ju}^2-2\delta_{rs}^2)(4k^2-4+\delta_{ju}^2+2\delta_{rs}^2)}}{4k^2+6k-4+\delta_{ju}^2+2\delta_{rs}^2}\right). \tag{A.27}$$

Bibliography

[1] S. R. Beane, K. Orginos and M. J. Savage, Nucl. Phys. B **768**, 38 (2007) [arXiv:hep-lat/0605014].

[2] S. R. Beane, P. F. Bedaque, T. C. Luu, K. Orginos, E. Pallante, A. Parreno and M. J. Savage [NPLQCD Collaboration], arXiv:hep-lat/0612026.

[3] C. W. Bernard and M. F. L. Golterman, Phys. Rev. D **49**, 486 (1994) [arXiv:hep-lat/9306005].

[4] S. R. Sharpe, Phys. Rev. D **56**, 7052 (1997) [Erratum-ibid. D **62**, 099901 (2000)] [arXiv:hep-lat/9707018].

[5] M. F. L. Golterman and K. C. L. Leung, Phys. Rev. D **57**, 5703 (1998) [arXiv:hep-lat/9711033].

[6] S. R. Sharpe and N. Shoresh, Phys. Rev. D **62**, 094503 (2000) [arXiv:hep-lat/0006017].

[7] J. N. Labrenz and S. R. Sharpe, Phys. Rev. D **54**, 4595 (1996) [arXiv:hep-lat/9605034].

[8] J. W. Chen and M. J. Savage, Phys. Rev. D **65**, 094001 (2002) [arXiv:hep-lat/0111050].

[9] A. Adams, N. Arkani-Hamed, S. Dubovsky, A. Nicolis, and R. Rattazzi, JHEP **0610**, 014 (2006) [arXiv:hep-th/0602178].

[10] M. L. Graesser, I. Low and M. B. Wise, Phys. Rev. D **72**, 115016 (2005) [arXiv:hep-th/0509180].

[11] T. D. Lee and G. C. Wick, Nucl. Phys. B **9**, 209 (1969).

[12] T. D. Lee and G. C. Wick, Phys. Rev. D **2**, 1033 (1970).

[13] T. G. Rizzo, arXiv:0704.3458 [hep-ph].

[14] D. O'Connell and M. J. Savage, Phys. Lett. B **633**, 319 (2006) [arXiv:hep-lat/0508009].

[15] J. W. Chen, D. O'Connell, R. S. Van de Water and A. Walker-Loud, Phys. Rev. D **73**, 074510 (2006) [arXiv:hep-lat/0510024].

[16] J. W. Chen, D. O'Connell and A. Walker-Loud, Phys. Rev. D **75**, 054501 (2007) [arXiv:hep-lat/0611003].

[17] D. O'Connell, M. J. Ramsey-Musolf and M. B. Wise, Phys. Rev. D **75**, 037701 (2007) [arXiv:hep-ph/0611014].

[18] A. Jenkins and D. O'Connell, arXiv:hep-th/0609159.

[19] D. O'Connell, Phys. Lett. B **643**, 379 (2006) [arXiv:hep-th/0602240].

[20] B. Grinstein, D. O'Connell and M. B. Wise, arXiv:0704.1845 [hep-ph].

[21] The LANSCE EDM Experiment. http://p25ext.lanl.gov/edm/edm.html .

[22] S. Aoki and A. Gocksch, Phys. Rev. Lett. **63**, 1125 (1989) [Erratum-ibid. **65**, 1172 (1990)].

[23] S. Aoki, A. Gocksch, A. V. Manohar and S. R. Sharpe, Phys. Rev. Lett. **65**, 1092 (1990).

[24] D. Guadagnoli, V. Lubicz, G. Martinelli and S. Simula, JHEP **0304**, 019 (2003) [arXiv:hep-lat/0210044].

[25] F. Berruto, T. Blum, K. Orginos and A. Soni, Nucl. Phys. Proc. Suppl. **140**, 411 (2005) [arXiv:hep-lat/0411003].

[26] E. Shintani et al., Phys. Rev. D **72**, 014504 (2005) [arXiv:hep-lat/0505022].

[27] F. Berruto, T. Blum, K. Orginos and A. Soni, PoS **LAT2005**, 010 (2006).

[28] J. Gasser, H. Leutwyler and M. E. Sainio, Phys. Lett. B **253**, 252 (1991).

[29] M. M. Pavan, I. I. Strakovsky, R. L. Workman and R. A. Arndt, PiN Newslett. **16**, 110 (2002) [arXiv:hep-ph/0111066].

[30] R. J. Crewther, P. Di Vecchia, G. Veneziano and E. Witten, Phys. Lett. B **88**, 123 (1979) [Erratum-ibid. B **91**, 487 (1980)].

[31] W. H. Hockings and U. van Kolck, Phys. Lett. B **605**, 273 (2005) [arXiv:nucl-th/0508012].

[32] A. Pich and E. de Rafael, Nucl. Phys. B **367**, 313 (1991).

[33] P. G. Harris et al., Phys. Rev. Lett. **82**, 904 (1999).

[34] J. Gasser and H. Leutwyler, Nucl. Phys. B **307**, 763 (1988).

[35] P. Hasenfratz and H. Leutwyler, Nucl. Phys. B **343**, 241 (1990).

[36] M. Luscher, Commun. Math. Phys. **104**, 177 (1986).

[37] M. Lüscher, Lecture given at Cargese Summer Inst., Cargese, France (Sep 1-15, 1983).

[38] G. Colangelo, S. Dürr and R. Sommer, Nucl. Phys. Proc. Suppl. **119**, 254 (2003) [arXiv:hep-lat/0209110].

[39] G. Colangelo and S. Dürr, Eur. Phys. J. C **33**, 543 (2004) [arXiv:hep-lat/0311023].

[40] S. R. Sharpe, Phys. Rev. D **46**, 3146 (1992) [arXiv:hep-lat/9205020].

[41] M. F. L. Golterman and K. C. Leung, Phys. Rev. D **56**, 2950 (1997) [arXiv:hep-lat/9702015].

[42] M. F. L. Golterman and K. C. L. Leung, Phys. Rev. D **58**, 097503 (1998) [arXiv:hep-lat/9805032].

[43] C. J. D. Lin, G. Martinelli, E. Pallante, C. T. Sachrajda and G. Villadoro, Nucl. Phys. B **650**, 301 (2003) [arXiv:hep-lat/0208007].

[44] D. Becirevic and G. Villadoro, Phys. Rev. D **69**, 054010 (2004) [arXiv:hep-lat/0311028].

[45] D. Arndt and C. J. D. Lin, Phys. Rev. D **70**, 014503 (2004) [arXiv:hep-lat/0403012].

[46] G. Colangelo and C. Haefeli, Phys. Lett. B **590**, 258 (2004) [arXiv:hep-lat/0403025].

[47] A. Ali Khan et al. [QCDSF Collaboration], Nucl. Phys. Proc. Suppl. **119**, 419 (2003) [arXiv:hep-lat/0209111].

[48] A. Ali Khan et al. [QCDSF Collaboration], Nucl. Phys. Proc. Suppl. **129**, 176 (2004) [arXiv:hep-lat/0309133].

[49] A. Ali Khan et al. [QCDSF Collaborations], arXiv:hep-lat/0312029.

[50] A. Ali Khan et al. [QCDSF-UKQCD Collaboration], Nucl. Phys. B **689**, 175 (2004) [arXiv:hep-lat/0312030].

[51] A. S. Kronfeld, arXiv:hep-lat/0205021.

[52] S. R. Beane, Phys. Rev. D **70**, 034507 (2004) [arXiv:hep-lat/0403015].

[53] S. R. Beane and M. J. Savage, Phys. Rev. D **70**, 074029 (2004) [arXiv:hep-ph/0404131].

[54] R. D. Young, D. B. Leinweber and A. W. Thomas, Phys. Rev. D **71**, 014001 (2005) [arXiv:hep-lat/0406001].

[55] A. W. Thomas, J. D. Ashley, D. B. Leinweber and R. D. Young, J. Phys. Conf. Ser. **9**, 321 (2005) [arXiv:hep-lat/0502002].

[56] W. Detmold and M. J. Savage, Phys. Lett. B **599**, 32 (2004) [arXiv:hep-lat/0407008].

[57] S. R. Sharpe and N. Shoresh, Int. J. Mod. Phys. A **16S1C**, 1219 (2001) [arXiv:hep-lat/0011089].

[58] S. R. Sharpe and N. Shoresh, Phys. Rev. D **64**, 114510 (2001) [arXiv:hep-lat/0108003].

[59] S. R. Beane and M. J. Savage, Nucl. Phys. A **709**, 319 (2002) [arXiv:hep-lat/0203003].

[60] E. Jenkins and A. V. Manohar, Phys. Lett. B **255**, 558 (1991).

[61] E. Jenkins and A. V. Manohar, Phys. Lett. B **259**, 353 (1991).

[62] E. Jenkins, Nucl. Phys. B **368**, 190 (1992).

[63] E. Jenkins and A. V. Manohar, "Baryon chiral perturbation theory," Talks presented at the workshop on *Effective Field Theories of the Standard Model*, Dobogoko, Hungary (Aug 1991).

[64] M. Golterman and E. Pallante, JHEP **0110**, 037 (2001) [arXiv:hep-lat/0108010].

[65] M. Golterman and E. Pallante, arXiv:hep-lat/0108029.

[66] C. Bernard et al., Nucl. Phys. Proc. Suppl. **119**, 170 (2003) [arXiv:hep-lat/0209086].

[67] S. R. Beane, Nucl. Phys. **B695**, 192 (2004) [arXiv:hep-lat/0403030].

[68] L. Susskind, Phys. Rev. **D16**, 3031 (1977).

[69] C. T. H. Davies et al. (HPQCD), Phys. Rev. Lett. **92**, 022001 (2004) [arXiv:hep-lat/0304004].

[70] C. Aubin et al. (MILC), Phys. Rev. **D70**, 114501 (2004) [arXiv:hep-lat/0407028].

[71] S. Durr, PoS **LAT2005**, 021 (2005) [arXiv:hep-lat/0509026].

[72] W.-J. Lee and S. R. Sharpe, Phys. Rev. **D60**, 114503 (1999) [arXiv:hep-lat/9905023].

[73] C. Aubin and C. Bernard, Phys. Rev. **D68**, 034014 (2003) [arXiv:hep-lat/0304014].

[74] C. Aubin and C. Bernard, Phys. Rev. **D68**, 074011 (2003) [arXiv:hep-lat/0306026].

[75] S. R. Sharpe and R. S. Van de Water, Phys. Rev. **D71**, 114505 (2005) [arXiv:hep-lat/0409018].

[76] R. S. Van de Water and S. R. Sharpe, Phys. Rev. **D73**, 014003 (2006) [arXiv:hep-lat/0507012].

[77] M. F. L. Golterman and J. Smit, Nucl. Phys. **B245**, 61 (1984).

[78] M. F. L. Golterman, Nucl. Phys. **B273**, 663 (1986).

[79] M. F. L. Golterman and J. Smit, Nucl. Phys. **B255**, 328 (1985).

[80] M. F. L. Golterman, Nucl. Phys. **B278**, 417 (1986).

[81] J. A. Bailey and C. Bernard, PoS **LAT2005**, 047 (2005) [arXiv:hep-lat/0510006].

[82] P. H. Ginsparg and K. G. Wilson, Phys. Rev. **D25**, 2649 (1982).

[83] M. Luscher, Phys. Lett. **B428**, 342 (1998) [arXiv:hep-lat/9802011].

[84] D. B. Kaplan, Phys. Lett. **B288**, 342 (1992) [arXiv:hep-lat/9206013].

[85] Y. Shamir, Nucl. Phys. **B406**, 90 (1993) [arXiv:hep-lat/9303005].

[86] V. Furman and Y. Shamir, Nucl. Phys. **B439**, 54 (1995) [arXiv:hep-lat/9405004].

[87] R. Narayanan and H. Neuberger, Nucl. Phys. **B412**, 574 (1994) [arXiv:hep-lat/9307006].

[88] R. Narayanan and H. Neuberger, Phys. Rev. Lett. **71**, 3251 (1993) [arXiv:hep-lat/9308011].

[89] R. Narayanan and H. Neuberger, Nucl. Phys. **B443**, 305 (1995) [arXiv:hep-th/9411108].

[90] A. D. Kennedy, Nucl. Phys. Proc. Suppl. **140**, 190 (2005) [arXiv:hep-lat/0409167].

[91] D. B. Renner et al. (LHP), Nucl. Phys. Proc. Suppl. **140**, 255 (2005) [arXiv:hep-lat/0409130].

[92] K. C. Bowler, B. Joo, R. D. Kenway, C. M. Maynard, and R. J. Tweedie (UKQCD), JHEP **08**, 003 (2005) [arXiv:hep-lat/0411005].

[93] F. D. R. Bonnet, R. G. Edwards, G. T. Fleming, R. Lewis, and D. G. Richards (Lattice Hadron Physics), Phys. Rev. **D72**, 054506 (2005) [arXiv:hep-lat/0411028].

[94] S. R. Beane, P. F. Bedaque, K. Orginos, and M. J. Savage (NPLQCD), Phys. Rev. **D73**, 054503 (2006) [arXiv:hep-lat/0506013].

[95] S. R. Sharpe, R. Gupta, and G. W. Kilcup, Nucl. Phys. **B383**, 309 (1992).

[96] R. Gupta, A. Patel, and S. R. Sharpe, Phys. Rev. **D48**, 388 (1993) [arXiv:hep-lat/9301016].

[97] S. Aoki et al. (JLQCD), Phys. Rev. **D66**, 077501 (2002) [arXiv:hep-lat/0206011].

[98] T. Yamazaki et al. (CP-PACS), Phys. Rev. **D70**, 074513 (2004) [arXiv:hep-lat/0402025].

[99] S. Aoki et al. (CP-PACS), Phys. Rev. **D71**, 094504 (2005) [arXiv:hep-lat/0503025].

[100] O. Bar, G. Rupak, and N. Shoresh, Phys. Rev. **D67**, 114505 (2003) [arXiv:hep-lat/0210050].

[101] O. Bar, G. Rupak, and N. Shoresh, Phys. Rev. **D70**, 034508 (2004) [arXiv:hep-lat/0306021].

[102] B. C. Tiburzi, Nucl. Phys. **A761**, 232 (2005) [arXiv:hep-lat/0501020].

[103] O. Bar, C. Bernard, G. Rupak, and N. Shoresh, Phys. Rev. **D72**, 054502 (2005) [arXiv:hep-lat/0503009].

[104] B. C. Tiburzi, Phys. Rev. **D72**, 094501 (2005) [arXiv:hep-lat/0508019].

[105] S. Weinberg, Phys. Rev. Lett. **17**, 616 (1966).

[106] J. Gasser and H. Leutwyler, Ann. Phys. **158**, 142 (1984).

[107] J. Gasser and H. Leutwyler, Nucl. Phys. **B250**, 465 (1985).

[108] M. Knecht, B. Moussallam, J. Stern, and N. H. Fuchs, Nucl. Phys. **B457**, 513 (1995) [arXiv:hep-ph/9507319].

[109] J. Bijnens, G. Colangelo, G. Ecker, J. Gasser, and M. E. Sainio, Phys. Lett. **B374**, 210 (1996) [arXiv:hep-ph/9511397].

[110] J. Bijnens, G. Colangelo, G. Ecker, J. Gasser, and M. E. Sainio, Nucl. Phys. **B508**, 263 (1997) [arXiv:hep-ph/9707291].

[111] J. Bijnens, P. Dhonte, and P. Talavera, JHEP **01**, 050 (2004) [arXiv:hep-ph/0401039].

[112] S. R. Sharpe and R. S. Van de Water, Phys. Rev. **D69**, 054027 (2004) [arXiv:hep-lat/0310012].

[113] M. Luscher, Commun. Math. Phys. **105**, 153 (1986).

[114] M. Luscher, Nucl. Phys. **B354**, 531 (1991).

[115] C. W. Bernard and M. Golterman, Nucl. Phys. Proc. Suppl. **34**, 331 (1994) [arXiv:hep-lat/9311070].

[116] L. Maiani and M. Testa, Phys. Lett. **B245**, 585 (1990).

[117] K. Rummukainen and S. A. Gottlieb, Nucl. Phys. **B450**, 397 (1995) [arXiv:hep-lat/9503028].

[118] C. H. Kim, C. T. Sachrajda, and S. R. Sharpe, Nucl. Phys. **B727**, 218 (2005) [arXiv:hep-lat/0507006].

[119] C. W. Bernard and M. F. L. Golterman, Phys. Rev. **D53**, 476 (1996) [arXiv:hep-lat/9507004].

[120] G. Colangelo and E. Pallante, Nucl. Phys. **B520**, 433 (1998) [arXiv:hep-lat/9708005].

[121] C. J. D. Lin, G. Martinelli, E. Pallante, C. T. Sachrajda, and G. Villadoro, Phys. Lett. **B553**, 229 (2003) [arXiv:hep-lat/0211043].

[122] S. R. Beane and M. J. Savage, Phys. Rev. **D67**, 054502 (2003) [arXiv:hep-lat/0210046].

[123] C. J. D. Lin, G. Martinelli, E. Pallante, C. T. Sachrajda, and G. Villadoro, Phys. Lett. **B581**, 207 (2004) [arXiv:hep-lat/0308014].

[124] M. Golterman, T. Izubuchi, and Y. Shamir, Phys. Rev. **D71**, 114508 (2005) [arXiv:hep-lat/0504013].

[125] S. R. Beane, P. F. Bedaque, A. Parreno, and M. J. Savage, Phys. Lett. **B585**, 106 (2004) [arXiv:hep-lat/0312004].

[126] P. F. Bedaque and J.-W. Chen, Phys. Lett. **B616**, 208 (2005) [arXiv:hep-lat/0412023].

[127] S. R. Sharpe and J. Singleton, Robert, Phys. Rev. **D58**, 074501 (1998) [arXiv:hep-lat/9804028].

[128] K. Symanzik, Nucl. Phys. **B226**, 205 (1983).

[129] K. Symanzik, Nucl. Phys. **B226**, 187 (1983).

[130] J.-W. Chen and M. J. Savage, Phys. Rev. **D66**, 074509 (2002) [arXiv:hep-lat/0207022].

[131] G. Rupak and N. Shoresh, Phys. Rev. **D66**, 054503 (2002) [arXiv:hep-lat/0201019].

[132] S. Aoki, O. Bar, S. Takeda, and T. Ishikawa, Phys. Rev. **D73**, 014511 (2006) [arXiv:hep-lat/0509049].

[133] K. G. Wilson, Phys. Rev. **D10**, 2445 (1974).

[134] J. B. Kogut and L. Susskind, Phys. Rev. **D11**, 395 (1975).

[135] R. G. Edwards et al. (LHPC), Phys. Rev. Lett. **96**, 052001 (2006) [arXiv:hep-lat/0510062].

[136] S. R. Beane, P. F. Bedaque, K. Orginos, and M. J. Savage, Phys. Rev. Lett. **97**, 012001 (2006) [arXiv:hep-lat/0602010].

[137] S. R. Beane, K. Orginos, and M. J. Savage (2006), arXiv:hep-lat/0604013.

[138] S. R. Beane, P. F. Bedaque, K. Orginos, and M. J. Savage, Phys. Rev. D **75**, 094501 (2007) (2006) [arXiv:hep-lat/0606023].

[139] C. Alexandrou, T. Leontiou, J. W. Negele, and A. Tsapalis, Phys. Rev. Lett. **98**, 052003 (2007) (2006) [arXiv:hep-lat/0607030].

[140] S. R. Beane, P. F. Bedaque, T. C. Luu, K. Orginos, E. Pallante, A. Parreno and M. J. Savage, Phys. Rev. D **74**, 114503 (2006) [arXiv:hep-lat/0607036].

[141] O. Bar, K. Jansen, S. Schaefer, L. Scorzato and A. Shindler, arXiv:hep-lat/0609039.

[142] C. W. Bernard et al., Phys. Rev. **D64**, 054506 (2001), http://qcd.nersc.gov/ [arXiv:hep-lat/0104002].

[143] K. Orginos and D. Toussaint (MILC), Phys. Rev. **D59**, 014501 (1998) [arXiv:hep-lat/9805009].

[144] K. Orginos, D. Toussaint, and R. L. Sugar (MILC), Phys. Rev. **D60**, 054503 (1999) [arXiv:hep-lat/9903032].

[145] T. B. Bunton, F. J. Jiang, and B. C. Tiburzi, Phys. Rev. **D74**, 034514 (2006) [arXiv:hep-lat/0607001].

[146] C. Aubin, J. Laiho and R. S. Van de Water, Phys. Rev. D **75**, 034502 (2007) [arXiv:hep-lat/0609009].

[147] J. Gasser and H. Leutwyler, Nucl. Phys. **B250**, 465 (1985).

[148] D. O'Connell, arXiv:hep-lat/0609046.

[149] P. H. Damgaard and K. Splittorff, Phys. Rev. **D62**, 054509 (2000) [arXiv:hep-lat/0003017].

[150] S. R. Sharpe, PoS **LAT2006**, 022 (2006) [arXiv:hep-lat/0610094].

[151] C. W. Bernard and M. F. L. Golterman, Phys. Rev. **D46**, 853 (1992) [arXiv:hep-lat/9204007].

[152] E. B. Gregory, A. C. Irving, C. C. McNeile, S. Miller, and Z. Sroczynski, PoS **LAT2005**, 027 (2006) [arXiv:hep-lat/0510066].

[153] S. Prelovsek, Phys. Rev. **D73**, 014506 (2006) [arXiv:hep-lat/0510080].

[154] C. W. Bernard, C. DeTar, Z. Fu, and S. Prelovsek (2006) [arXiv:hep-lat/0610031].

[155] B. Sheikholeslami and R. Wohlert, Nucl. Phys. **B259**, 572 (1985).

[156] R. Frezzotti, P. A. Grassi, S. Sint, and P. Weisz (Alpha), JHEP **08**, 058 (2001) [arXiv:hep-lat/0101001].

[157] S. R. Sharpe and J. M. S. Wu, Phys. Rev. **D71**, 074501 (2005) [arXiv:hep-lat/0411021].

[158] A. Walker-Loud, Nucl. Phys. **A747**, 476 (2005) [arXiv:hep-lat/0405007].

[159] B. C. Tiburzi and A. Walker-Loud, Nucl. Phys. **A748**, 513 (2005) [arXiv:hep-lat/0407030].

[160] W. Detmold and C. J. D. Lin, Phys. Rev. **D71**, 054510 (2005) [arXiv:hep-lat/0501007].

[161] B. C. Tiburzi and A. Walker-Loud, Nucl. Phys. **A764**, 274 (2006) [arXiv:hep-lat/0501018].

[162] W. Detmold, B. C. Tiburzi, and A. Walker-Loud, Phys. Rev. **D73**, 114505 (2006) [arXiv:hep-lat/0603026].

[163] A. Walker-Loud, Ph.D. thesis, University of Washington (2006) [arXiv:hep-lat/0608010].

[164] R. G. Edwards et al. (LHPC), PoS **LAT2005**, 056 (2006) [arXiv:hep-lat/0509185].

[165] P. F. Bedaque, I. Sato, and A. Walker-Loud, Phys. Rev. **D73**, 074501 (2006) [arXiv:hep-lat/0601033].

[166] H. W. Hamber, E. Marinari, G. Parisi, and C. Rebbi, Nucl. Phys. **B225**, 475 (1983).

[167] Private communications with Silas Beane.

[168] J. Stern, H. Sazdjian, and N. H. Fuchs, Phys. Rev. **D47**, 3814 (1993) [arXiv:hep-ph/9301244].

[169] G. Colangelo, J. Gasser, and H. Leutwyler, Phys. Lett. **B488**, 261 (2000) [arXiv:hep-ph/0007112].

[170] G. Colangelo, J. Gasser, and H. Leutwyler, Phys. Rev. Lett. **86**, 5008 (2001) [arXiv:hep-ph/0103063].

[171] G. Colangelo, J. Gasser, and H. Leutwyler, Nucl. Phys. **B603**, 125 (2001) [arXiv:hep-ph/0103088].

[172] J. Bijnens, G. Colangelo, and P. Talavera, JHEP **05**, 014 (1998) [arXiv:hep-ph/9805389].

[173] B. Ananthanarayan, G. Colangelo, J. Gasser, and H. Leutwyler, Phys. Rept. **353**, 207 (2001) [arXiv:hep-ph/0005297].

[174] S. Pislak et al. (BNL-E865), Phys. Rev. Lett. **87**, 221801 (2001) [arXiv:hep-ex/0106071].

[175] S. Pislak et al., Phys. Rev. **D67**, 072004 (2003) [arXiv:hep-ex/0301040].

[176] DIRAC, URL `http://dirac.web.cern.ch/DIRAC/future.html`.

[177] V. Bernard, N. Kaiser, and U. G. Meissner, Nucl. Phys. **B357**, 129 (1991).

[178] V. Bernard, N. Kaiser, and U. G. Meissner, Phys. Rev. **D43**, R2757 (1991).

[179] B. Kubis and U.-G. Meissner, Nucl. Phys. **A699**, 709 (2002) [arXiv:hep-ph/0107199].

[180] B. Kubis and U.-G. Meissner, Phys. Lett. **B529**, 69 (2002) [arXiv:hep-ph/0112154].

[181] J. Bijnens, P. Dhonte, and P. Talavera, JHEP **05**, 036 (2004) [arXiv:hep-ph/0404150].

[182] C. Bernard, Phys. Rev. **D73**, 114503 (2006) [arXiv:hep-lat/0603011].

[183] J. Bijnens and N. Danielsson, Phys. Rev. **D74**, 054503 (2006) [arXiv:hep-lat/0606017].

[184] R. G. Edwards et al., arXiv:hep-lat/0610007.

[185] S. L. Glashow and S. Weinberg, Phys. Rev. D **15**, 1958 (1977).

[186] R. S. Chivukula and H. Georgi, Phys. Lett. B **188**, 99 (1987); L. J. Hall and L. Randall, Phys. Rev. Lett. **65**, 2939 (1990); G. D'Ambrosio, G. F. Giudice, G. Isidori and A. Strumia, Nucl. Phys. B **645**, 155 (2002) [arXiv:hep-ph/0207036].

[187] R. N. Cahn, Rept. Prog. Phys. **52**, 389 (1989); J. F. Gunion, H. E. Haber, G. Kane and S. Dawson, *The Higgs Hunter's Guide*, Frontiers in Physics, Perseus Publishing, Cambridge M.A. (1990); L. Reina, arXiv:hep-ph/0512377.

[188] N. V. Krasnikov, Phys. Lett. B **291**, 89 (1992); N. V. Krasnikov, Mod. Phys. Lett. A **13**, 893 (1998) [arXiv:hep-ph/9709467]; A. Datta and A. Raychaudhuri, Phys. Rev. D **57**, 2940 (1998) [arXiv:hep-ph/9708444]; D. G. Cerdeno, A. Dedes and T. E. J. Underwood, JHEP **0609**, 067 (2006) [arXiv:hep-ph/0607157].

[189] J. Ellis, J. F. Gunion, H. E. Haber, L. Roszkowski and F. Zwirner, Phys. Rev. D **39**, 844 (1989); U. Ellwanger, J. F. Gunion and C. Hugonie, arXiv:hep-ph/0111179; U. Ellwanger, J. F. Gunion, C. Hugonie and S. Moretti, arXiv:hep-ph/0401228; R. Dermisek and J. F. Gunion, Phys. Rev. Lett. **95**, 041801 (2005) [arXiv:hep-ph/0502105]; R. Dermisek and J. F. Gunion, Phys. Rev. D **73**, 111701(R) (2006) [arXiv:hep-ph/0510322].

[190] V. Barger, P. Langacker, H. S. Lee and G. Shaughnessy, Phys. Rev. D **73**, 115010 (2006) [arXiv:hep-ph/0603247].

[191] M. Voloshin and V. Zakharov, Phys. Rev. Lett. **45**, 688 (1980); M. Voloshin, Sov. J. Nucl. Phys. **44**, 478 (1986); R. S. Chivukula, A. G. Cohen, H. Georgi, B. Grinstein and A. V. Manohar, Annals Phys. **192**, 93 (1989).

[192] W. M. Yao et al. [Particle Data Group], J. Phys. G **33**, 1 (2006).

[193] R. E. Shrock and M. Suzuki, Phys. Lett. B **110**, 250 (1982); L. F. Li, Y. Liu and L. Wolfenstein, Phys. Lett. B **159**, 45 (1985); A. S. Joshipura and J. W. Valle, Nucl. Phys. B **397**, 105 (1993).

[194] A. V. Manohar and M. B. Wise, Phys. Lett. B **636**, 107 (2006) [arXiv:hep-ph/0601212]; A. V. Manohar and M. B. Wise, Phys. Rev. D **74**, 035009 (2006) [arXiv:hep-ph/0606172].

[195] R. Barate et al. [LEP Working Group for Higgs boson searches], Phys. Lett. B **565**, 61 (2003) [arXiv:hep-ex/0306033].

[196] CTEQ Collaboration, http://www.phys.psu.edu/~cteq/ .

[197] J. D. Barrow and A. C. Ottewill, J. Phys. A **16**, 2757 (1983).

[198] V. Müller and H. J. Schmidt, Gen. Rel. Grav. **17**, 769 (1985).

[199] A. De Felice, M. Hindmarsh and M. Trodden, JCAP **0608**, 005 (2006) [arXiv:astro-ph/0604154].

[200] N. Arkani-Hamed, H. C. Cheng, M. A. Luty and S. Mukohyama, JHEP **0405**, 074 (2004) [arXiv:hep-th/0312099].

[201] S. D. H. Hsu, A. Jenkins, and M. B. Wise, Phys. Lett. B **597**, 270 (2004) [arXiv:astro-ph/0406043].

[202] D. Krotov, C. Rebbi, V. A. Rubakov, and V. Zakharov, Phys. Rev. D **71**, 045014 (2005) [arXiv:hep-ph/0407081].

[203] N. Arkani-Hamed, H. C. Cheng, M. A. Luty, S. Mukohyama and T. Wiseman, JHEP **0701**, 036 (2007) [arXiv:hep-ph/0507120].

[204] J. Distler, B. Grinstein, R. A. Porto and I. Z. Rothstein, Phys. Rev. Lett. **98**, 041601 (2007) [arXiv:hep-ph/0604255].

[205] M. L. Graesser, I. Low, and M. B. Wise, Phys. Rev. D **72**, 115016 (2005) [arXiv:hep-th/0509180].

[206] S. Mukohyama, arXiv:hep-th/0610254.

[207] T. N. Pham and T. N. Truong, Phys. Rev. D **31**, 3027 (1985).

[208] B. Ananthanarayan, D. Toublan, and G. Wanders, Phys. Rev. D **51**, 1093 (1995) [arXiv:hep-ph/9410302].

[209] M. R. Pennington and J. Portoles, Phys. Lett. B **344**, 399 (1995) [arXiv:hep-ph/9409426].

[210] M. L. Graesser, A. Jenkins, and M. B. Wise, Phys. Lett. B **613**, 5 (2005) [arXiv:hep-th/0501223].

[211] S. M. Carroll and E. A. Lim, Phys. Rev. D **70**, 123525 (2004) [arXiv:hep-th/0407149].

[212] B. Z. Foster and T. Jacobson, Phys. Rev. D **73**, 064015 (2006) [arXiv:gr-qc/0509083].

[213] G. D. Moore and A. E. Nelson, JHEP **0109**, 023 (2001) [arXiv:hep-ph/0106220].

[214] J. W. Elliott, G. D. Moore, and H. Stoica, JHEP **0508**, 066 (2005) [arXiv:hep-ph/0505211].

[215] Y. Kats, L. Motl, and M. Padi, arXiv:hep-th/0606100.

[216] N. Arkani-Hamed, P. Creminelli, S. Mukohyama and M. Zaldarriaga, JCAP **0404**, 001 (2004) [arXiv:hep-th/0312100].

[217] S. L. Dubovsky, JCAP **0407**, 009 (2004) [arXiv:hep-ph/0403308].

[218] M. Peloso and L. Sorbo, Phys. Lett. B **593**, 25 (2004) [arXiv:hep-th/0404005].

[219] B. Holdom, JHEP **0407**, 063 (2004) [arXiv:hep-th/0404109].

[220] A. V. Frolov, Phys. Rev. D **70**, 061501 (2004) [arXiv:hep-th/0404216].

[221] N. Arkani-Hamed, H. C. Cheng, M. Luty and J. Thaler, JHEP **0507**, 029 (2005) [arXiv:hep-ph/0407034].

[222] S. Mukohyama, Phys. Rev. D **71**, 104019 (2005) [arXiv:hep-th/0502189].

[223] A. Anisimov and A. Vikman, JCAP **0504**, 009 (2005) [arXiv:hep-ph/0411089].

[224] I. Montvay and G. Munster, *Quantum fields on a lattice*, Cambridge University Press (1994).

[225] R. E. Cutkosky, P. V. Landshoff, D. I. Olive and J. C. Polkinghorne, Nucl. Phys. B **12**, 281 (1969).

[226] N. Nakanishi, Phys. Rev. D **3**, 811 (1971).

[227] T. D. Lee and G. C. Wick, Phys. Rev. D **3**, 1046 (1971).

[228] S. Coleman, In *Erice 1969, Ettore Majorana School On Subnuclear Phenomena*, New York, 282 (1970).

[229] K. Jansen, J. Kuti and C. Liu, Phys. Lett. B **309**, 119 (1993) [arXiv:hep-lat/9305003]; K. Jansen, J. Kuti and C. Liu, Phys. Lett. B **309**, 127 (1993) [arXiv:hep-lat/9305004].

[230] D. G. Boulware and D. J. Gross, Nucl. Phys. B **233**, 1 (1984).

[231] D. Evens, J. W. Moffat, G. Kleppe and R. P. Woodard, Phys. Rev. D **43**, 499 (1991); J. W. Moffat, arXiv:hep-ph/0003171.

[232] M. Gell-Mann, P. Ramond and R. Slansky, In *Supergravity*, P. van Nieuwenhuizen & D.Z. Freedman (eds.), North Holland Publ. Co. (1979); T. Yanagida, In *Proceedings of the Workshop on the Baryon Number of the Universe and Unified Theories, Tsukuba, Japan, 13-14 Feb 1979* ; R. N. Mohapatra and G. Senjanovic, Phys. Rev. Lett. **44**, 912 (1980); R. N. Mohapatra and G. Senjanovic, Phys. Rev. D **23**, 165 (1981).

[233] J. A. Casas, J. R. Espinosa and I. Hidalgo, JHEP **0411**, 057 (2004) [arXiv:hep-ph/0410298]; F. Vissani, Phys. Rev. D **57**, 7027 (1998) [arXiv:hep-ph/9709409]; J. A. Casas, V. Di Clemente, A. Ibarra and M. Quiros, Phys. Rev. D **62**, 053005 (2000) [arXiv:hep-ph/9904295].